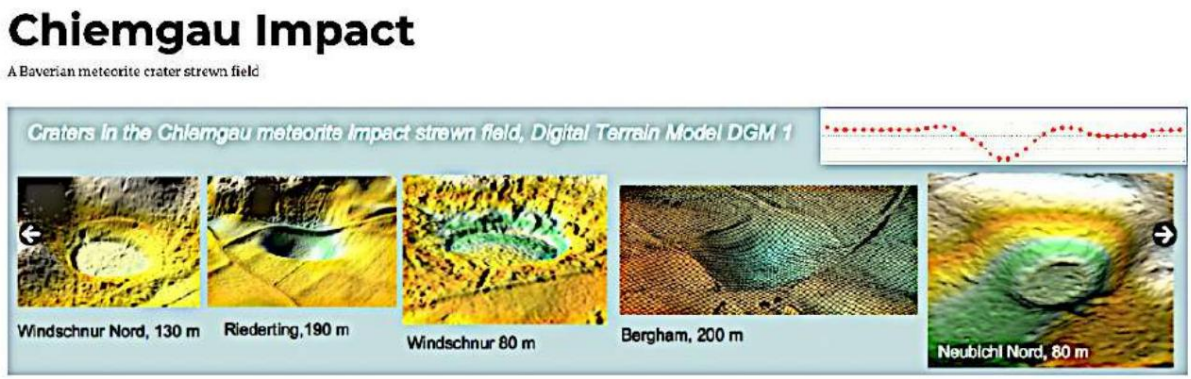

Eggstätt-Hemhofen Lakes (Upper Bavaria): "Touchdown" airburst impact instead of kettle holes in a landscape of glacial disintegration

The lake district in the new light of impact research: Chiemgau airburst impact - Digital terrain model - Hydrocode models - Rayleigh-Taylor/Kelvin-Helmholtz instabilities

by Kord Ernstson1 and Jens Poßekel2

Summary: - The Eggstätt-Hemhofen lake district, with an area of approximately 14 km² (roughly 20 km² including four more distant lakes), located northwest of Lake Chiemsee in Upper Bavaria, is described in Bavarian Ice Age research as a model glacial meltwater landscape and is listed by the Bavarian State Office for the Environment as a significant and valuable geotope. Its origin as a relic of dead ice during the last (Würm) glaciation is described in detail by Darga (2009). This interpretation of the 18 lakes as kettle holes, which is generally plausible, is presented here as no longer tenable. According to the latest topographic data from the extremely high-resolution Digital Terrain Model DGM 1, the geologically structurally unproven origin of the lakes as dead ice must be seen as the result of a "touchdown" airburst impact within the now established Chiemgau crater strewn field. The distinctive morphologies of all the lakes, which definitively rule out a kettle hole origin as impact craters, include more or less pronounced ring rims, inner rings and central bulges, perfect morphological symmetries over hundreds of meters, as well as complex crater morphologies with finger-like, mushroom-like, and wave-like structures and block-like, jagged crater rims, consistent with the instability models of Rayleigh-Taylor and Kelvin-Helmholtz. These features do not occur individually but are documented across the entire lake district and its surrounding area. The sharp overprinting of the agricultural traces of ridge and furrow fields by the impact dates the formation of the lake district to a later period than the Bronze Age, when the first ridge and furrow fields were presumably created. This corresponds to the more recent dating of the Chiemgau impact to 900–600 BC. For the first time in impact research at Chiemgau, a large impact crater strewn field was used.

Hydrocode modeling is compatible with the structure of the Eggstätt-Hemhofen lake district.
With this new possibility of definitively proving impact structures, previously necessary evidence such as shock effects or projectile remnants becomes unnecessary for specific objects.

---

[1]Faculty of Philosophy I, University of 97074 Würzburg, (kernstson@ernstson.de); [2] Geophysics Poßekel Mülheim Possekeljens@gmail.com

1 Introduction

1.1 The outdated Ice Age ideas

The Chiemgau impact strewn field, discovered and subsequently established at the beginning of the new millennium and dated to 900–600 BC in the Bronze Age/Iron Age (Rappenglück, B. et al. 2023) [1], comprises well over 100 mostly walled craters scattered across an area approximately 60 km long and 30 km wide (now extending further to the southwest and north) in the far southeast of Germany. Crater diameters range from a few meters to 1,300 m. Geologically, the craters are located in Pleistocene moraine and fluvioglacial sediments. A fragmented, loosely bound asteroid of about 1,000 m in diameter with low density or a fragmented comet is suspected as the impactor to explain the extensive strewn field.

The Chiemgau incident is now considered to have been caused by an airburst touchdown impact (Moore et al. 2004)[2] [3] (Ernstson and Poßekel 2025).

Since the discovery of the impact began over 20 years ago by a group of
Local historians and amateur archaeologists are familiar with the impact phenomenon from the Bavarian
Ice Age research by the LfU and by local and regional Ice Age geologists up to the present day
The day was denied and fought against, and instead the origin of the Bavarian
Pre-Alpine lakes in glacial meltwater landscapes with kettle holes, kettle pools and kettle basins
persists.

The model of kettle hole formation for the Bavarian Alpine foothill lakes is an “invention” of geographers at the turn of the 20th century. Since then, this model has been passed down from generation to generation of geographers and geologists without this hypothesis ever being supported by field studies. There is no geological or other geoscientific evidence for such a formation for any of the kettle holes/basins in the Alpine foothills (Martin 2014)[4]. A typical example of a probable formation at

Misinterpretation is the kettle hole Wolf's Pit

Dachau/Fürstenfeldbruck, which the Bavarian State Office for the Environment (LfU) considers one of the most beautiful geotopes in Bavaria, probably has a completely different origin. More critical Ice Age researchers (e.g. [4]) question the uniqueness of kettle holes anyway and can cite a whole series

other possible origins. In the case of the Tüttensee crater of the Chiemgau impact, however, it can no longer be said that the local and regional geologists were mistaken, since the geologists of the Bavarian State Office for the Environment (LfU) ignored all the geological, geophysical, mineralogical, geochemical and strictly impact-specific evidence that had been presented in recent years for a meteorite crater (Ernstson et al. 2010[5], Rappenglück et al. 2017[6] and extensive citations therein; [3]Ernstson & Poßekel 2025), they also declared the Tüttensee a Bavarian Ice Age dead-ice geotope and thus made themselves quite ridiculous (CIRT 2019)[7].

For over 100 years, and continuing to this day, the geographers' "invention" at the turn of the last century has been treated as established, irrefutable textbook knowledge, supported by extensive literature consisting of images and descriptions of the Ice Age, and an alternative explanation has never been considered. This is the starting point for this article on the Eggstätt-Hemhofen lake district (Figs. 1, 2), in which we demonstrate once again that, with the postulated paradigm shift in impact research (Ernstson & Poßekel 2024)[8], the dead-ice hypothesis for the Alpine foreland can no longer be considered valid by Ice Age geologists and geomorphologists when using the extremely high-resolution Digital Terrain Model DTM 1, and that general considerations regarding the advance of the

ice was required during the Würm glaciation.

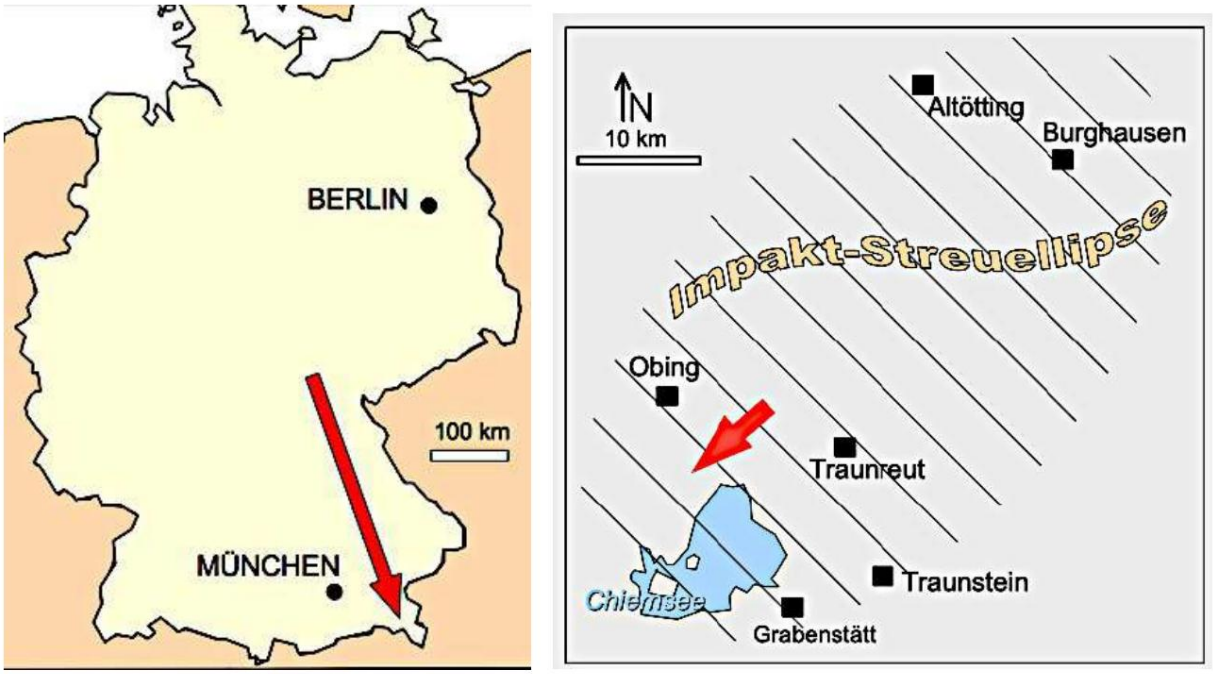

Fig. 1. Site plan of the Eggstätt-Hemhofer lake district northwest of Lake Chiemsee (arrow).

Fig. 2. The Eggstätt-Hemhofen lake district in a Google Earth aerial image. Scale shown in Fig. 3.

1.2 The Digital Terrain Model DTM 1

The digital terrain model (DTM), with its inexhaustible possibilities in geology, hydrogeology, and engineering geophysics, is presented here as another example of a specific application in impact research. It is based on airborne LiDAR survey data of the Earth's surface in a regular meter grid with extremely high vertical resolution. This allows for the precise identification of features, particularly in young meteorite craters and impact structures in general, that would never be discovered during fieldwork or on topographic maps. The pure Earth's surface is displayed independently of buildings and vegetation, even in dense forests. (X,Y,Z) files are provided online for download by the responsible authorities, in this case the Bavarian State Office for Surveying and Geoinformation, and can be used with data processing programs (filtering, gradient calculation, etc., SURFER program) to create various map displays and terrain profiles. In Bavaria, for example, this service is offered free of charge, providing coverage and access to approximately 70,000 tiles measuring 1 km x 1 km, with a 1 m x 1 m grid and a height resolution of approximately 10 cm (DGM 1) for online download within minutes. Furthermore, the SURFER program allows for the already extremely high resolution to be reduced to the decimeter and centimeter range through interpolation.

A significant advantage of DGM mapping is that the extremely high-resolution morphology of the craters, due to their mostly perfect symmetry down to the centimeter range, excludes geogenic and anthropogenic origins, while point-like explosions with spherical shock propagation to the Earth's surface produce exactly what forms an essential basis for the following explanations.

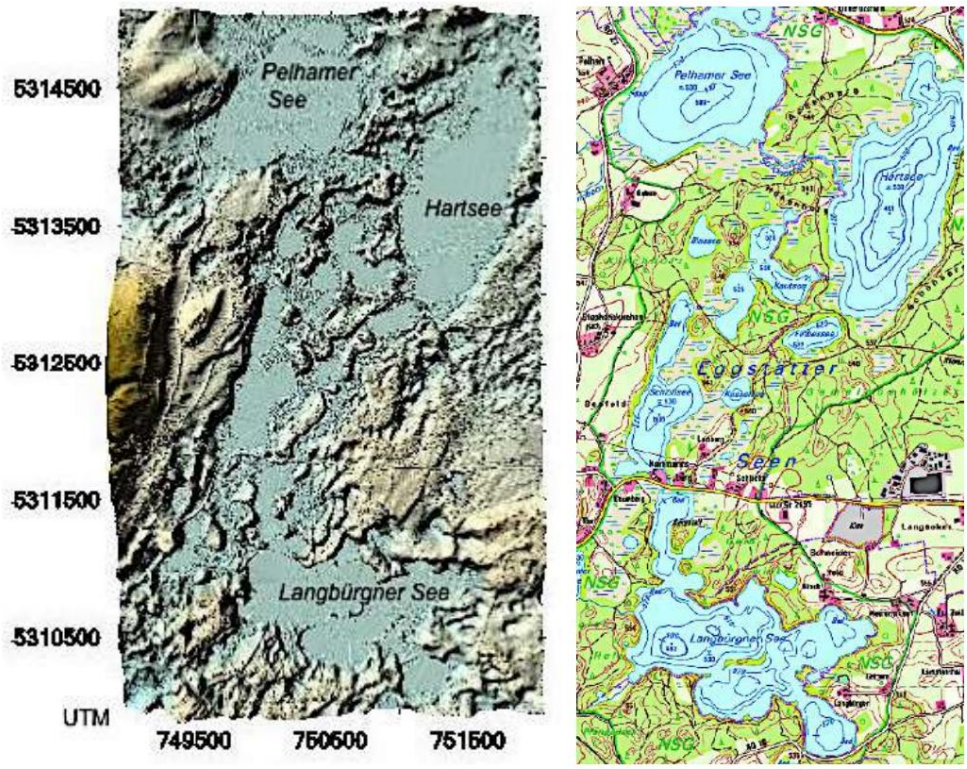

Fig. 3. Digital terrain model DTM 1. 3D block image of the terrain surface with the main lakes and official digital topographic map (BayernAtlas). With DTM 1, and also in the other maps, it should be noted that the 3D terrain usually appears considerably exaggerated, but it makes the essential structures particularly clear, which is especially emphasized by this comparison.

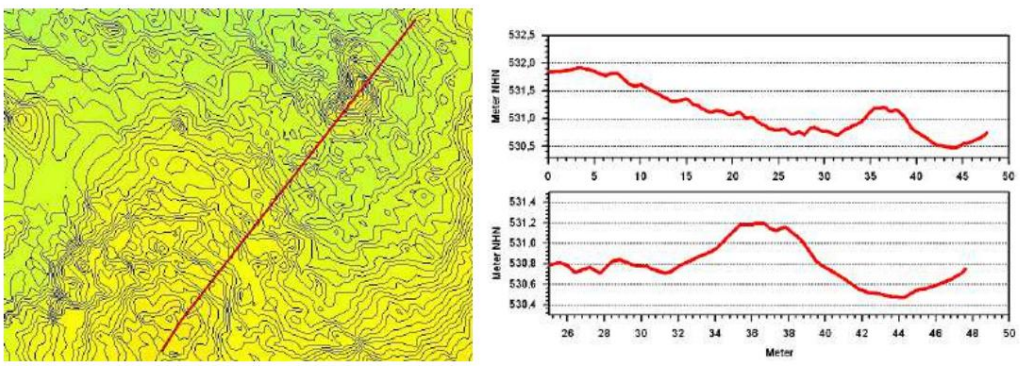

Fig. 4. DGM 1 topographic map, section of the shore area of Hofsee near Eggstätt.
The contour line spacing is interpolated to 5 cm with an interpolated grid spacing of 50 cm. These figures also apply to the resolution of the extracted elevation profile. Anticipating later explanations, the track-symmetric bulge at the end of the profile shows one of the many RTI "mushroom" structures of the impact (see section 1.3 below).

1.3 Rayleigh-Taylor/Kelvin-Helmholtz instabilities

Distinctive features in impact craters, frequently observed in laboratory experiments, can be caused by Rayleigh-Taylor (RT) and Kelvin-Helmholtz (KH) fluid instabilities, which are related to differences in viscosity, inertia, density, and velocity (Google AI review 2006)[9]. RT occurs during density reversal during deceleration and forms diapirs, while KH occurs during velocity shear and produces wave-like deformations. Both phenomena result in complex mixed layers. RT in impact craters (mushrooming) occurs when a denser liquid or solid ejecta material encounters a less dense landing material, and deceleration destabilizes the interface, forcing the less dense material upward and the denser material downward. This creates mushroom-shaped diapirs or fingers that grow outward from the point of impact. While this process is frequently observed in laboratory experiments with liquid impacts, it is less common in large terrestrial craters, where it can occur due to other physical processes such as vaporization or shock waves. KH occurs at the interface between two layers with

Different velocities are encountered, generating velocity shear that forms wave-like patterns. While RT can lead to diapir (mushroom) formation during impacts leading to central elevations (in addition to, for example, elastic rebound), KH can occur in turbulent impact ejecta or mixing zones and contribute to complex dynamics. Therefore, RT generates mushroom and finger structures, while KH instability is velocity-dependent and can cause wave-like impact phenomena. It is understandable that both processes can interact in the formation of impact structures. Here, we report apparent RT and KH instabilities observed in the extremely high-resolution digital terrain models with the aforementioned crater features (fingers, mushrooms, waves, block formations) from the Eggstätt-Hemhofen airburst impact area.

are.

1.4 Hydrocode Modeling

Hydrocode modeling of impacts uses computer programs to simulate extreme, short-term events such as impact craters. It models the behavior of materials under extreme conditions, e.g., shock waves, simulating pressures, temperatures, stresses, as well as material deformations and movements where physical tests are impossible or too costly. Here, we refer to a hydrocode modeling, performed for the first time in impact research, for a very large crater field, that of the Chiemgau impact, which was formed by a low-altitude airburst over largely unconsolidated sediments (West et al. 2006)[10].

2 Geology - the subsurface - Geological map sheet 8040 Eggstätt and explanations

Apart from the glacial discussions questioned here (e.g., [11]), the geology of the study area is described in great detail with a map and explanations on the Eggstätt sheet at a scale of 1:25,000. This sheet covers the lake district and the surrounding area with Pleistocene deposits from the Würm glaciation, as well as lowland areas around the lakes with mostly Holocene peat deposits. Even at this stage,

It should be noted that these recent overburdens surrounding most of the lakes make access to the postulated impact structures for sampling extremely difficult, if not impossible. In the future, this will be addressed using the precise maps of the DGM 1.

Fig. 5. The broad belt of fen peat around Laubensee and Eschenauer See, as with most lakes, makes access and impact sampling difficult. Excerpt: geological map of Bavaria, sheet 8040 Eggstätt and explanatory notes (GK25 1983).

The Würm deposits hit by the airburst impact consist of diverse
Alternating sequences, which are quoted here in simplified form from the legend of the Digital Geological Map:

Meltwater gravel, moraine (till), glacial till (till, matrix-supported), gravelly moraine (till, grain-supported), terminal or lateral moraine (till), gravelly terminal or lateral moraine (till, grain-supported), outcrop gravel.
(dGK25) https://www.lfu.bayern.de/geologie/geo_karten_schriften/dgk25_uab/index.htm

Typical stratigraphic deposits consist lithologically of loam, silt, clay, sand, gravel and any mixtures of these fractions, e.g. sandy loam, sandy silt, clayey sand, sandy gravel, as well as special formations such as interbedded layers of highly consolidated conglomerates (Nagelfluh).

With regard to the key parameters of KA and KH instabilities, the following density and viscosity differences can be assumed: The *densities* of the rocks involved can vary considerably and are (in g/cm³): dry sand 1.5–1.6, dry gravel 1.3–1.7, groundwater-saturated sand 1.9–2.0, clay 1.9–2.2, conglomerate 2.4, dry silt up to 1.0–1.2. The *viscosities* of the unconsolidated rocks affected by the impact differ by many orders of magnitude, with the viscosities before the impact, such as composition, grain size, texture, and water content, as well as the impact parameters such as temperature, pressure, and strain rate, playing an important role.

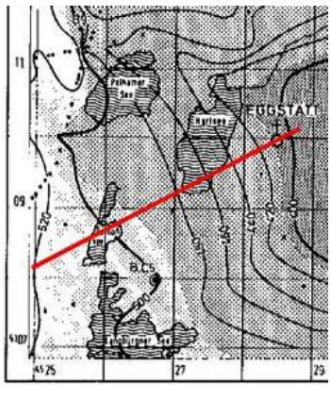

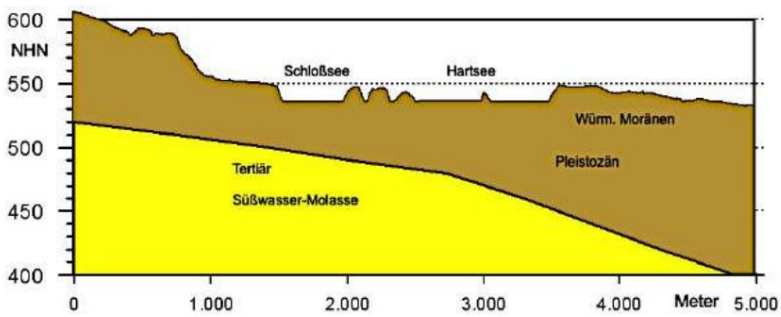

Fig. 6. Relief of the upper edge of the Molasse (map on the left from Eggstätt GK25 1983, explanations).

The extent to which Tertiary rocks of the freshwater molasse were also involved in the excavation and ejecta remains unanswered for the time being without suitable sample specimens. As shown in Figure 57, a supplementary copy of Figure 4, the greatest water depths of, for example, Schloßsee and Hartsee reach depths of 10 m and 20 m above the upper edge of the Tertiary. In the case of the roughly 600 m wide Schloßsee (wall crests), 10 m depth is not much, and in the course of complex RTI crater formation with ejecta backflow and mushroom and finger formations, Tertiary rocks may well have been affected by the impact, although the cross-section in Figure 6 at the Tertiary-Quaternary boundary is based on only a few widely spaced boreholes.

3 results

The following sections present explanations of the discussed lakes along with their well-known topographical names. Given the abundance of information, it is important that the overview is not lost in this compilation. Therefore, the numerous illustrations have not been integrated into a coherent text.
Instead, only the corresponding images are listed, each accompanied by more or less lengthy texts as "captions".

Regarding the maps and profile illustrations, it should be noted that all scales, heights above sea level (NHN) and distance measurements are given in meters.

In the illustrations with the digital terrain models, the different maps of 3D terrain, shaded relief and isoline topography are used alternately to adjust their respective expressiveness.

3.1 Pelhamer See

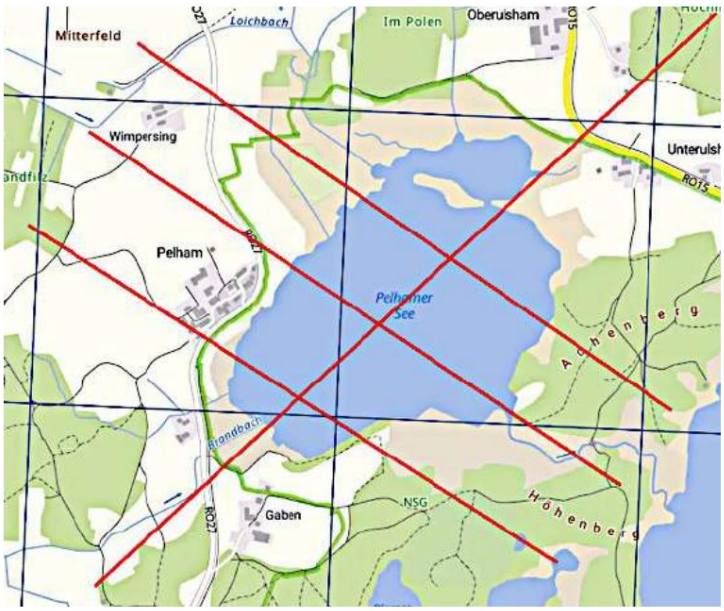

Fig. 7. Pelhamer See in the topographic map (BayernAtlas) with the profiles of Fig. 8.

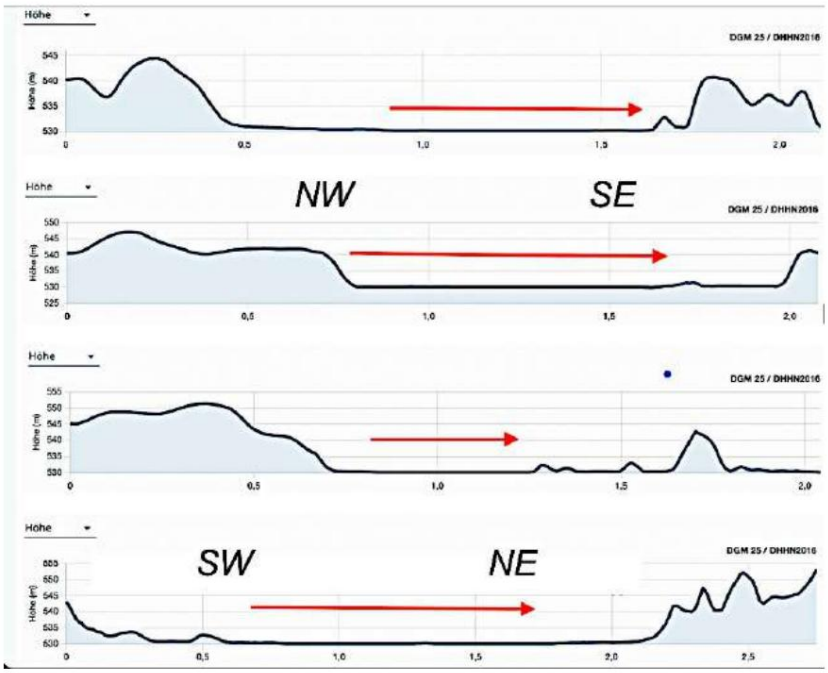

Fig. 8. In the elevation profiles of Lake Pelham, the lake's surface area is marked with arrows. This shows that the structure with the surrounding embankment is significantly larger, indicating a gradation towards the center. Many of the other lakes exhibit similar features, which will be documented later. An example for Lake Pelham is shown in Fig. 9.

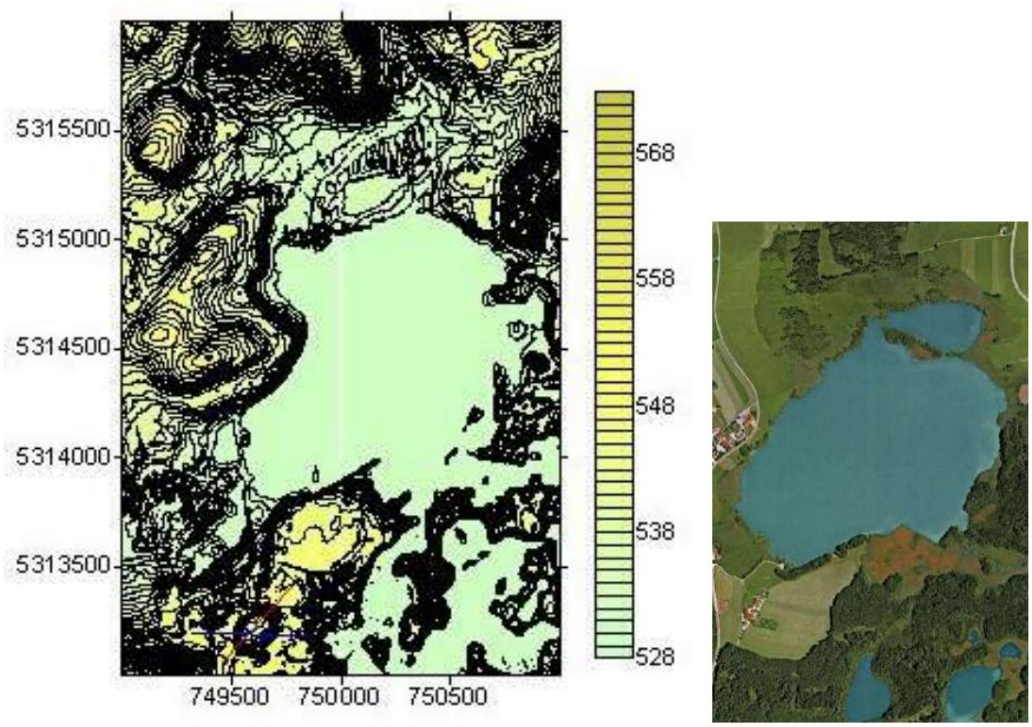

Fig. 7. Pelhamer See, DGM 1, topographic map, contour line spacing 1 m, compared to the water surface in the Google Earth aerial image.

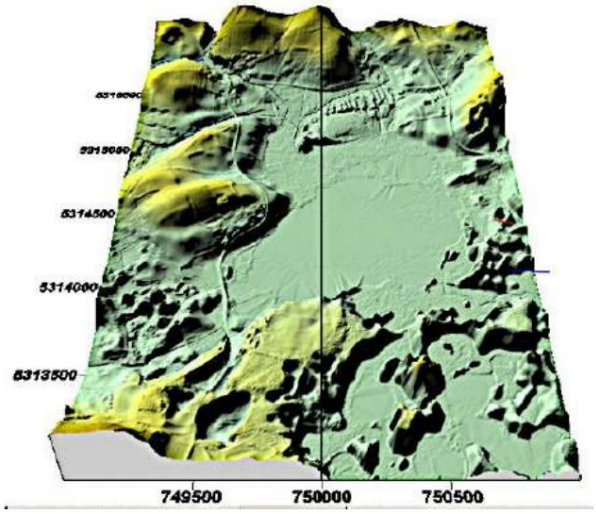

Fig. 8. Pelhamer See in the DGM 1 3D terrain surface; oblique view to the north. The deeply furrowed, partly radial marginal zones are reminiscent of the complex finger structures of Rayleigh-Taylor instabilities.

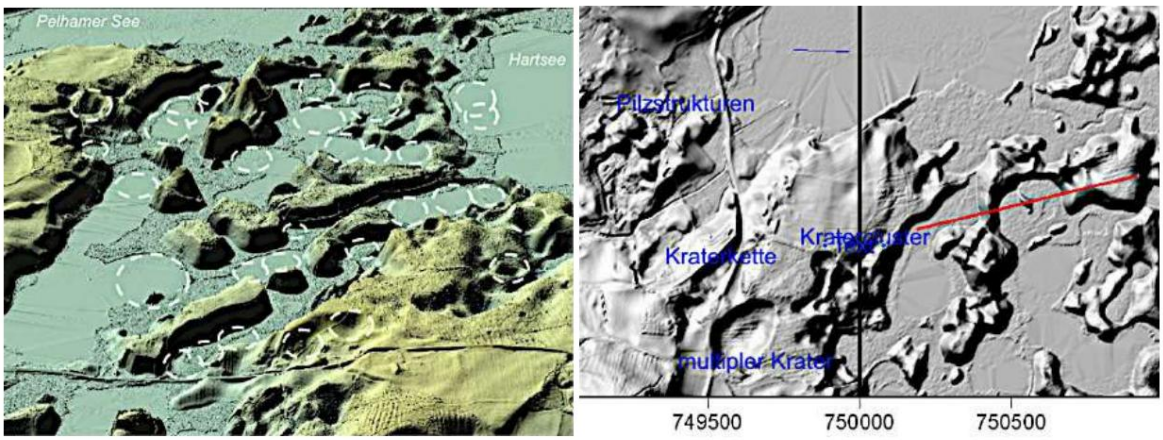

Fig. 9. The southern part of Lake Pelham and the transition to Lake Hartsee and Lake Schloßsee: The highly structured, waterless marginal zone with a cluster of circular structures and selected crater complexes (image on the right and Figs. 11-14). DEM 1 Terrain surface and shaded relief.

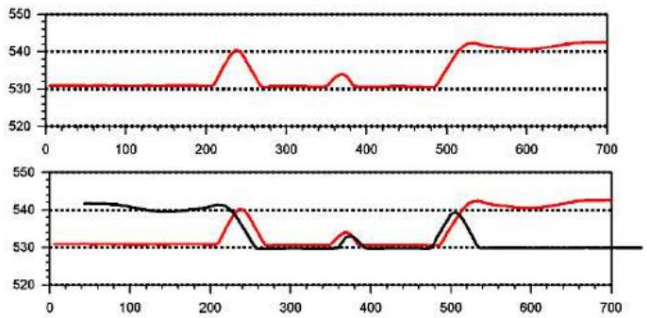

Fig. 10. Red profile line (WSW - ENE, mirrored in black), and above the crater on the right in Fig. 9. As in many other cases, the central hill rules out a kettle hole.

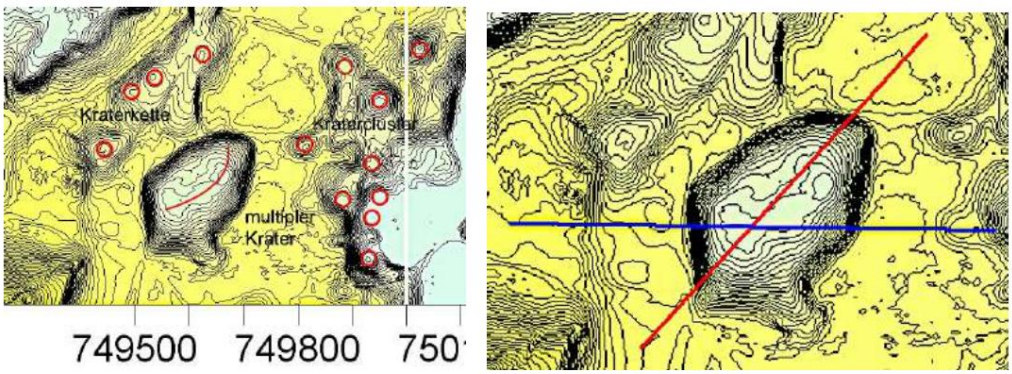

Fig. 11. Site plan for the following structures. DEM 1, topographic map. Scale according to the following elevation profiles. Right: Slightly embanked multiple crater.

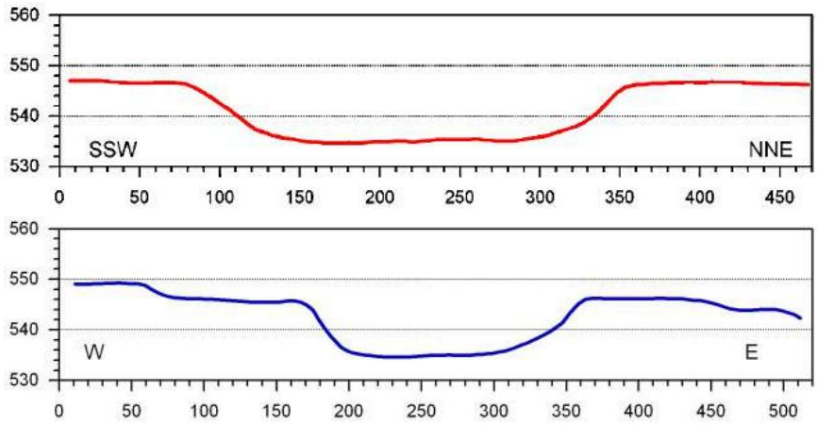

Fig. 12. The elevation profiles above the crater of Fig. 11 (right) show a very uniform rim zone and significant axial symmetries all around, as well as a slight central bulge. A kettle hole can be ruled out.

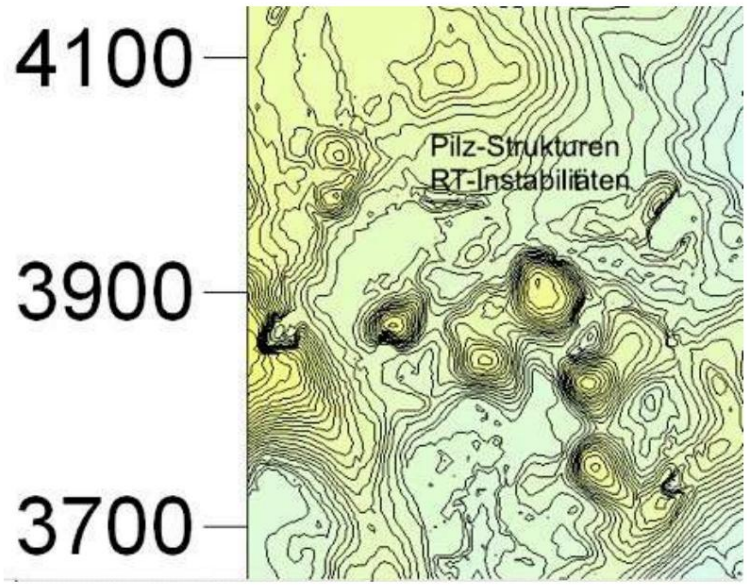

Fig. 13. Mushroom structures (“mushrooming” according to Rayleigh-Taylor).

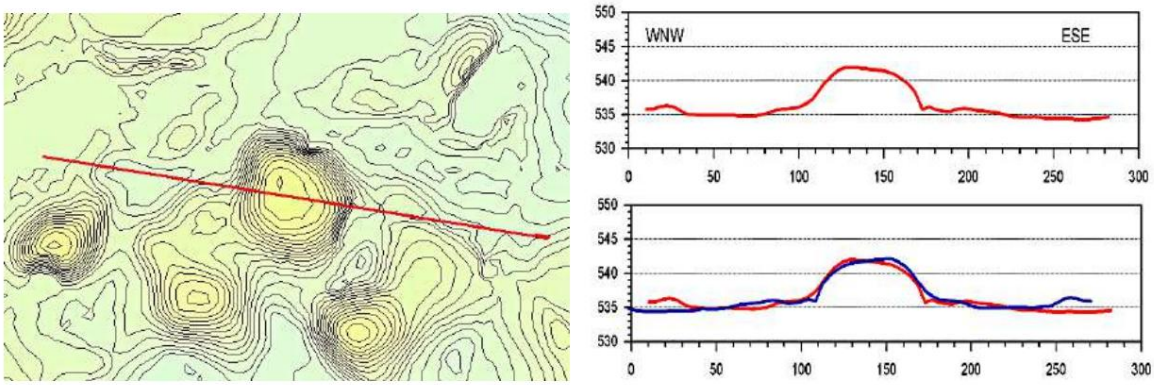

Fig. 14. Near-perfect axial symmetry over 200 m of the mushroom structure. Blue = mirrored profile.

3.2 Hartsee

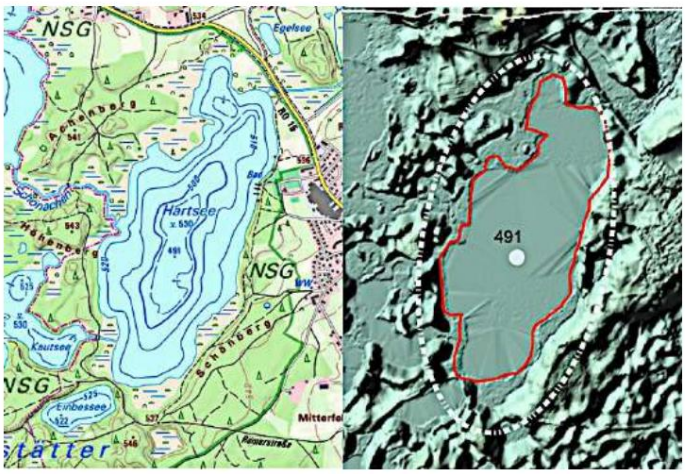

Fig. 15. Hartsee in the topographic map and as an impact structure in the DEM 1 terrain surface (with elliptical ridge border). Red = water area. 491 = central deepest lake. The lake is approximately 1.8 km long.

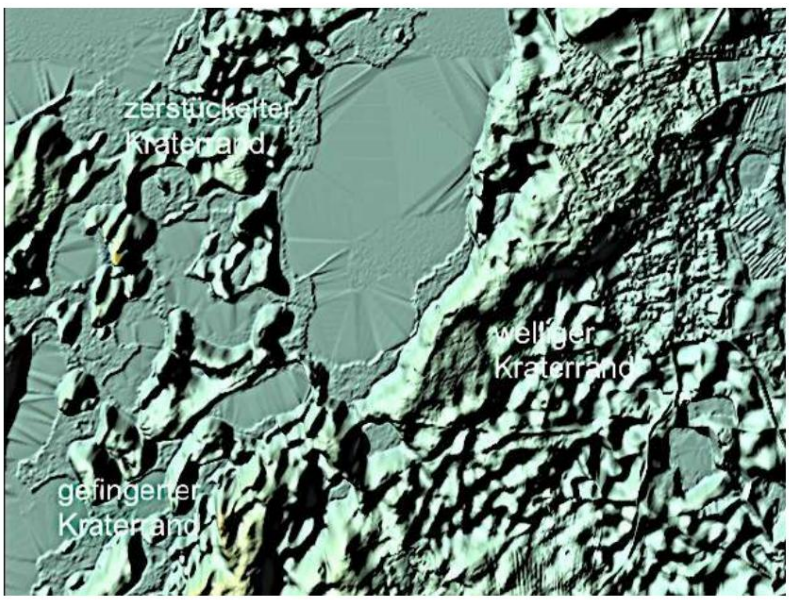

Fig. 16. The Hartsee impact with RT/KH instability structures.

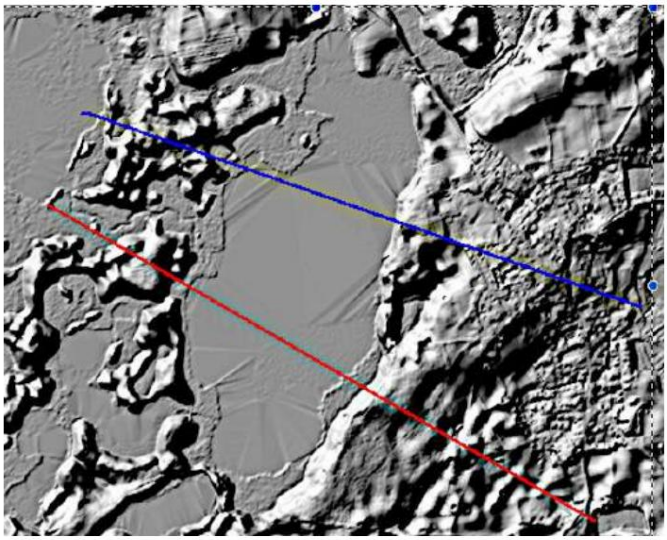

Fig. 17. DGM 1 shaded relief of Hartsee with the profiles of Fig. 18 (with the scale).

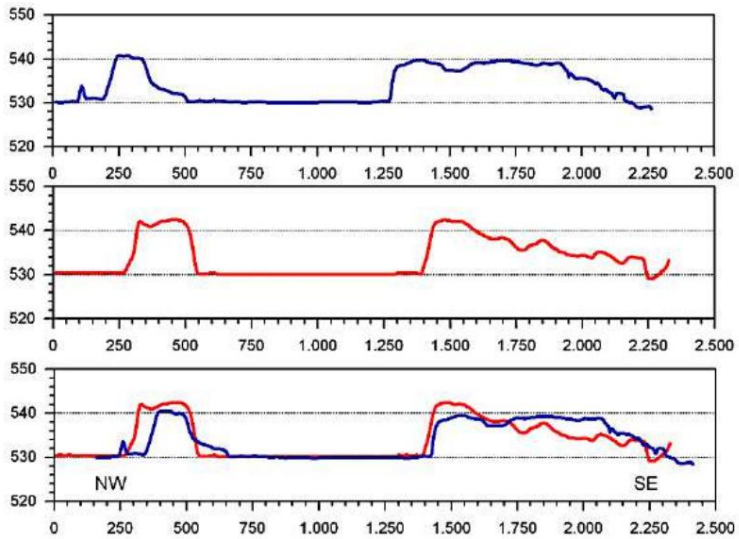

Fig. 18. DGM 1: The profiles, located approximately 400 m apart, have a remarkable

Height profile accurate to the meter.

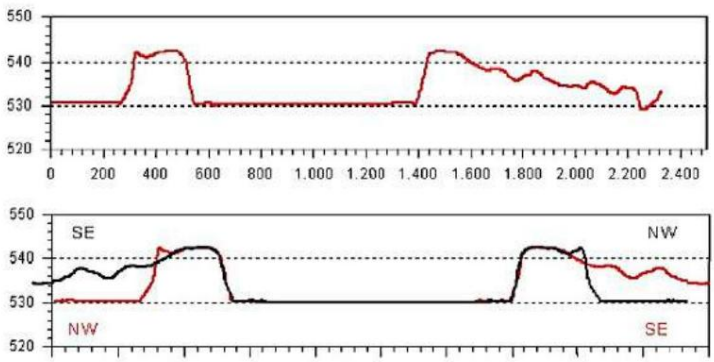

Fig. 19. The perfect axial symmetry over 1000 m for the edge of the red profile (mirrored in black) is also remarkable and poses problems in classifying it as an Ice Age relic.

explain.

3.3 Lake group Blassee, Kautsee, Einbessee and unnamed small crater

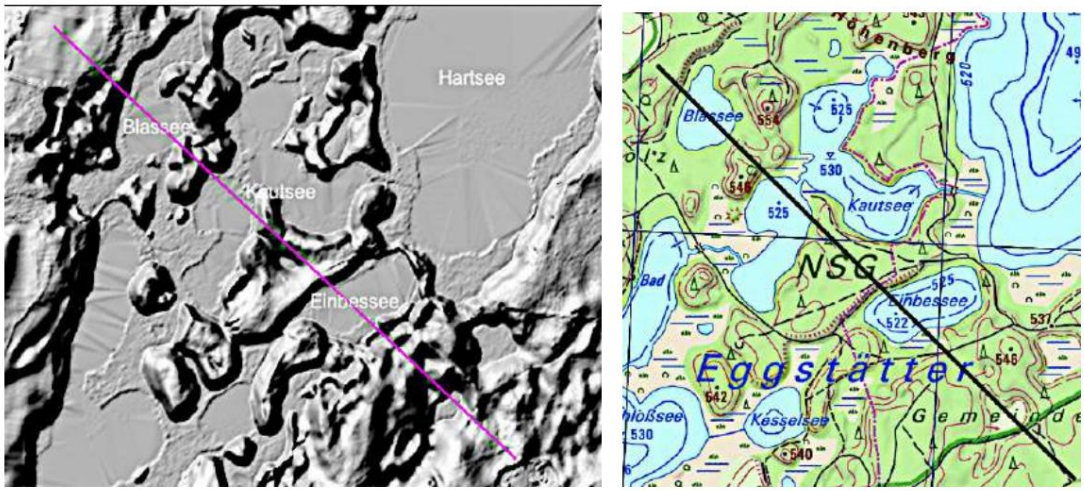

Fig. 20. DGM 1, shaded relief with profile line and topographic map, BayernAtlas.

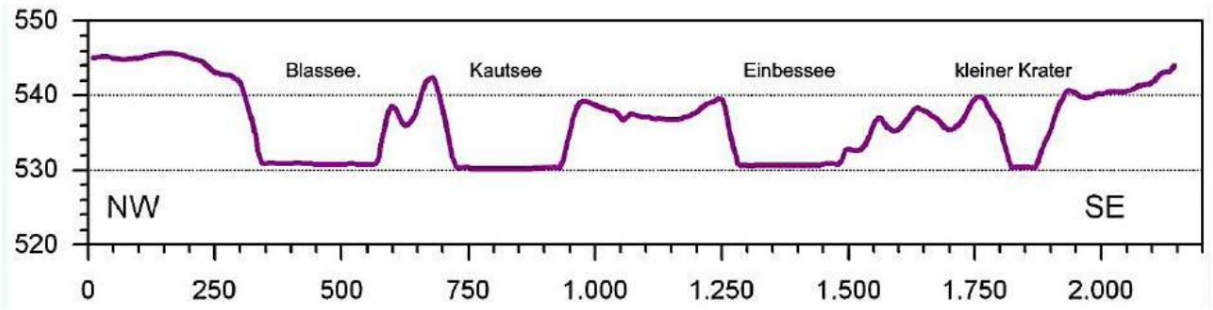

Fig. 21. DGM 1 profile, 10 cm height resolution. The characteristic marginal ridges argue against kettle holes.

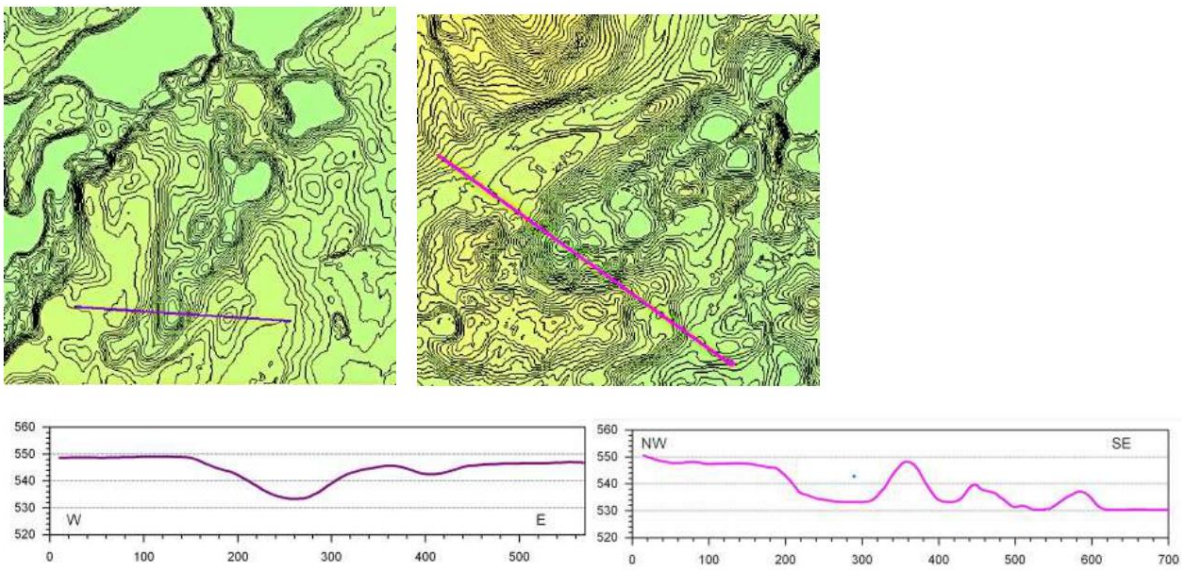

Fig. 22. DGM 1, topographic maps; accompanying crater chains and selected elevation profiles.

3.4 Schloßsee - Kesselsee - Dürnbiehler See

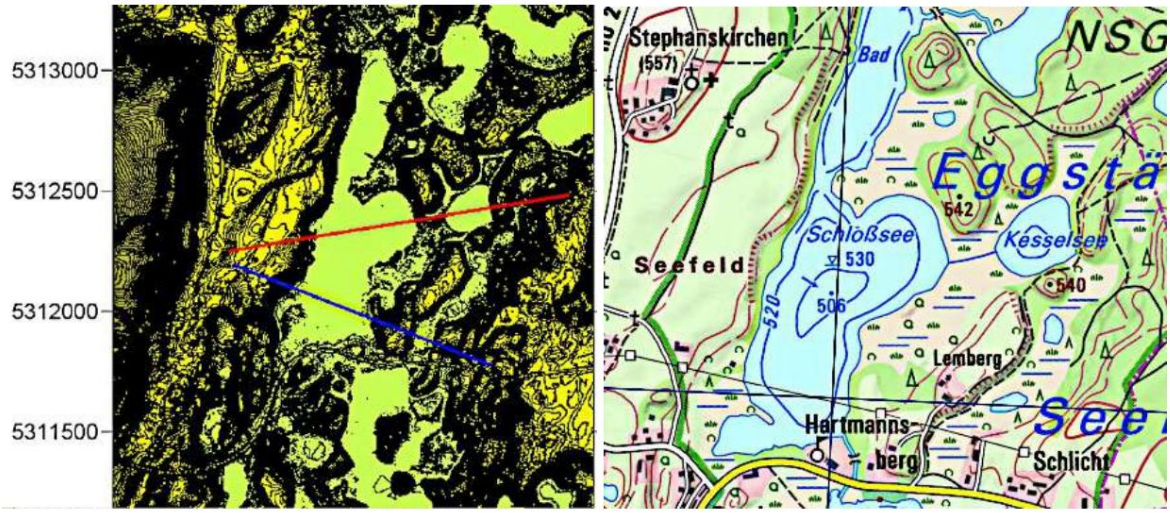

Fig. 23. DGM 1 Topography with elevation profiles (Fig. 24) and topographic map BayernAtlas. Dürnbiehler See above the east of Eggstätt.

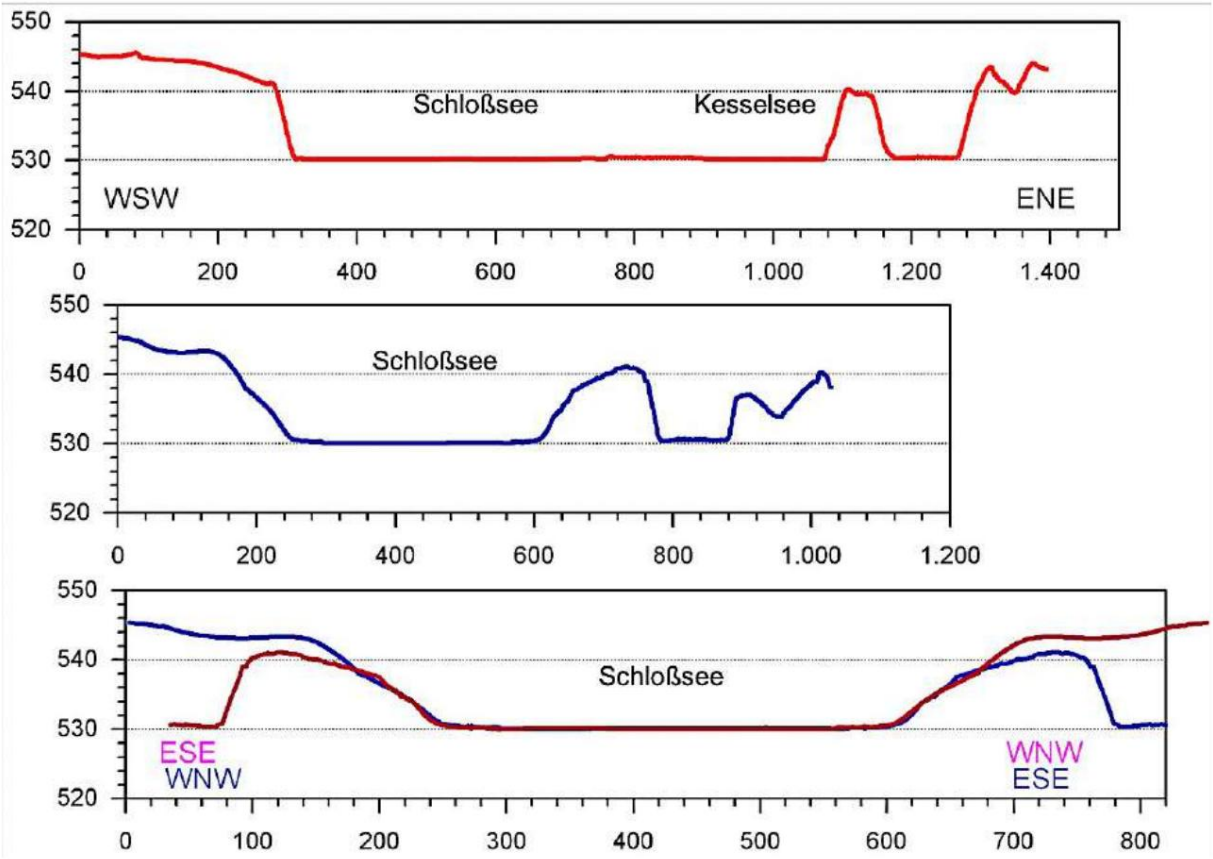

Fig. 24. DGM 1 profiles over Schloßsee and Kesselsee. Impressive in the blue profile above

The Schloßsee (castle lake) has the identical morphology of the mirrored crater edges 500 m away (profiles below).

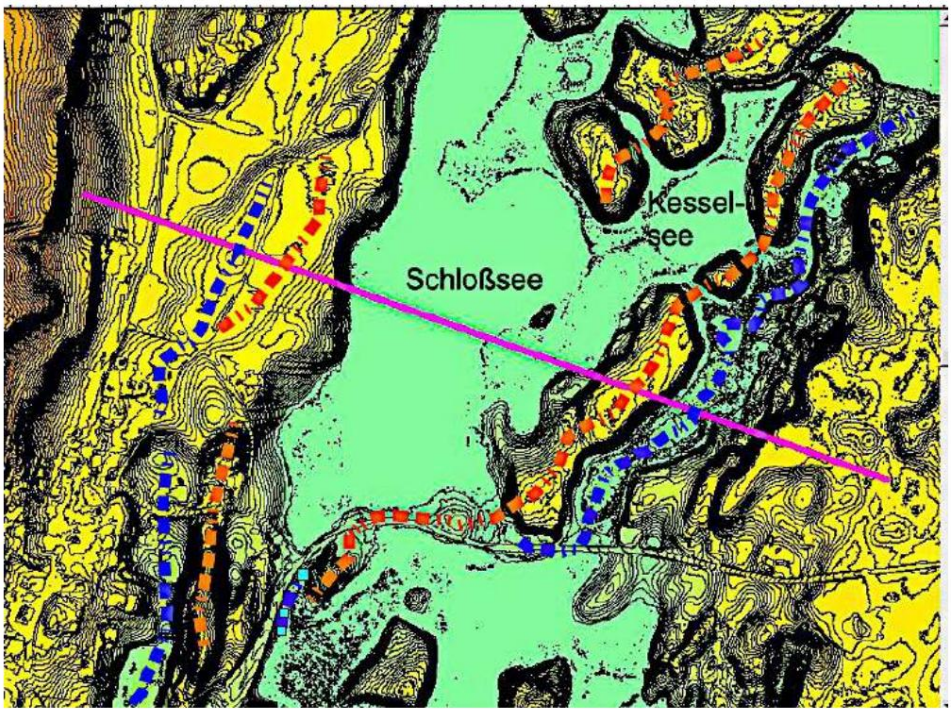

Fig. 25. The longer profile in the DEM 1 over the Schloßsee shows, as with many other lakes, that the mapped and photographed water surface only represents the inner, lower-lying area of the postulated impact. In fact, a more complex structural margin appears to exist, consisting of a sequence of ridge (marked in orange) and trough (blue), which is particularly clear in the mirrored profile in Fig. 26. Part of the blue-marked structure will be discussed in more detail later (Fig. 82).

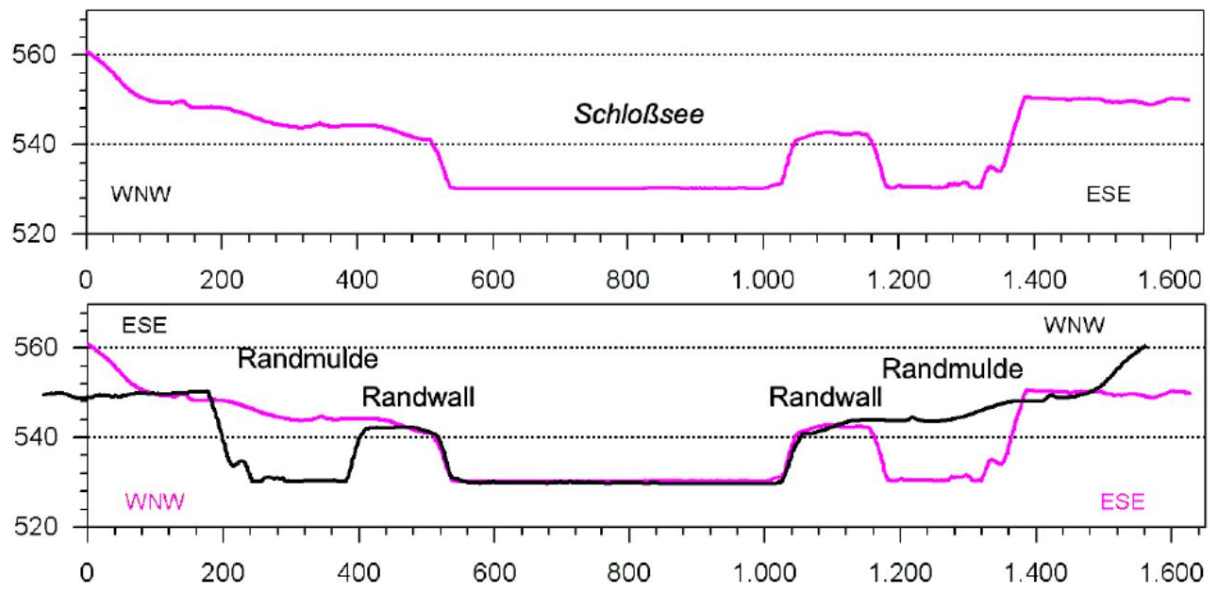

Fig. 26. The sequence of rim bulge and rim depression in the superposition of the mirrored profile indicates a construct according to a wave-like Kelvin-Helmholtz instability during impact.

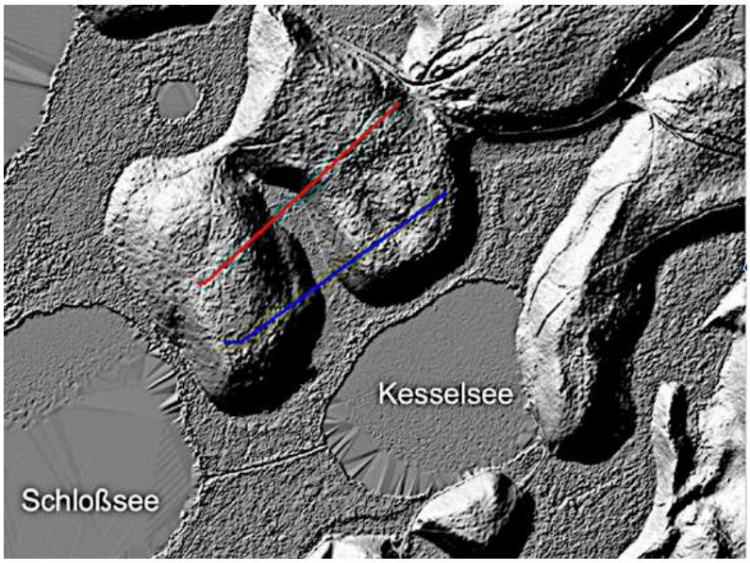

Fig. 27. Finger-shaped outpouching of the Kesselsee crater (according to RTI). DTM 1 profiles in Fig. 28.

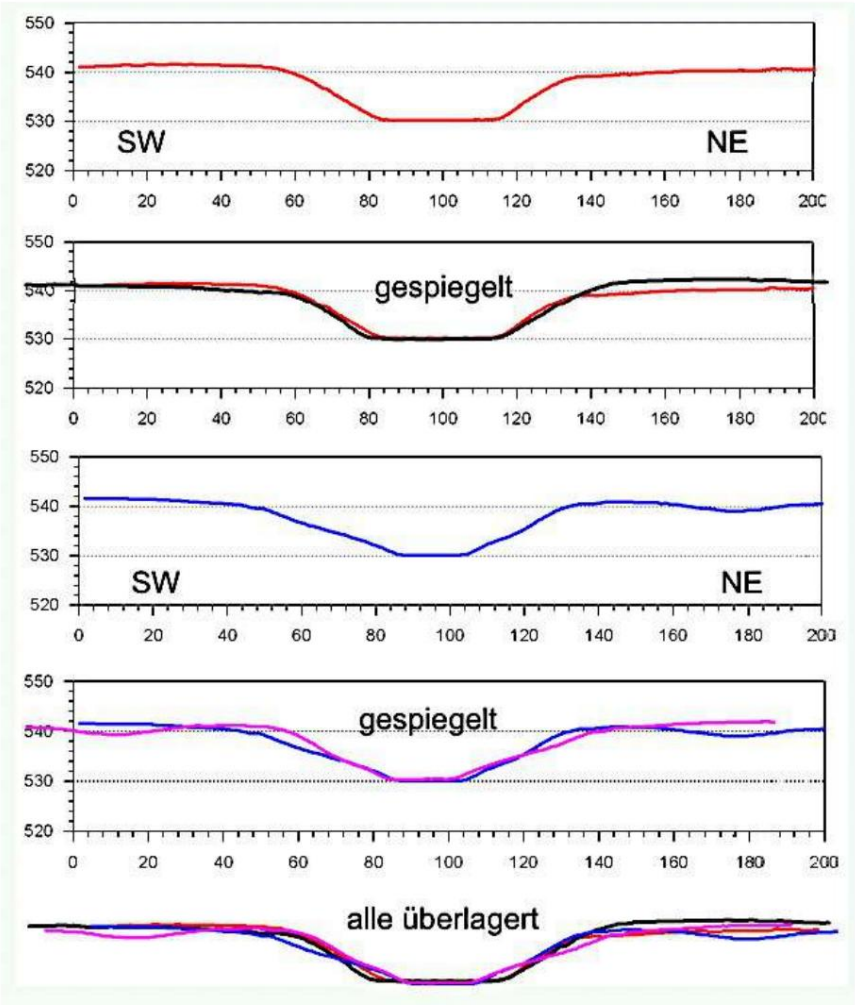

Fig. 28. DGM 1 profiles across the finger groove. The symmetries and the precise overlap are noteworthy.

Dürnbiehler See (location in Fig. 23)

Fig. 29. The name of the small Dürnbiehler See can now only be found on a map from 19th century (center). Left: Google Earth, right: DGM 1.

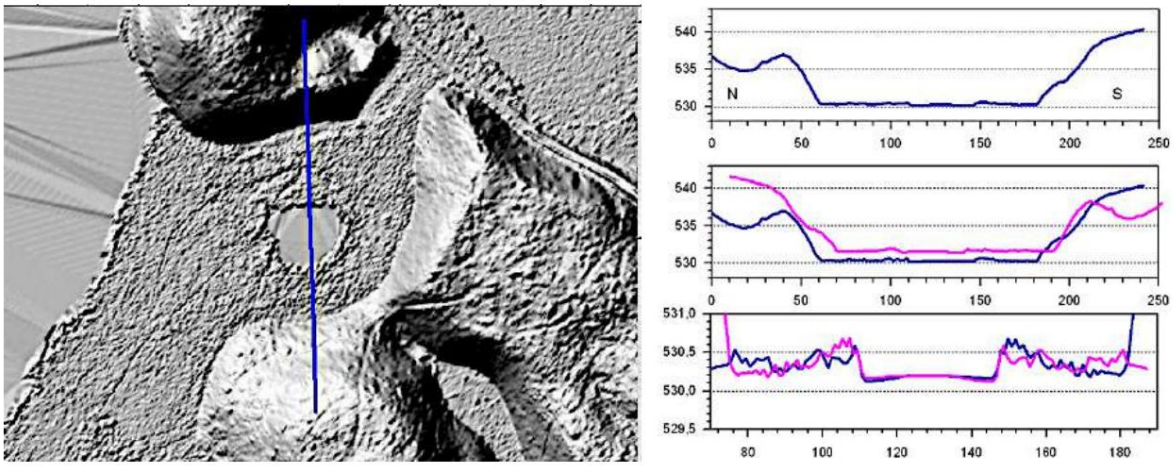

Fig. 30. Morphological symmetries for both the outer prominent crater rim and the inner lake rim, which traces an inner bulge, which will be discussed later.

3.5 Langbürgner See,

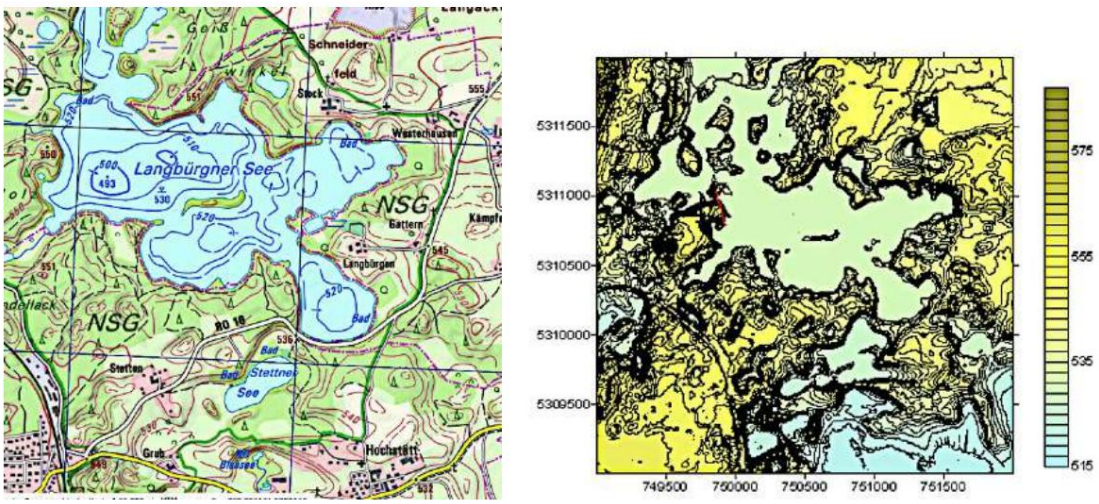

Fig. 30. Topographic map BayernAtlas with grid lines of the Bavarian DGM 1 (map on the right made of 9 tiles, 3 km x 3 km).

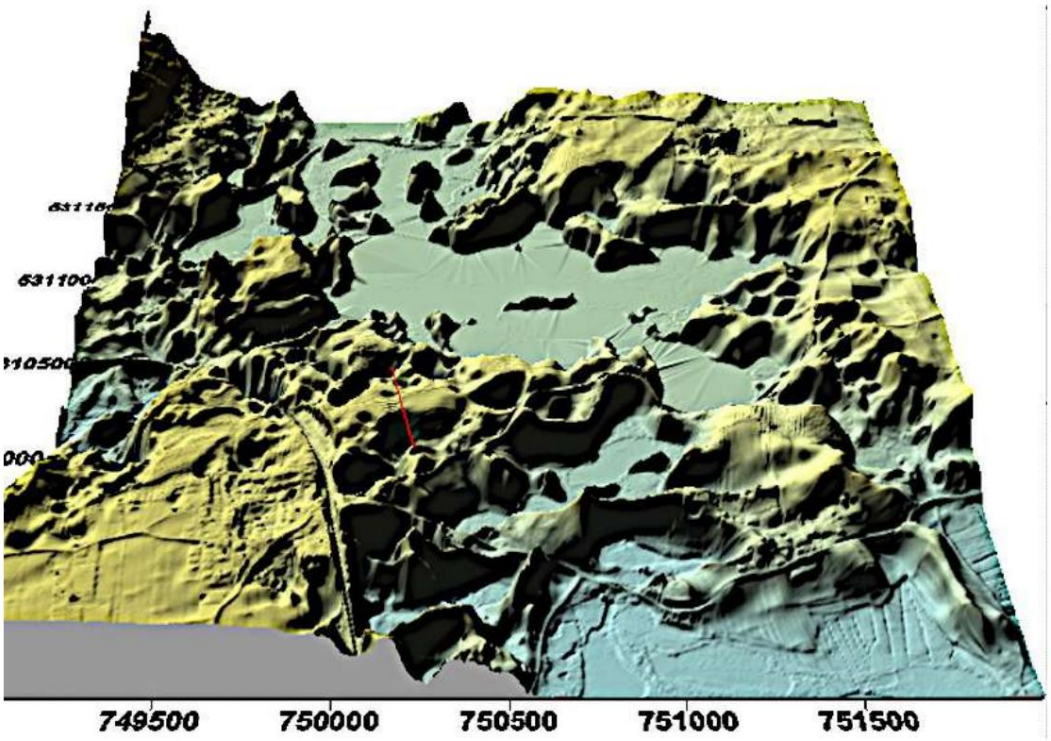

Fig. 31. The nine 3 km x 3 km DGM 1 tiles from Fig. 30. 3D surface viewed obliquely to the north. The strong exaggeration of the DGM 1 emphasizes the extremely fragmented, bowl-like outline of the present-day water surface of the lake.

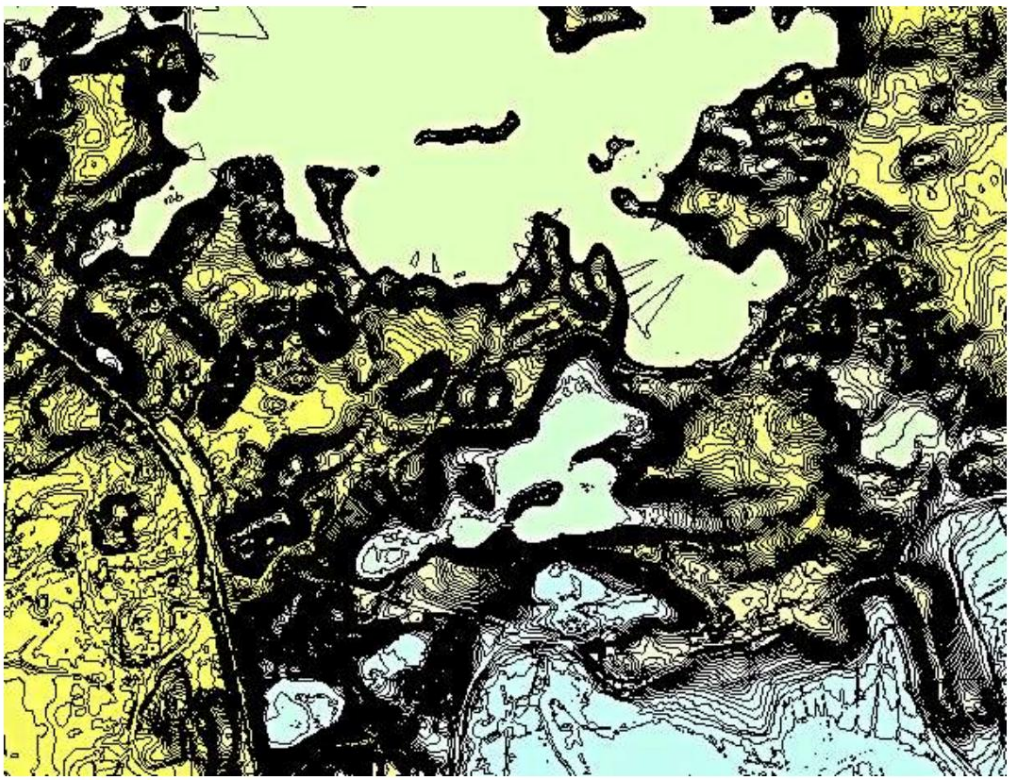

Fig. 32. The southern edge of the lake, which appears paved with hollows and humps, as shown by examples in Figs. 33 and 34 (where there is also a scale).

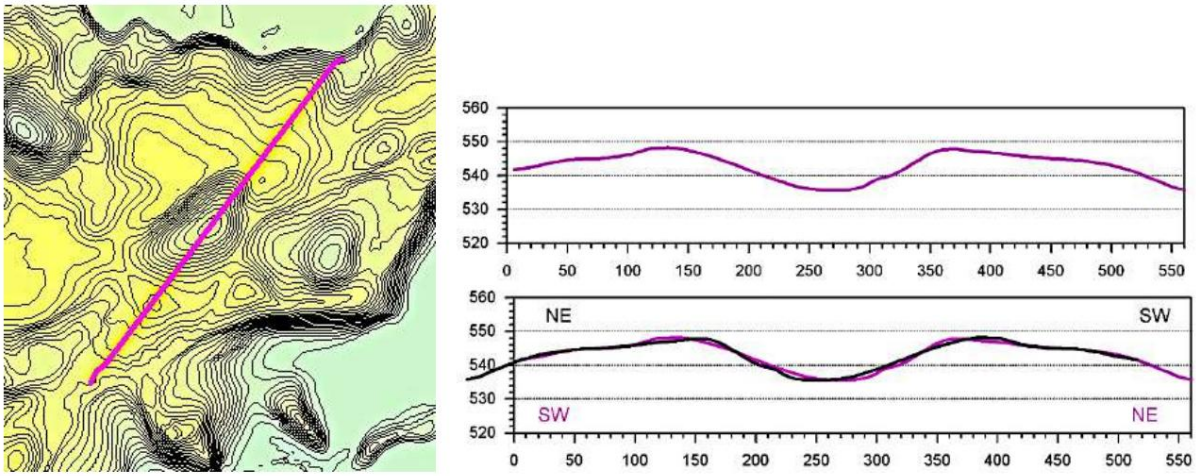

Fig. 33. DGM 1 Topography: Example from the cluster of Fig. 32. The 250 m (ramp crests)
The long trough shows extreme track symmetry in the superposition.

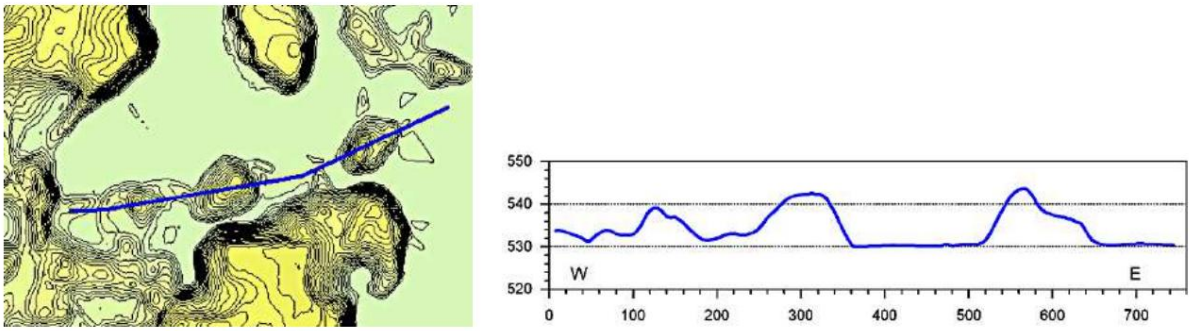

Fig. 34. Chain of three rounded bumps from the cluster in Fig. 33. The middle bump
It measures 100 m in length and is 10 m high.

3.6 Schernsee

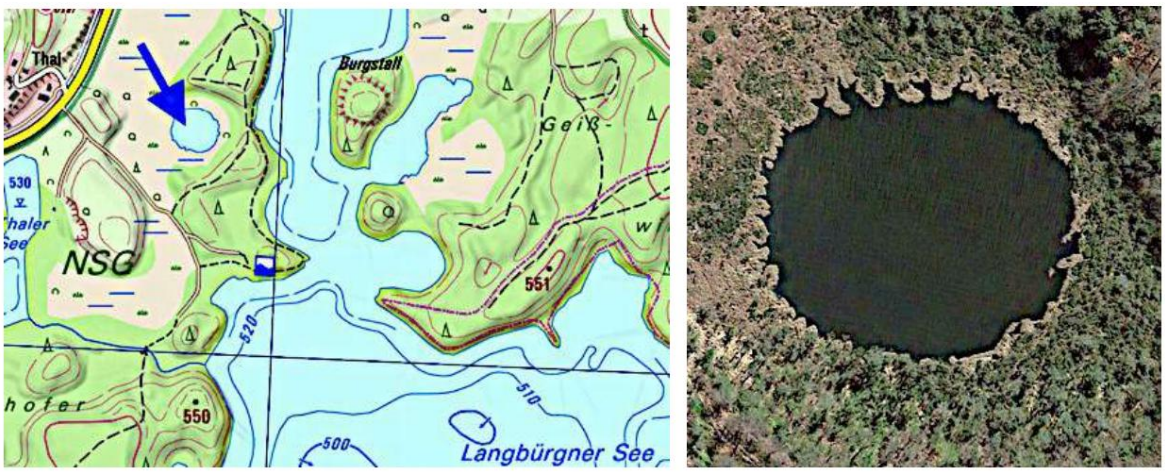

Fig. 35. Lake Schernsee near Lake Langbürgner; BayernAtlas and Google Earth. The sawtooth-like edge will be discussed later. Size: see Fig. 36.

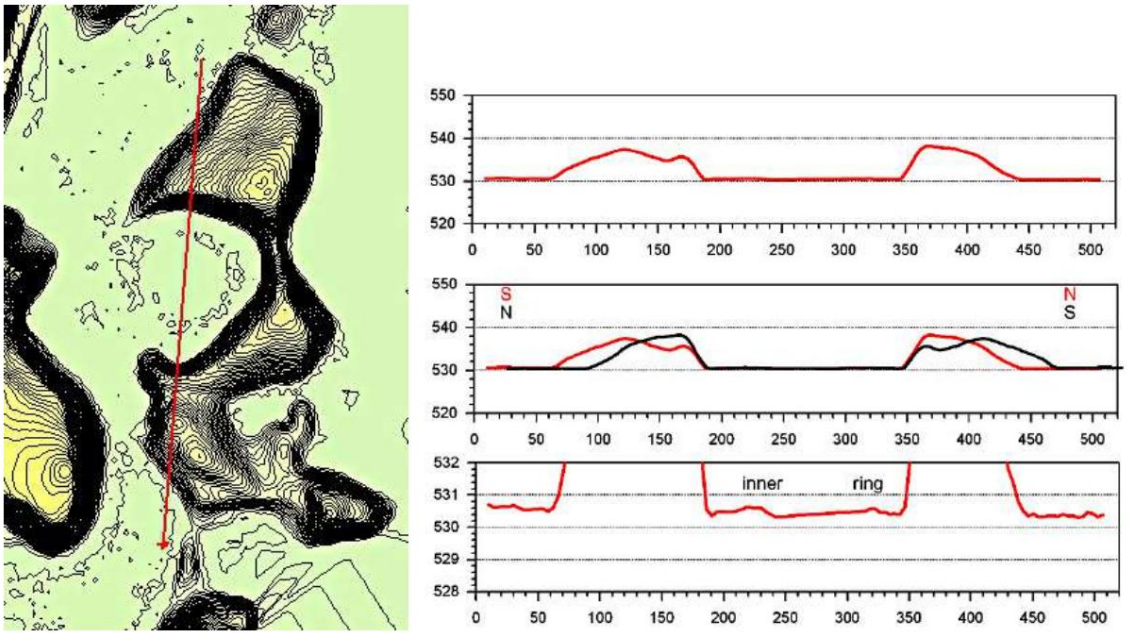

Fig. 36. Lake Schernsee in the DGM 1, topographic map and mirrored profile. The inner ring marks the lakeshore. The structure of Lake Schernsee will be discussed later.

3.7 Stettner See

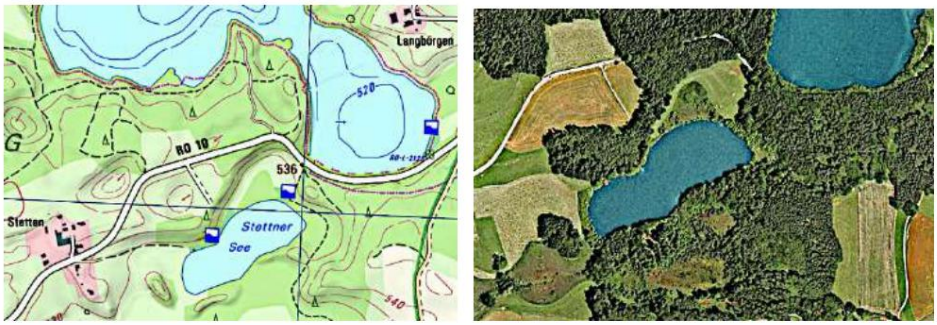

Fig. 37. Lake Stettner south of Lake Langbürgner; BayernAtlas and Google Earth. A detailed discussion will follow later.

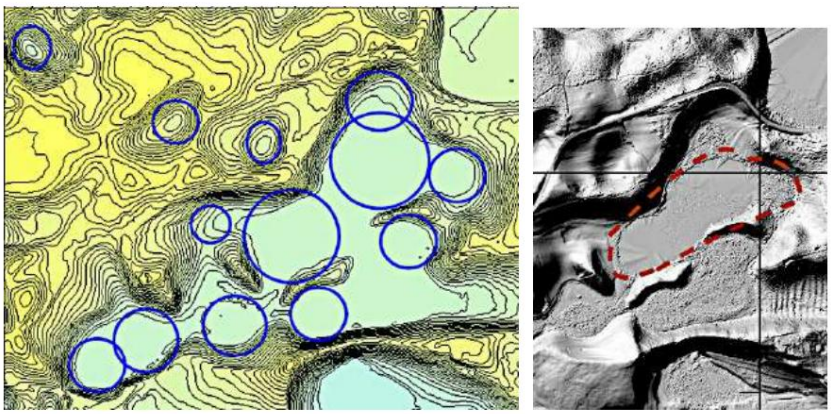

Fig. 38. DGM 1 topography and present-day lake (Fig. 37), traced in the shaded relief of DGM 1 (right). The morphological structure caused by the impact, which evidently left behind a whole cluster of separate impacts (image left), is considerably larger.

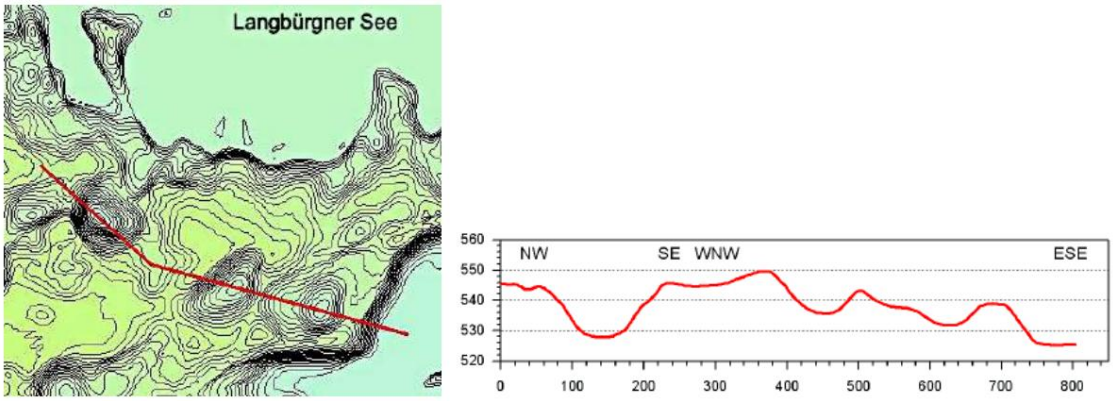

Fig. 39. Smaller accompanying craters from the Stettner See impact, all of which have a ring wall.

3.8 Liensee and neighboring structures

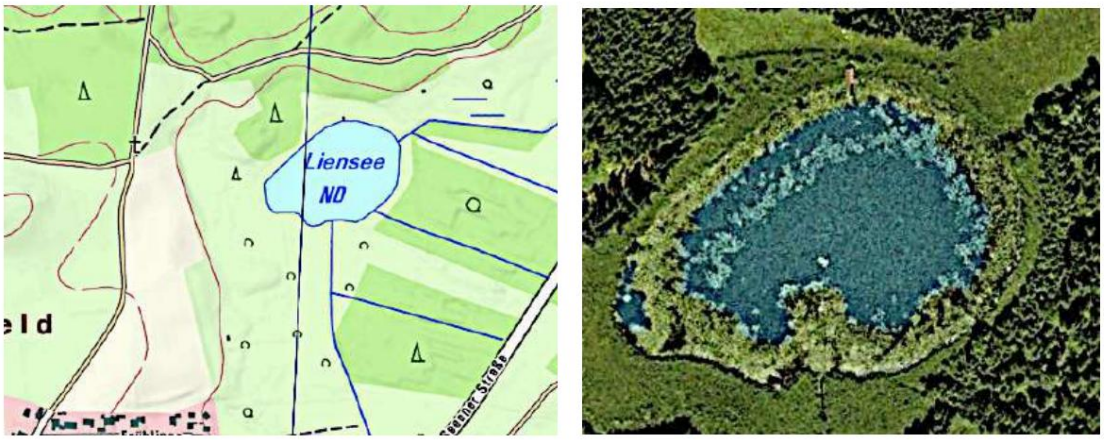

Fig. 41. The Liensee impact, BayernAtlas and Google Earth. The bright ring parallel to the
The lakeshore is defined as plant growth on a slope extending almost to the water's surface.
interpreted as an inner crater ring.

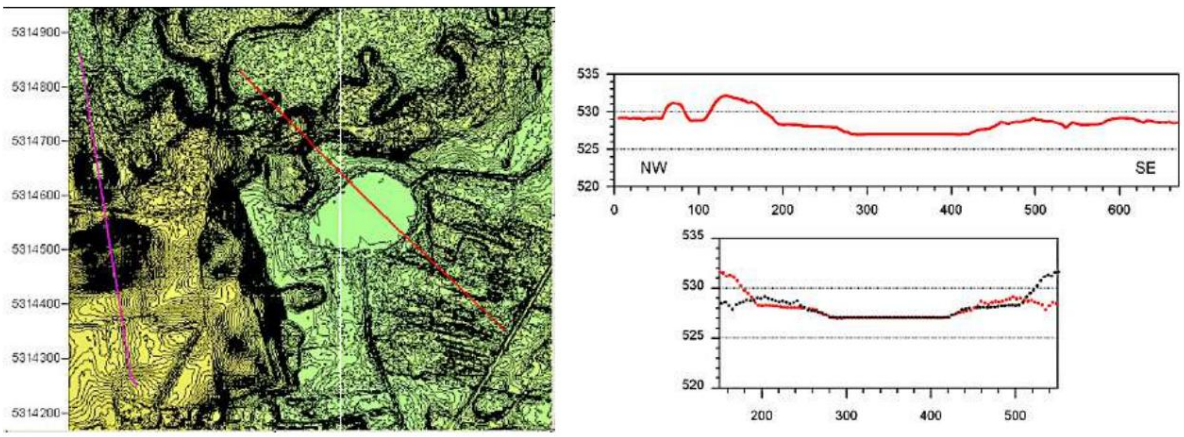

Fig. 41. The Liensee crater and accompanying structures to the west (crater and large hill).
Right: DGM 1 profile through the crater with an outer and an inner rim (around the lake).

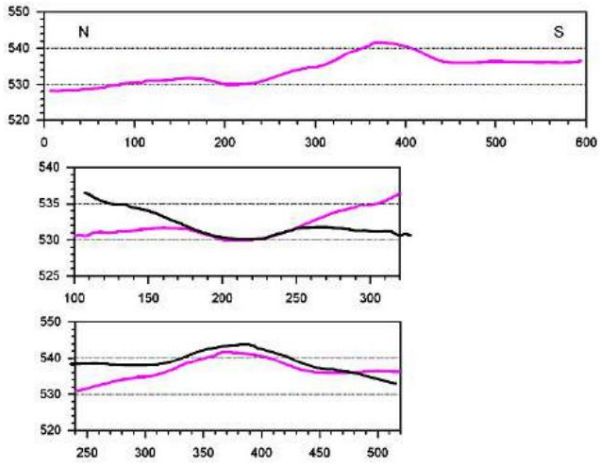

Fig. 42. DGM 1 profile over the 150 m wide and 10 m high hump. Below: The

Symmetrically mirrored profiles over craters and humps.

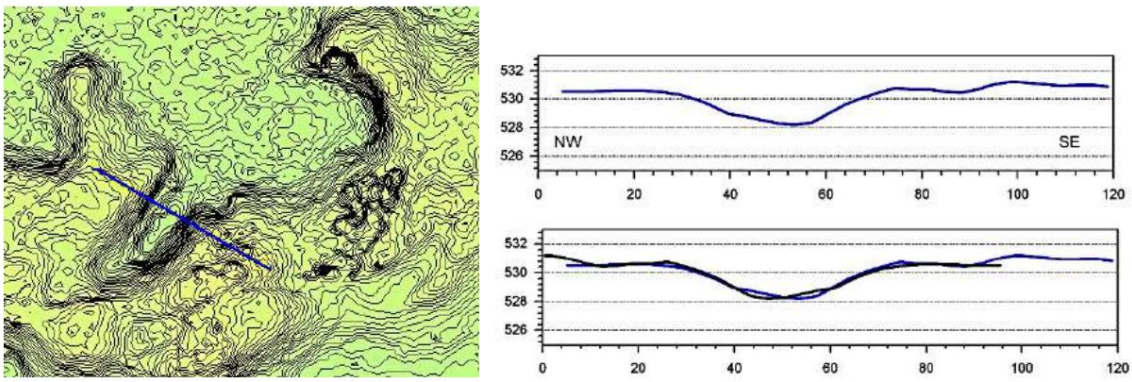

Fig. 43. The north-facing, walled crater with RTI finger structure north of Liensee (location Fig. 41). In profile, the rim and trough margin are strictly symmetrical.

3.9 Hofsee - Katzensee

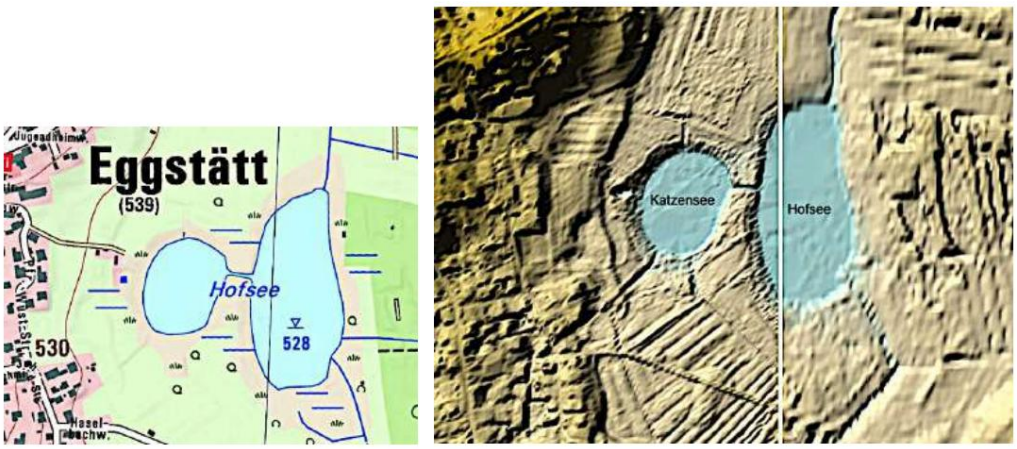

Fig. 44. An apparently related pair of craters on the eastern edge of Eggstätt. In the DGM 1 surface map, the ridge patterns are unrelated to the impact. They are likely so-called ridge and furrow fields, a special form of plowing from the early Middle Ages to possibly back to the Bronze Age, which is discussed in the section on dating.

will be discussed in detail.

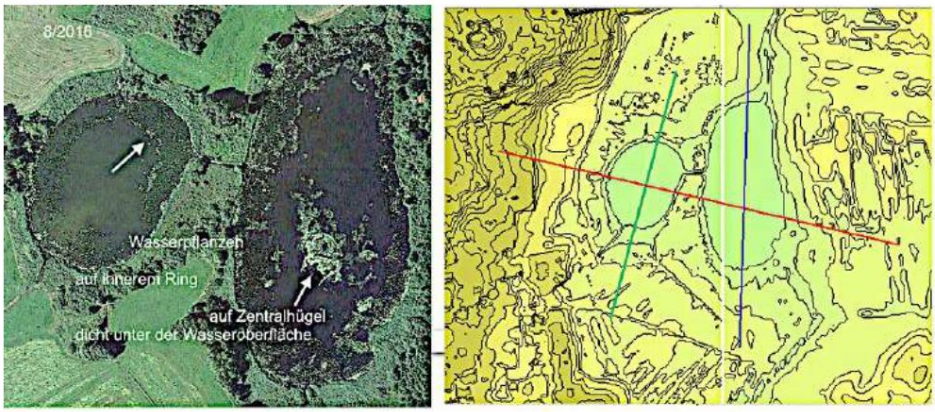

Fig. 45. Google Earth and DEM 1 topographic map. The colored inner and central rings (at Hofsee) are interpreted as reflective aquatic plant growth on rock outcrops extending close to the water's surface. The DEM 1 profiles can be found in Figs. 46-48.

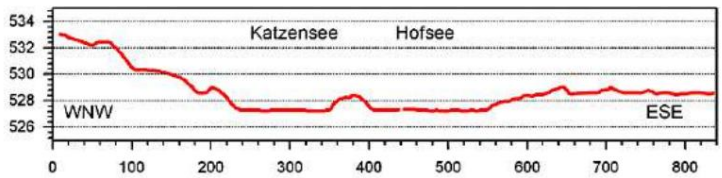

Fig. 46. DGM 1 profile across both lakes. The wavy edges could be an expression of Kelvin-Helmholtz instabilities.

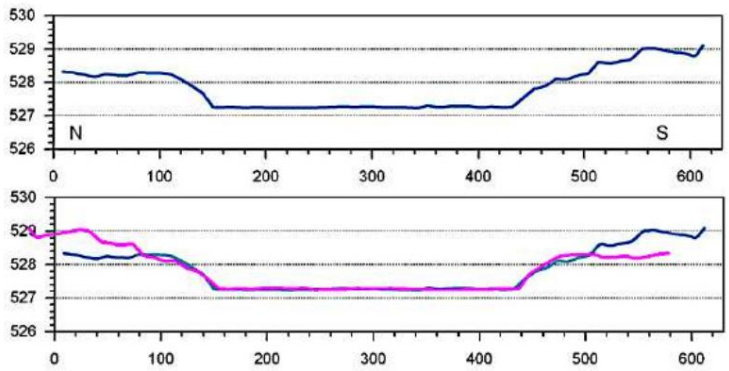

Fig. 47. Longitudinal profile of the Hofsee with mirror-symmetrical crater rims.

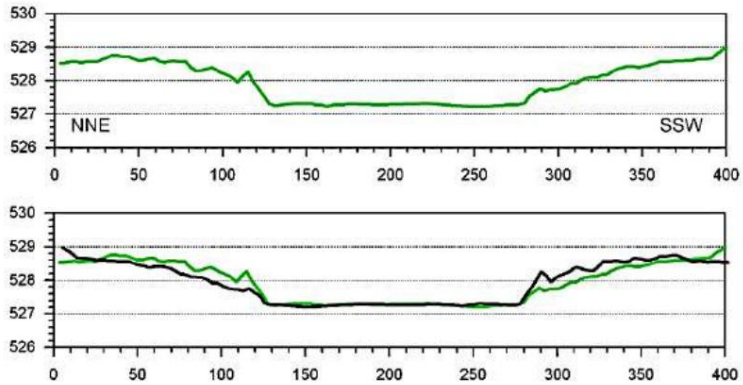

Fig. 48. Longitudinal profile across Lake Katzensee with mirror-symmetrical crater rims

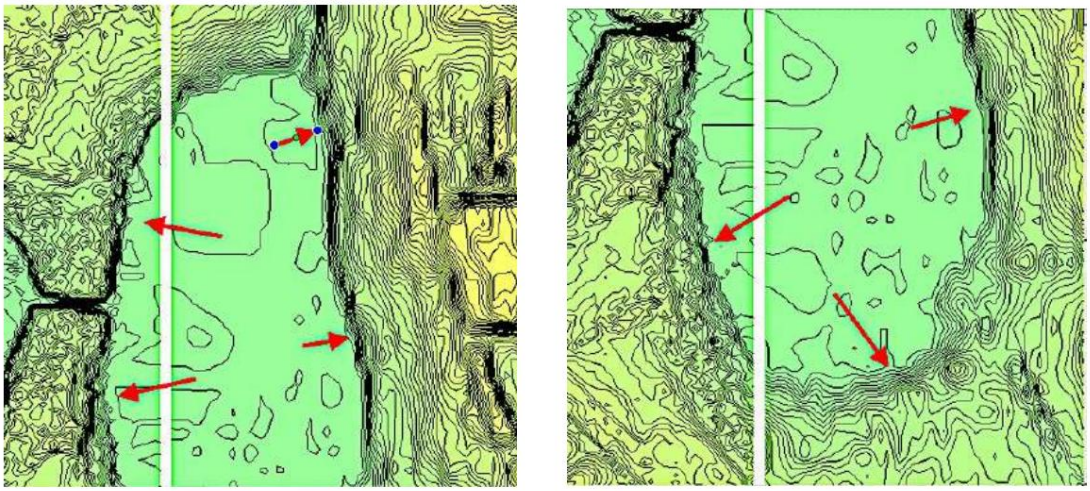

Fig. 49. Hofsee: Periodic block formations in the crater rim according to RTI. The impact direction could be documented in the tile-like offsets. A superposition with the impact-modified ridge and furrow structures (Fig. xy), especially on the western shore, which will be discussed later, is conceivable.

3.10 Laubensee

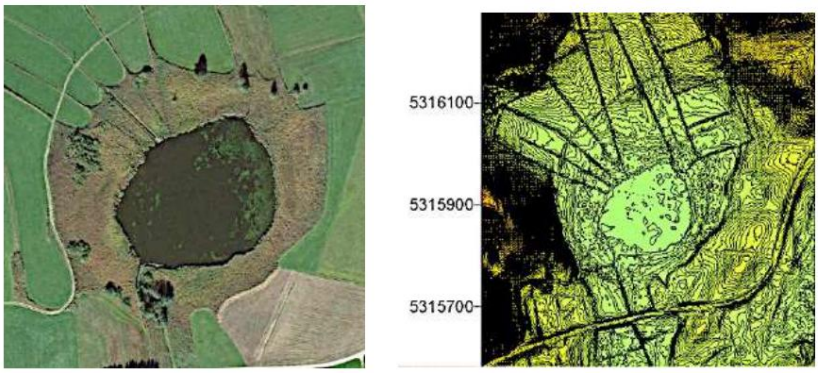

Fig. 50. Lake Laubensee, located just outside the main lake district, Google Earth and DGM 1 topographic contour map. The lake, almost 200 m in diameter, has a maximum depth of only 2 m.

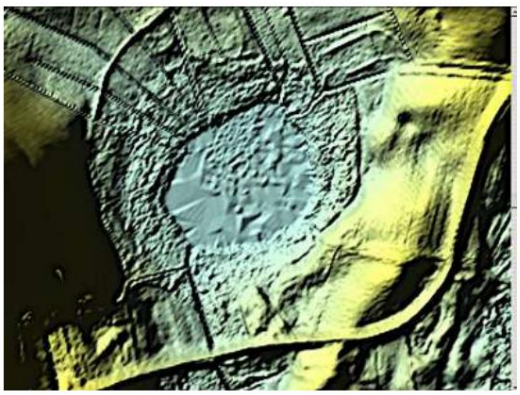

Fig. 51. DGM 1 3D: View to the NW. Block-shaped and wave-like terrace formations according to RTI and KHI. More on this in Fig. 56. An overprinting of pre-impact ridge-and-furrow structures (weakly developed at the right crater rim) is indicated, which will be discussed later in section 6 (Dating).

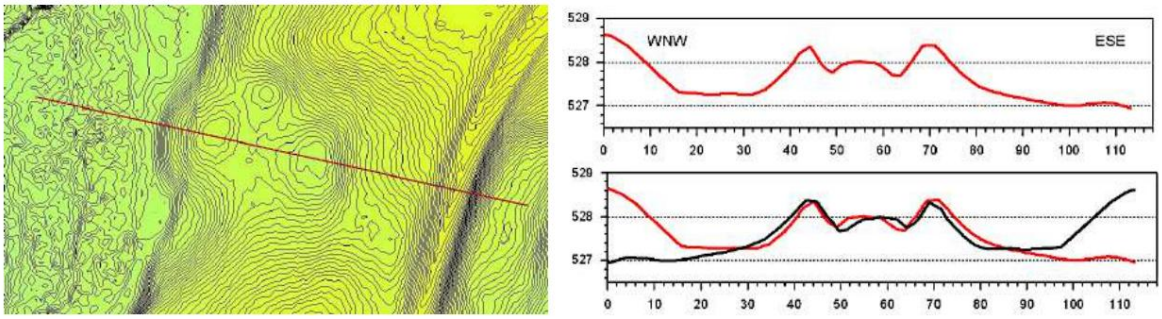

Fig. 52. DGM 1 profile of the northeastern small complex secondary crater.

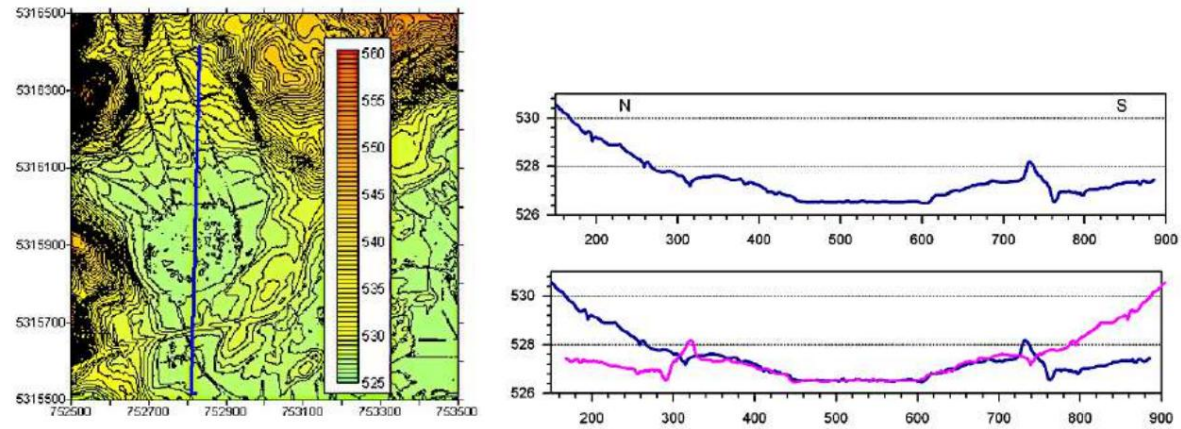

Fig. 53. DGM 1. The impact structure, which extends considerably beyond the lake and is elliptically elongated to the NE (Fig. 50 right), has an inner and an outer marginal ridge.
Plant growth could mark an inner ring parallel to the edge. The mirror symmetry, with deviations of only decimeters over a profile length of approximately 400 m, is remarkable.

3.11 Eschenauer See

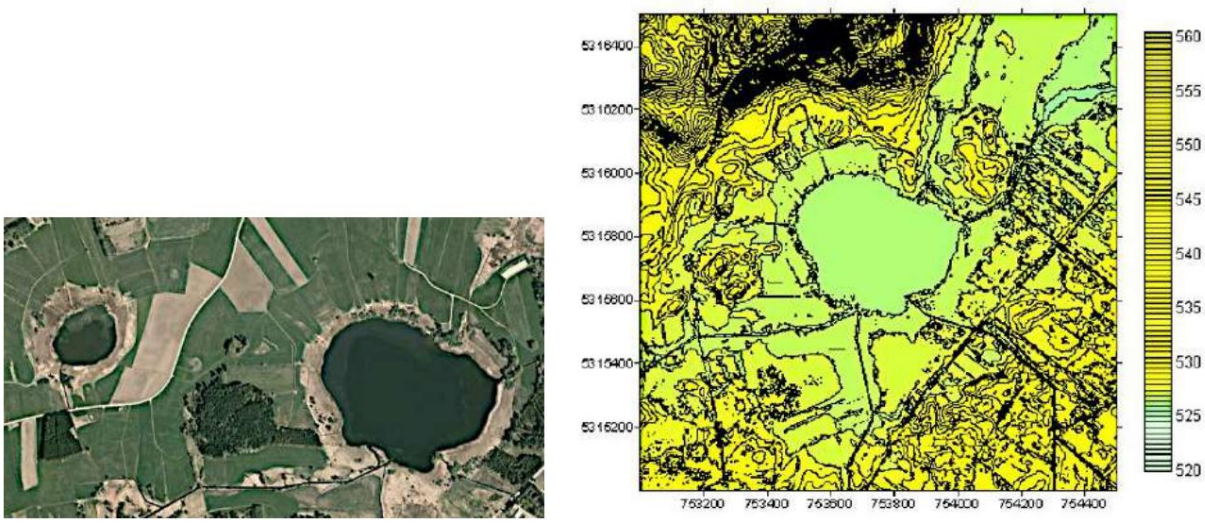

Fig. 54. The Eschenauer See east of the Laubensee; Google Earth and DGM 1, contour line spacing 50 cm.

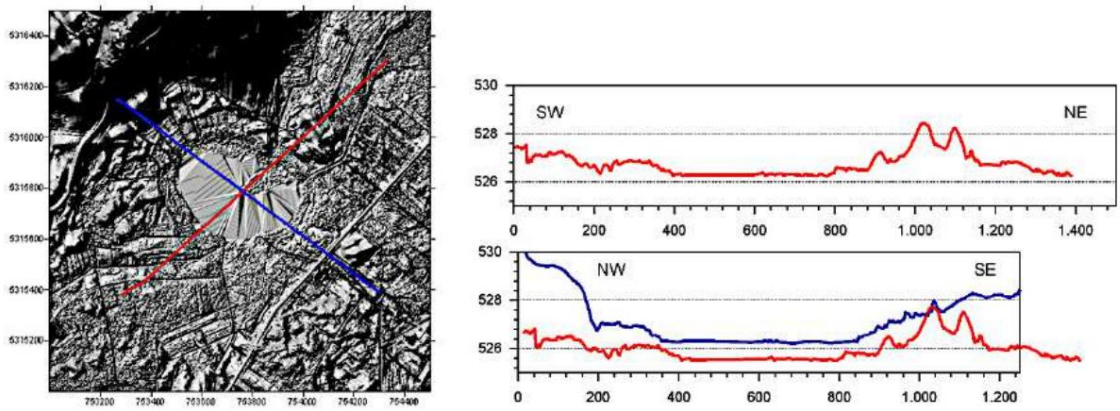

Fig. 55. DGM 1 shaded relief with profiles marking an outer embankment and an inner embankment (around the lake). The significantly elliptical structure has a remarkably almost identical outline when comparing the longitudinal and transverse profiles.

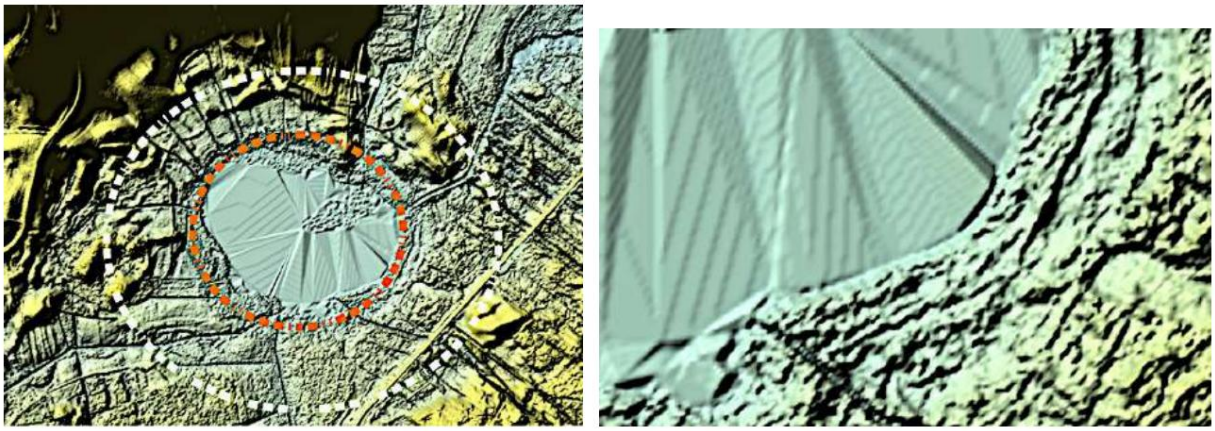

Fig. 56. Red: inner crater rim with undulating terrace formation (image right). White: block formation in the outer crater rim. Evidence of RT and KH instabilities.

4 Ejecta - Rayleigh-Taylor and Kelvin-Helmholtz instability Structures

Unlike conventional impacts with a simple bowl-shaped crater or complex structures surrounded by more or less geometrically simple ejecta, "touchdown" airburst impacts, with their typically very shallow crater scatter fields, can leave behind highly complex landforms. This is especially true for impacts into unconsolidated sedimentary sequences, where the RT and KH instabilities described earlier result in geometrically diverse structures both internally and externally.

can lead to this.

This appears to be almost entirely exemplified in the case of the impact lake district.

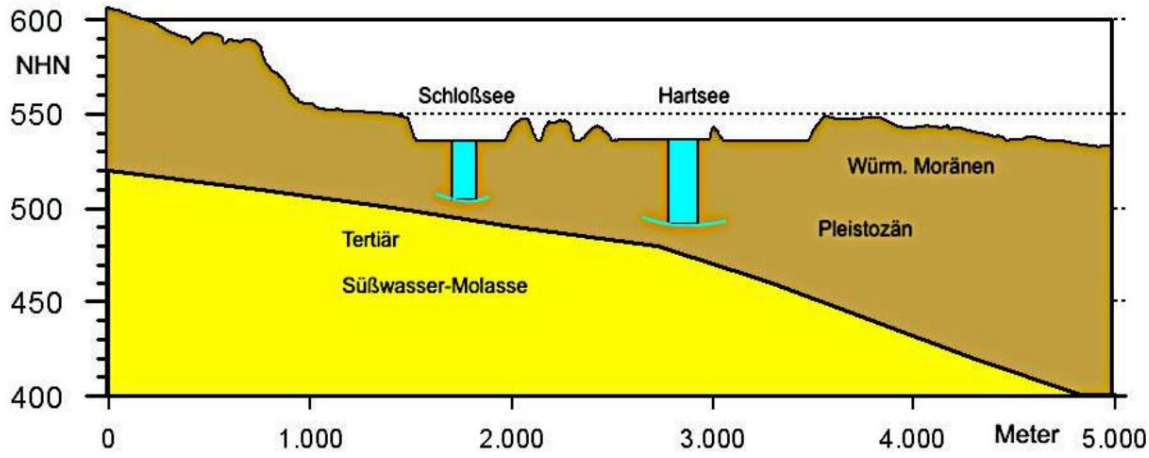

Fig. 57. Schematic geological section from Fig. 4 showing the maximum water depths of
Schlosssee and Hartsee. The values 10-20 m above the Tertiary top edge must not be considered
representative of the current impact investigation area, since the few and
widely spaced deep boreholes used to create the map in Fig. 4 may be locally higher.
Allow sufficient molasse. This could be useful for interpreting the DGM 1 maps and profiles.
This means that blocks and slabs occurring in a wide area, with high morphological resolution, are found in the
Marginal areas of the crater lakes and in the mushroom diapirs made of molasse bedrock such as
It consists of clay marls and calcareous marls, sometimes alternating with molasse sands and gravels.
In many cases, however, it can be assumed that pre-impact geometrically regular, partly self-contained
Intersecting ridge and furrow structures formed by the airburst explosion cloud, with the involvement of
RT and KH instabilities were jumbled together and could only be seen as block patterns.
It is evident that this will be explained later (dating).

4.1 Castle Lake

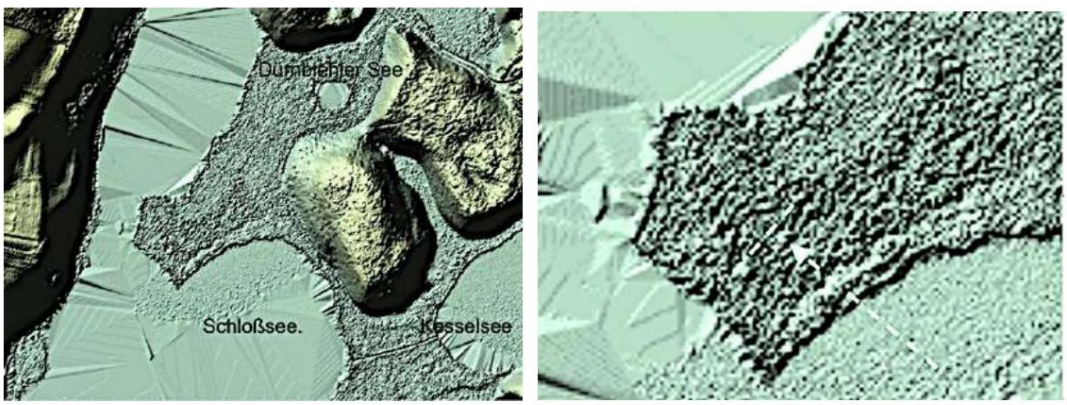

Fig. 58. Marginal areas of Schloßsee, Kesselsee and Dürnbiehler See in DGM 1. The terrain is covered by a relatively homogeneous, dense carpet of small, angular boulders, which is further analyzed in the following figures.

The wave pattern with SW-NE sweep could indicate ejecta transport from SE (arrow), although the block illumination from NW has an intensifying effect. However, the waves could also be a destroyed remnant of the previously mentioned ridge and furrow fields (Fig. 57).

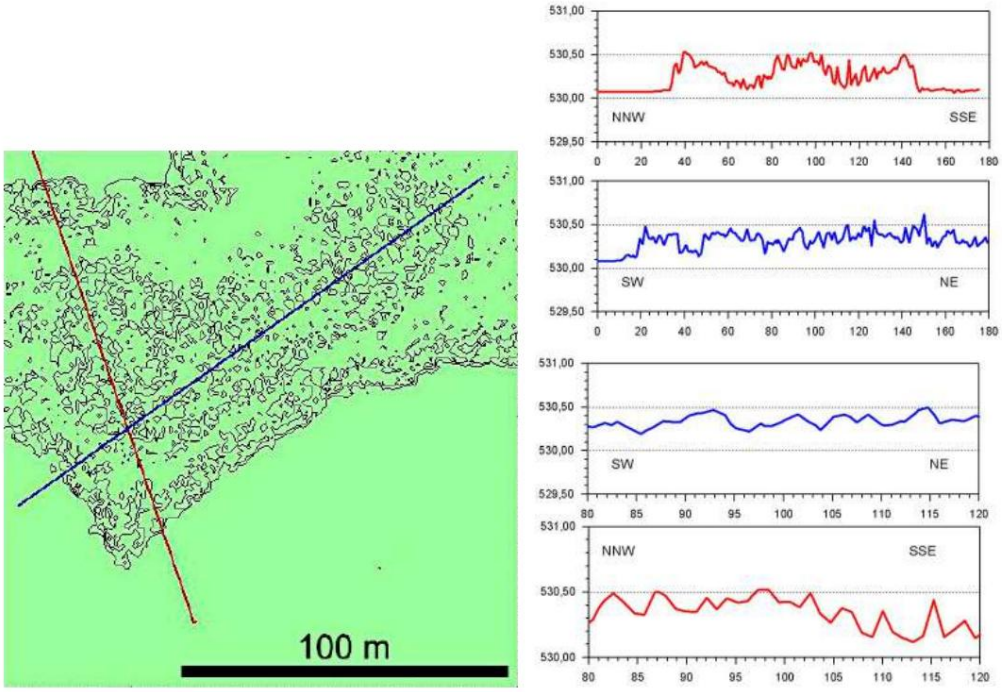

Fig. 59. Section of the DGM 1 as an isoline map of the northern edge of the castle lake with two Intersecting elevation profiles. A zonation parallel to the lake rim is noticeable. The elevation profiles show long- and short-period fragmentation, differing in orientation, which could correspond to the undulating nature in Fig. 58. The periods are roughly 50 m (red, faintly in blue) and 3–5 m (red and blue, sectioned profiles). This coarse, blocky blanket around the crater lakes, which can also be observed in many other craters, supports the assumption that the impact excavation partially reached down into the Molasse and ejected and/or uplifted larger components of the bedrock, or alternatively, that pre-existing ridge-and-furrow structures were overprinted, which is more likely in Fig. 60.

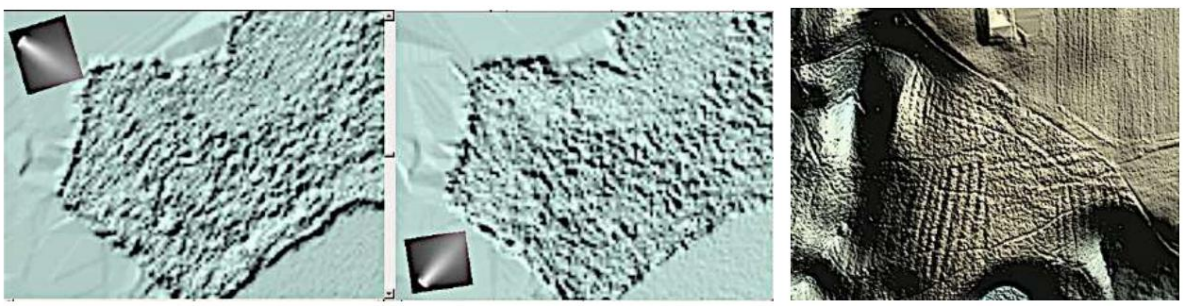

Fig. 60. The 3D digital terrain model (DTM) of Fig. 59, viewed under different lighting conditions, suggests that the block pattern represents a ridge ridge completely destroyed by the airburst. A better-preserved ridge ridge with intersecting tracks near Lake Langbürgner (image on the right) supports this.

4.2 Kesselsee South

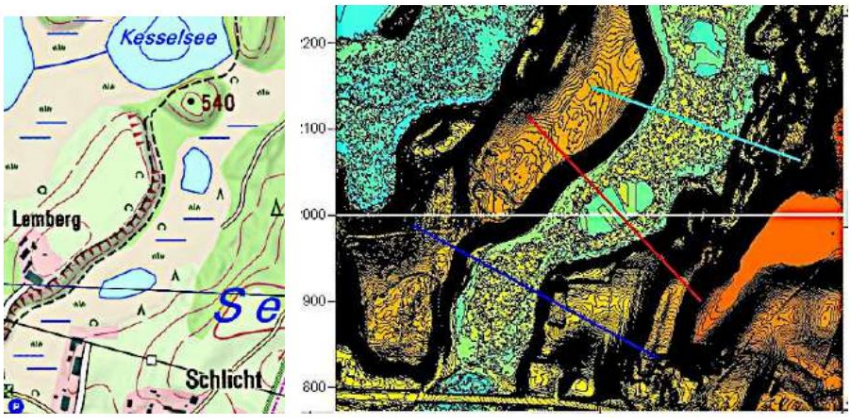

Fig. 61. Impact chain south of Kessel Lake with profiles on the DGM 1 contour map.

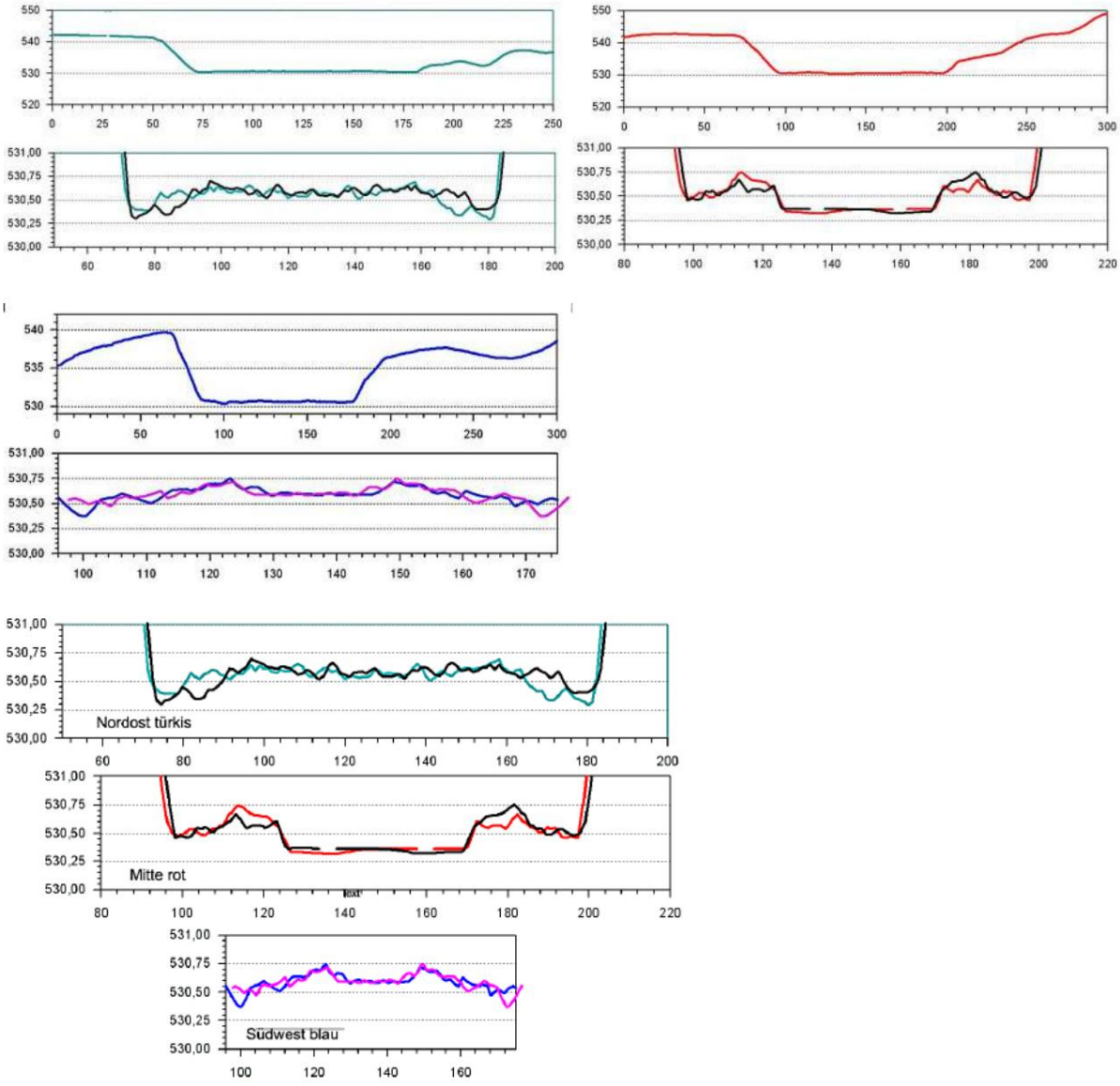

Fig. 62. The DGM 1 profiles from Fig. 61 with the superimposition of the respective mirror-symmetric profiles.

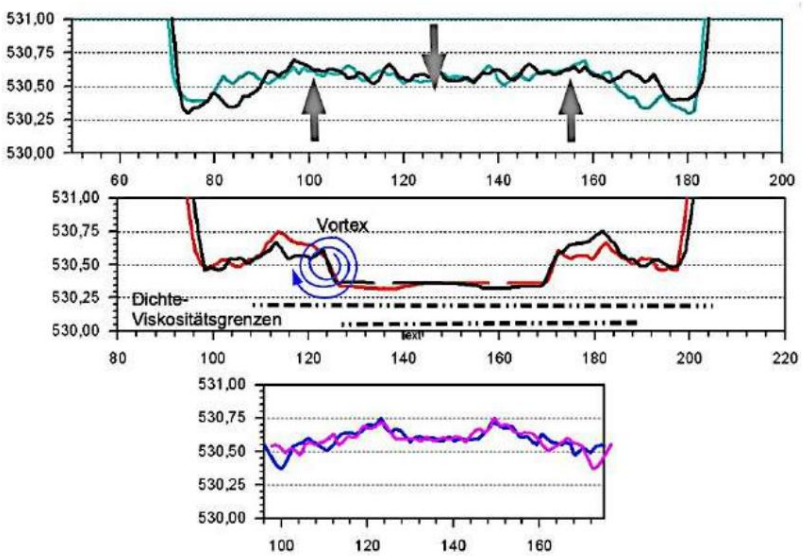

Fig. 63. Simple Rayleigh-Taylor instability models for the three DGM 1 profiles. The RTI cases discussed in the literature usually deal with two-dimensional, 2-density cases.

In the case of the impact presented here as pressure from above, it is particularly important to consider, apart from the 3D case, that we are dealing with multilayer systems of varying densities and viscosities, which also differ lithostructurally from place to place. This is impressively demonstrated here by the three lined-up impact structures with their differently shaped internal ring structures, which, however, suggest a very similar formation process, which we attribute here to effective RTI. As with the Schloßsee, the small-scale block formation here is probably not ejecta material from the depths, but rather a relic of airburst-shattered and moved RT and KH instabilities (Fig. 60).

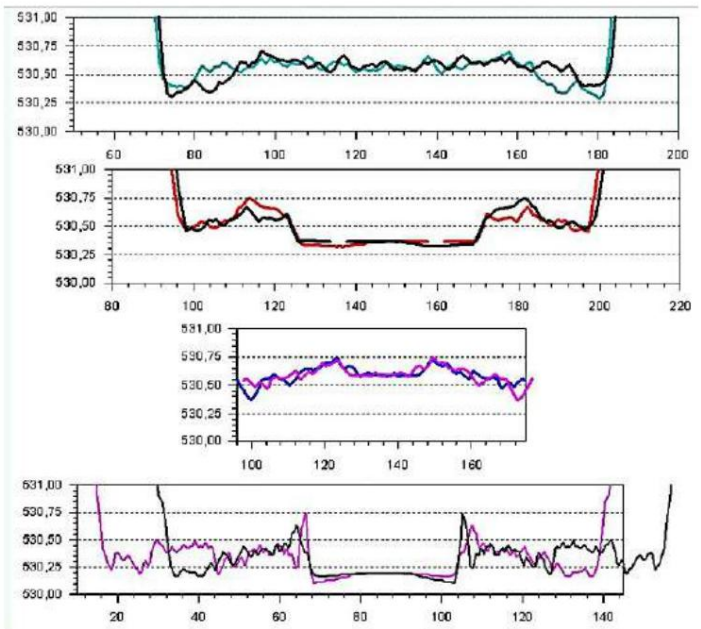

Fig. 64. In addition to the three southern Kesselsee profiles, a profile of the inner Kesselsee is shown below.

The Dürnbiehler See craters (4.3) are attached. It shows that in the lake district, the same physical processes lead to structurally similar, very complex shape symmetries in distant objects.

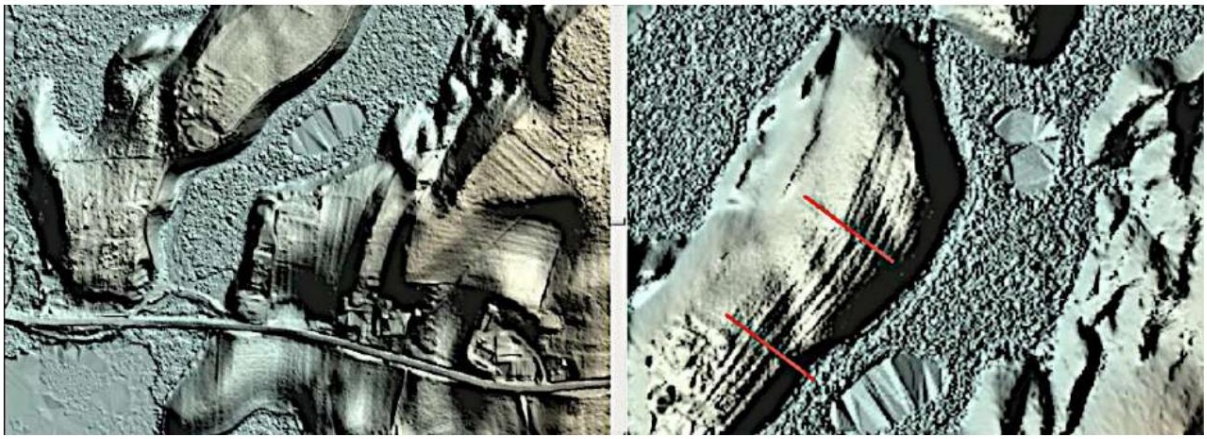

Fig. 65. DGM 1: 3D of sections of the Kesselsee South structure. The ridge and furrow fields on both sides. The structure, like that of the castle lake, suggests that the accompanying block pattern is a relic of destroyed ridge and furrow fields. Red: old field boundaries.

4.3 Dürnbiehler See

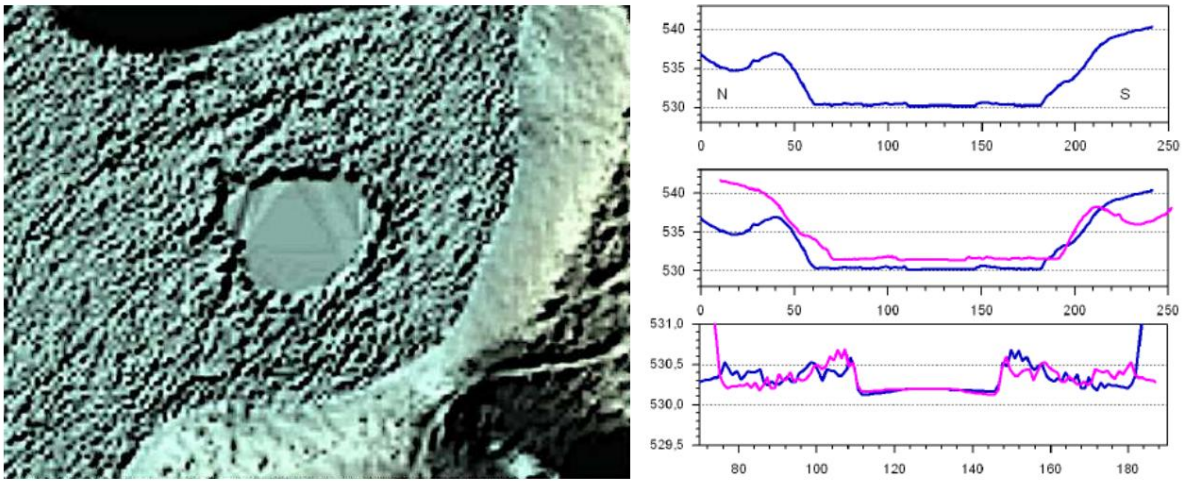

Fig. 66. DTM 1, 3D terrain and north-south profile. The internal structure shows a superposition of RTI and KHI structures. A ring of blocks and slabs up to roughly 10 m long is grouped around the 40 m diameter lake. This ring appears slightly uplifted along with the lake, which is reflected in the bottom profile on the right as an expression of an incipient RTI mushroom structure. Around the lake, faint rings can be discerned by the block sizes, which can be assigned to a wave pattern corresponding to a KHI.

The varying block sizes in the rings may reflect a layering in the subsoil, although it remains unclear whether the large blocks originate from Quaternary conglomerate slabs or the more solid Tertiary.

4.4 Schernsee

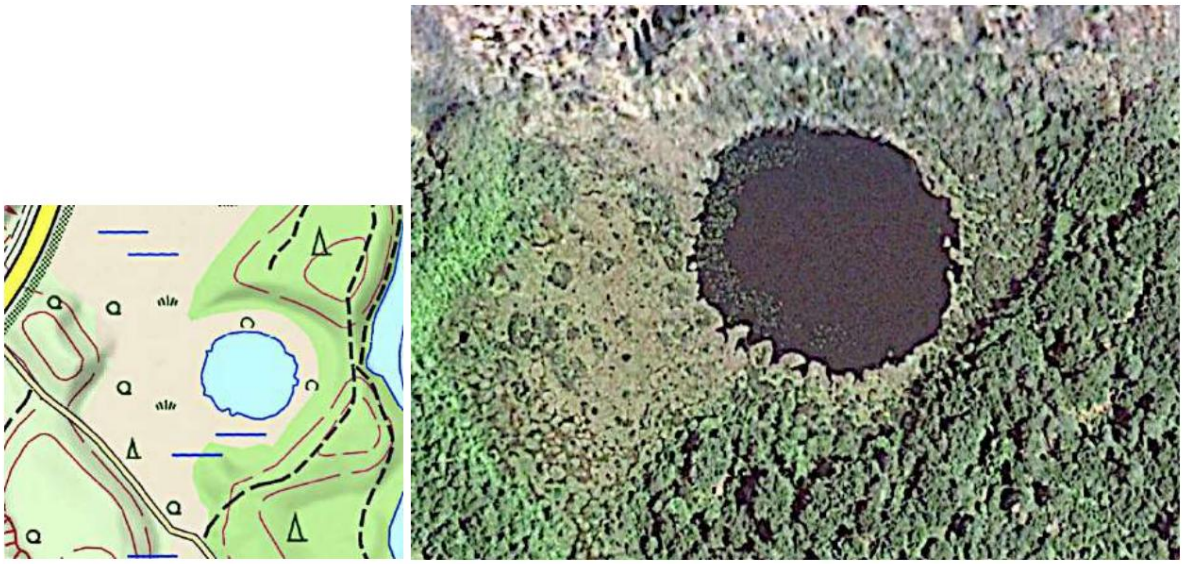

Fig. 67. The almost circular Schernsee lake as seen on the topographic map and in the Google Earth aerial image. The latter reveals the peculiar sawtooth pattern of the shoreline, which will be discussed further below.

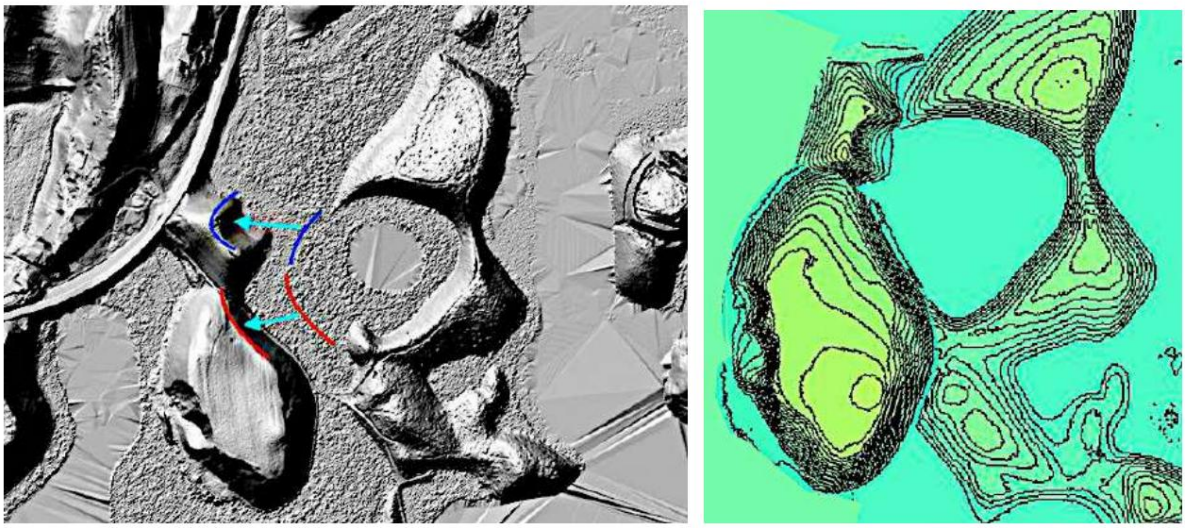

Fig. 68. Digital Terrain Model 1 (DTM 1), shaded relief and 1 m isoline map of the Schernsee crater. Here, the DTM 1 reveals a unique airburst impact process in a temporal sequence of primary crater formation, followed by the immediate disintegration of the previously formed outer ring wall. The DTM 1 images show the sequence of movements and the reconstruction of the primary structure. The accuracy is remarkable, despite some deformations that naturally occurred during transport.

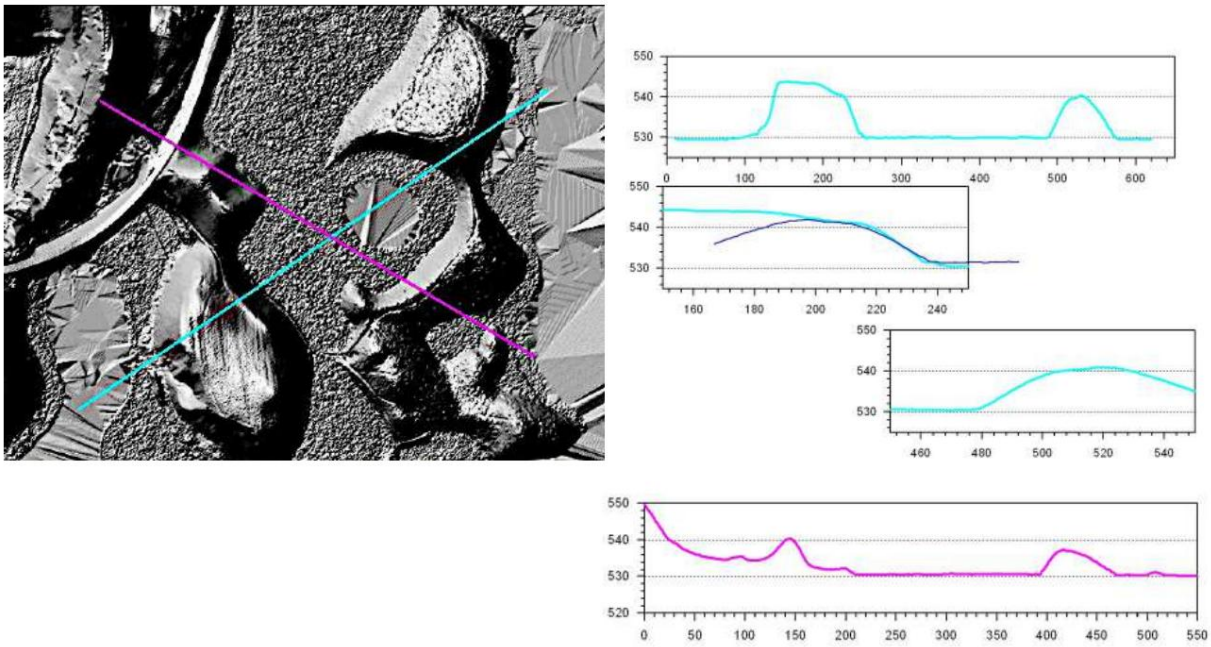

Fig. 69. The extracted DGM 1 profiles also support the reconstruction. The uppermost

The turquoise profile is shown in its full length, from which the turquoise sections of the rampart are derived. The black profile of the northeastern rampart is rotated and superimposed on the southwestern rampart profile. The identical course along the inner rampart edge suggests that the two rampart sections previously formed a single, continuous ring. The pink profile, with its dimensions, also emphasizes an original unity.

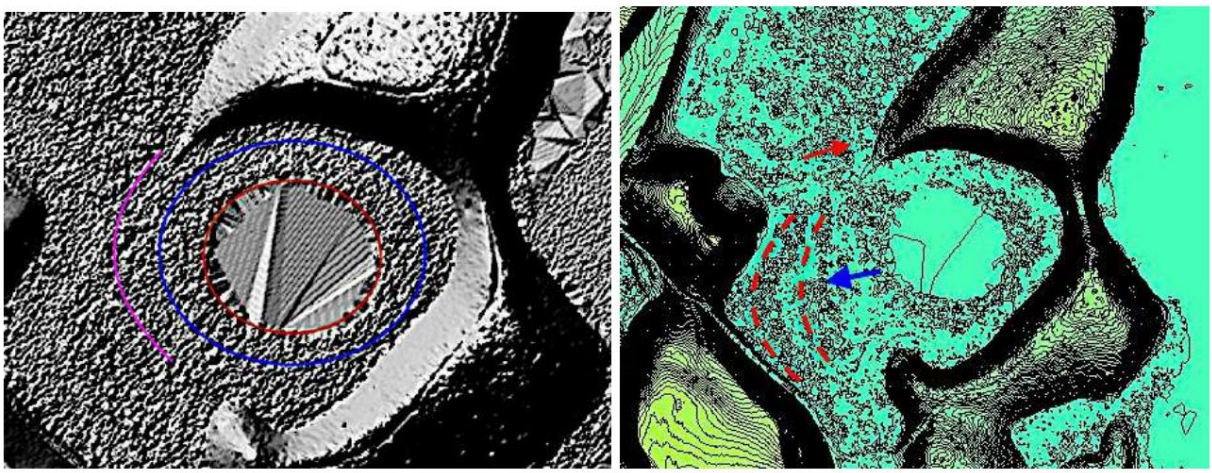

Fig. 70. DGM 1 Detailed structures marking the RT and KH instabilities and movements during the airburst impact. The elements running across the lake without elevation differences are interpolation artifacts of the LiDAR data.

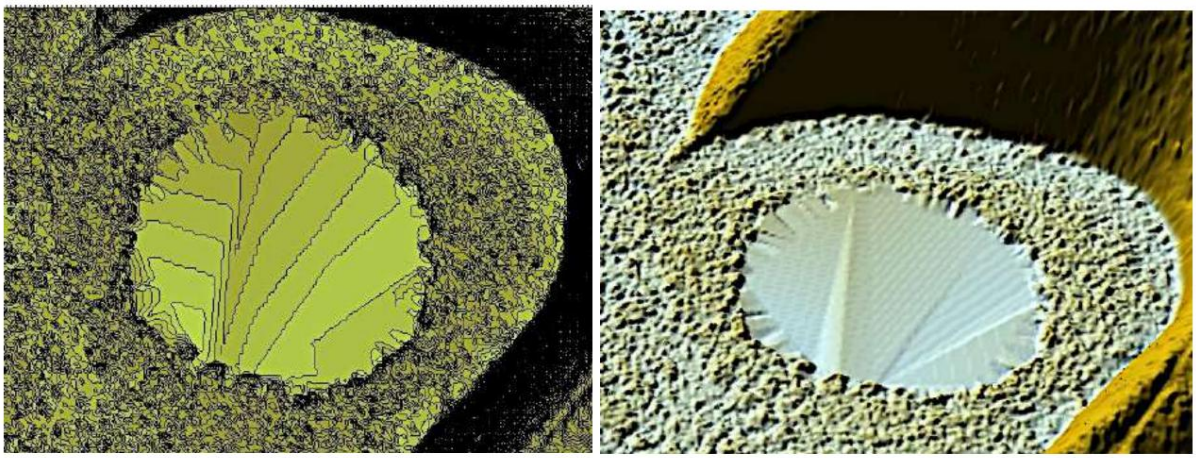

Fig. 71. The Schernsee crater as a DEM 1 topographic map (contour line spacing interpolated 5 cm in an interpolated 50 cm grid) and 3D block image of the terrain surface, slightly oblique view. The sawtooth pattern of the lake rim turns out to be a periodic alignment of approximately equally spaced, roughly equal-sized rock blocks, which almost ideally document a CTI movement structure that originated in a central circular impact.

Stettner See and companions

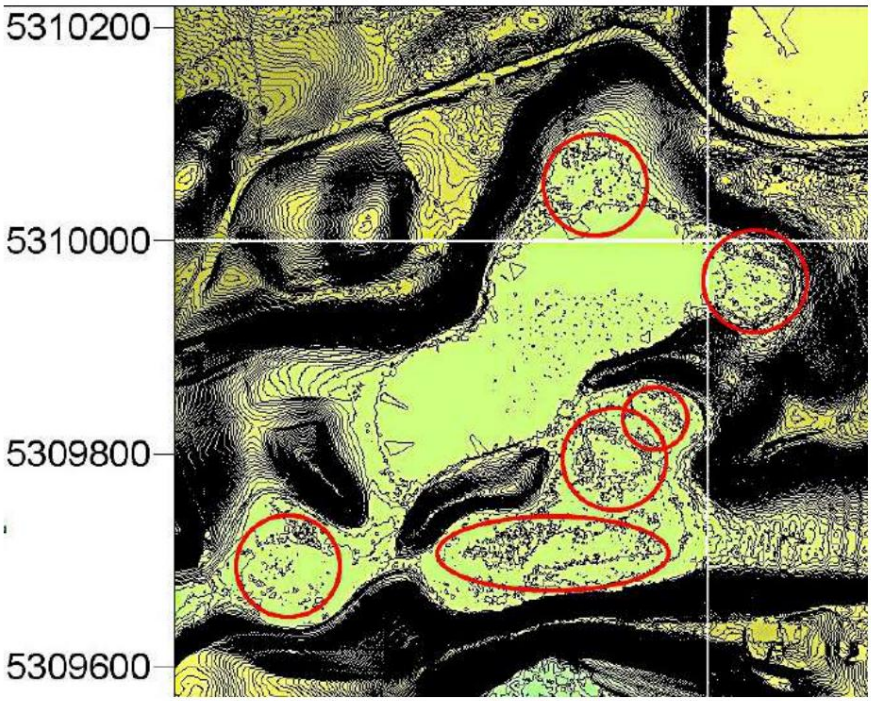

Fig. 72. Lake Stettner and, according to Fig. 38, its much larger impact structure, which is evidently formed by a cluster of several separate impacts. This is particularly evident from the inner rings marked in red, consisting of roughly rim-parallel, apparently upward-moving blocks of rock. The lake itself could also be divided into at least two sections.

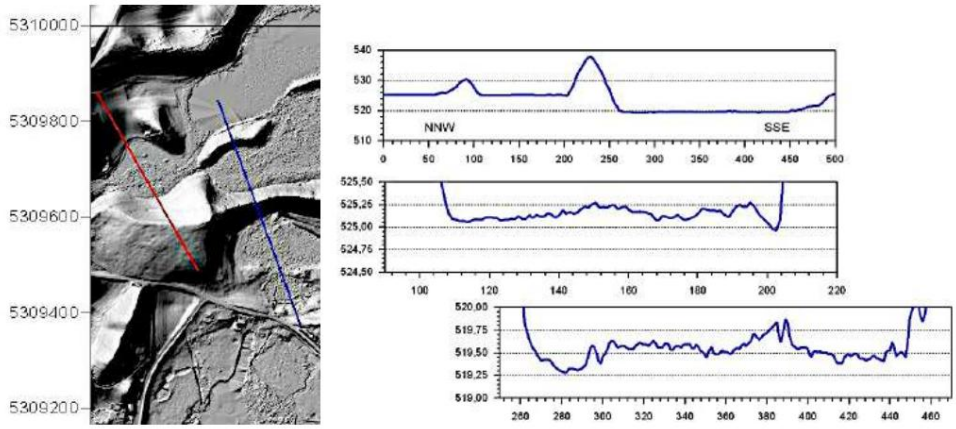

Fig. 73. DGM 1 Profiles over selected associated craters: blue.

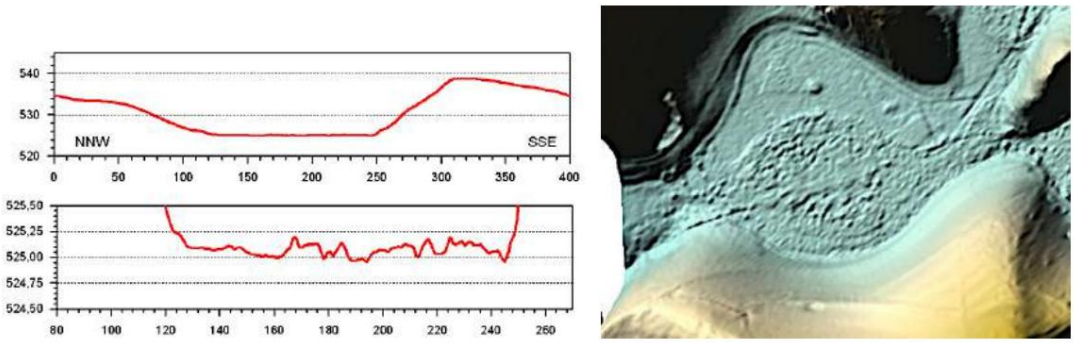

Fig. 74. DGM 1 profile over selected accompanying crater: red, with internal detail structure made of uplifted coarser rock material.

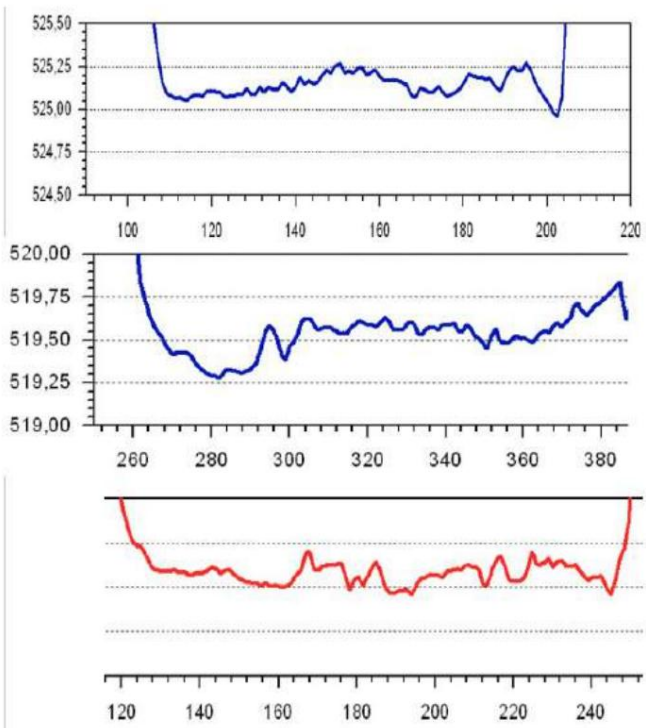

Fig. 75. Strikingly similar internal structures of the three craters with a central emphasis on coarsely sorted blocks, which underlines a synchronous formation during the airburst impact.

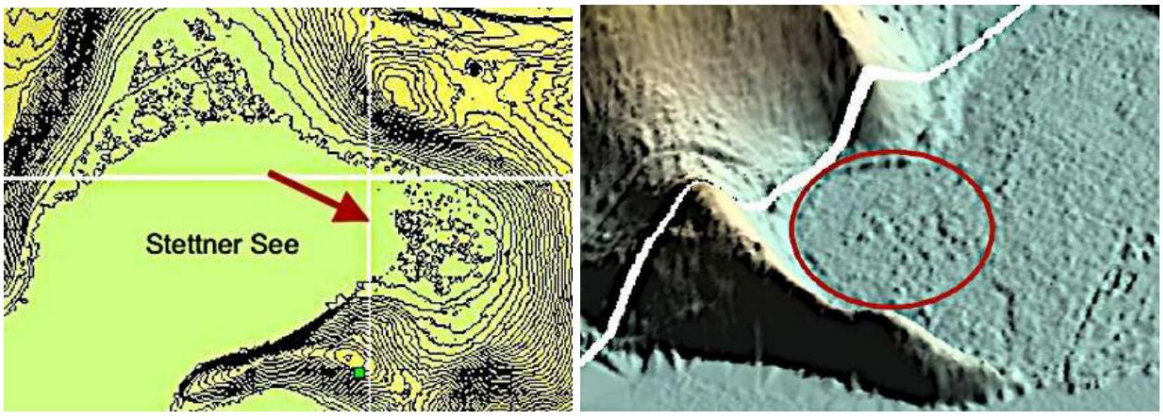

Fig. 76. DGM 1 topographic map and 3D block image, oblique view to the southeast. The circular basin with ring wall and central hummock cluster definitively rules out glacial formations (moraine, kettle hole).

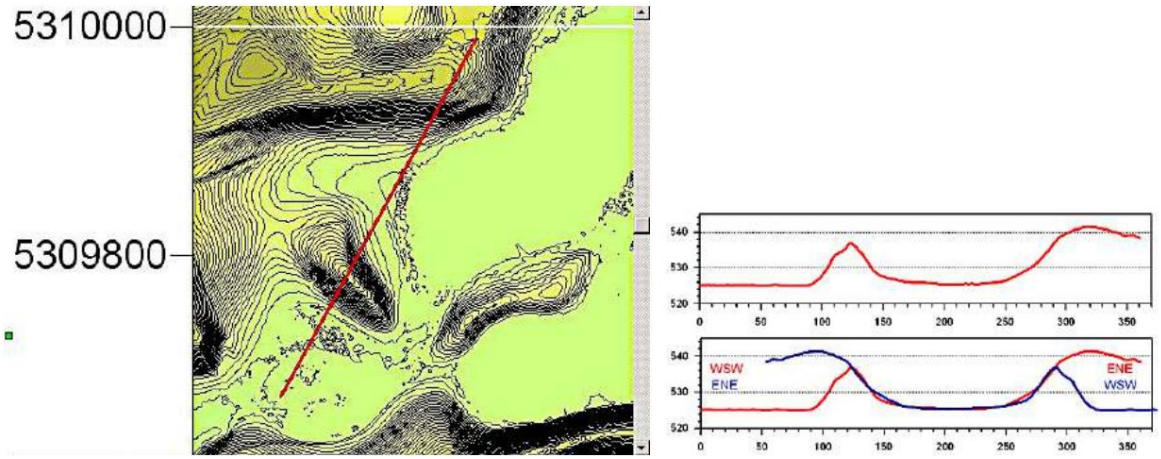

Fig. 77. Also belonging to the Stettner See impact: a marginal finger structure according to the RTI pattern with trace-symmetric border (profiles red - blue).

Eschenauer See

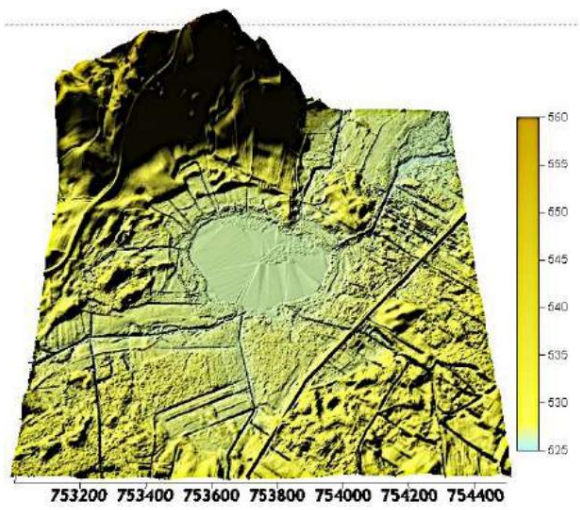

Fig. 78. DGM 1 3 surface. The Eschenau crater lake with a block-like, strongly fragmented outer ring wall according to the RTI model.

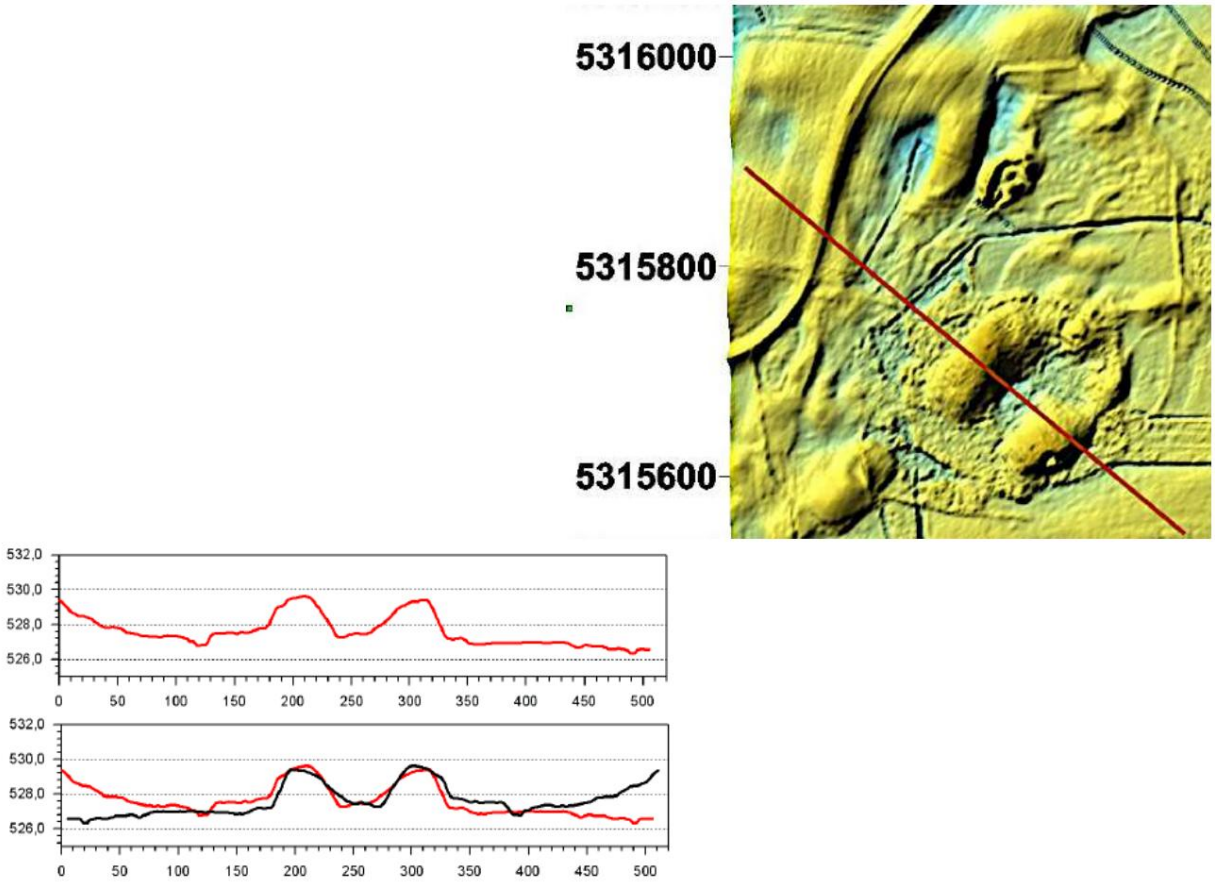

Fig. 79. DGM 1 3D surface, section of Fig. 78. Finger structures with astonishing track symmetry over 300 m; according to RTI in the ring wall (black mirrored from red).

5 Unique Impact Forms in the Lake District

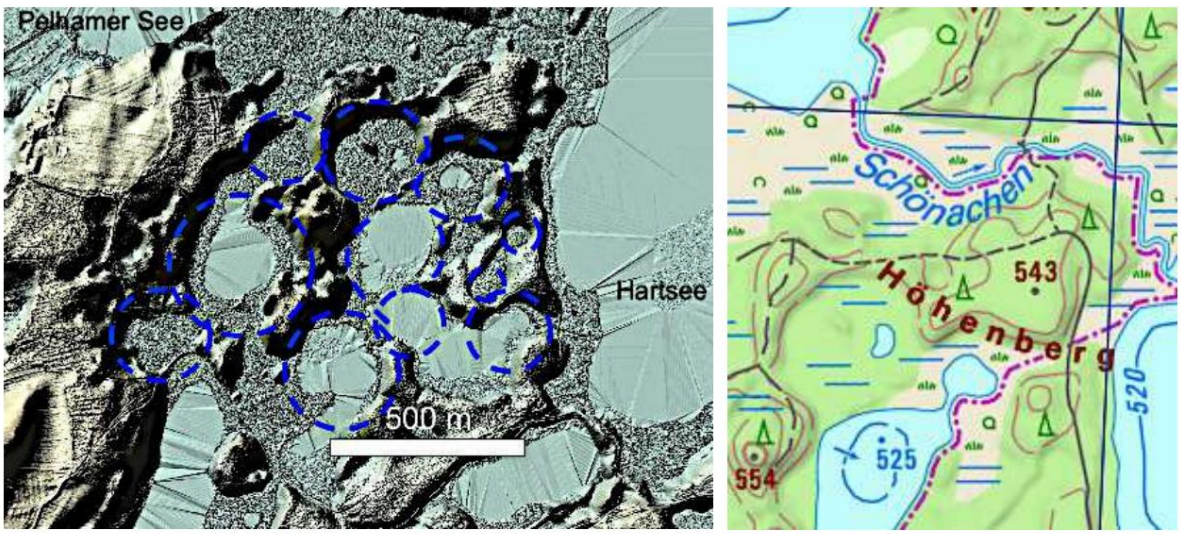

Fig. 80. A cluster of densely grouped impacts between Pelhamer See and Hartsee. Here, too, there is a consistent structural division into an outer, robust ring rim (aligned to form Höhenberg in the north) and inner, partially water-filled, but now mostly silted-up former crater lakes, surrounded by coarse material.

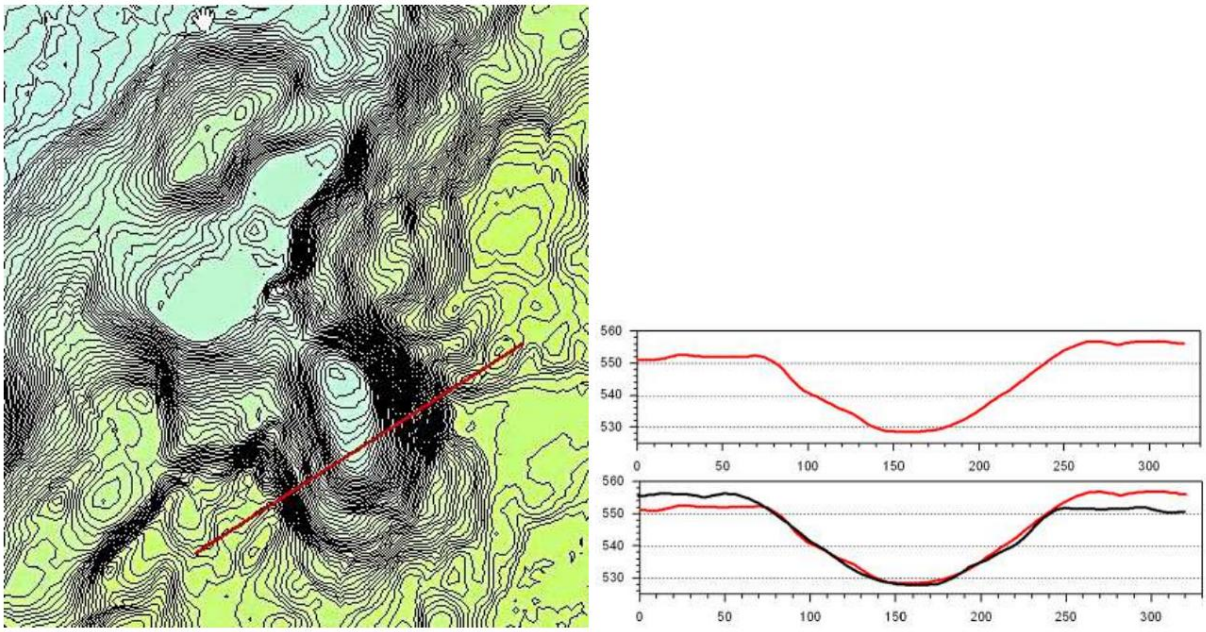

Fig. 81. DGM 1 Topography: Marginal area of the castle lake. Such highly irregular impact zones are common in the lake district, with trace-symmetrical structures like this one being a fundamental part of the morphological inventory.

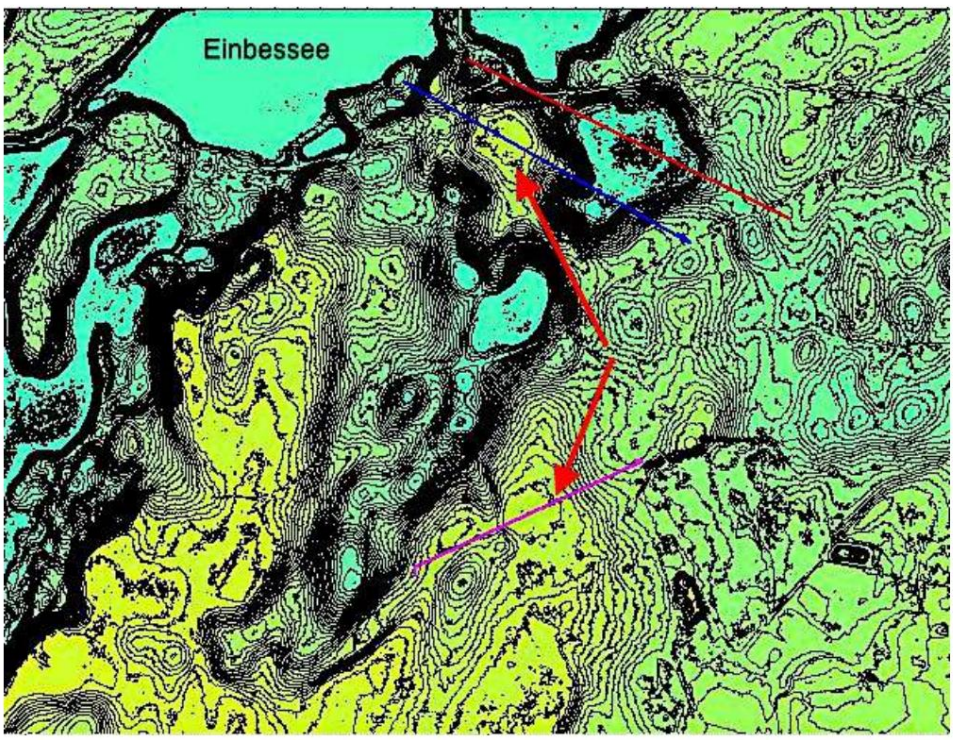

Fig. 82. DGM 1 Topographic map: Impact chain at Einbessee with profiles for the uppermost structure and subsequent profiles for the almost identical hummock structures marked with arrows.

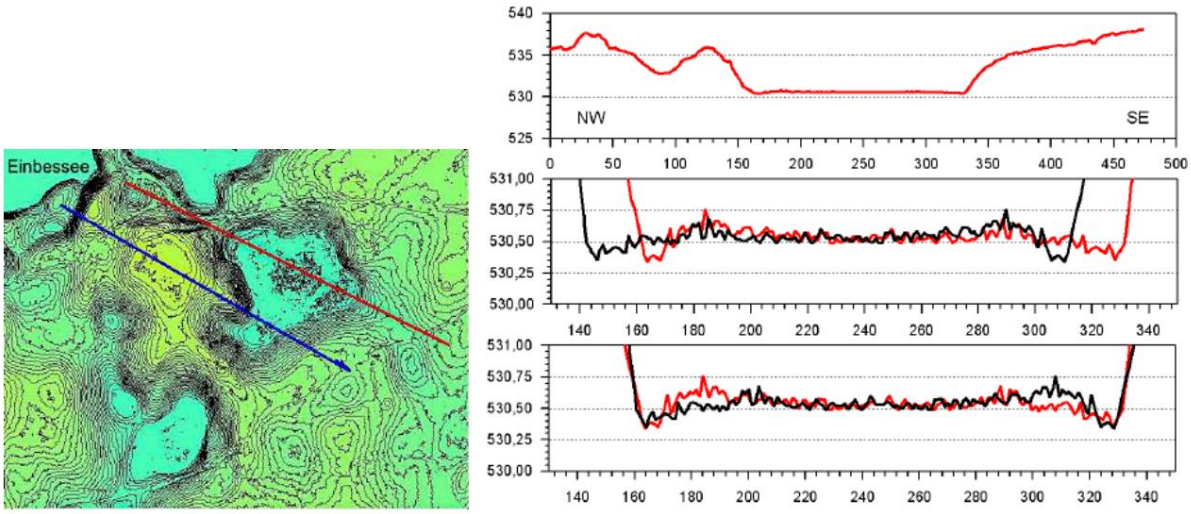

Fig. 83. The uppermost irregular structure with the complex, slight internal bulge made of coarse material. The blue profile is discussed in Fig. 84. The red profile is superimposed with its mirror image and, despite an asymmetrical position of the bulge, shows remarkable accuracy when a 20 m displacement is applied to the edge and center of both images.

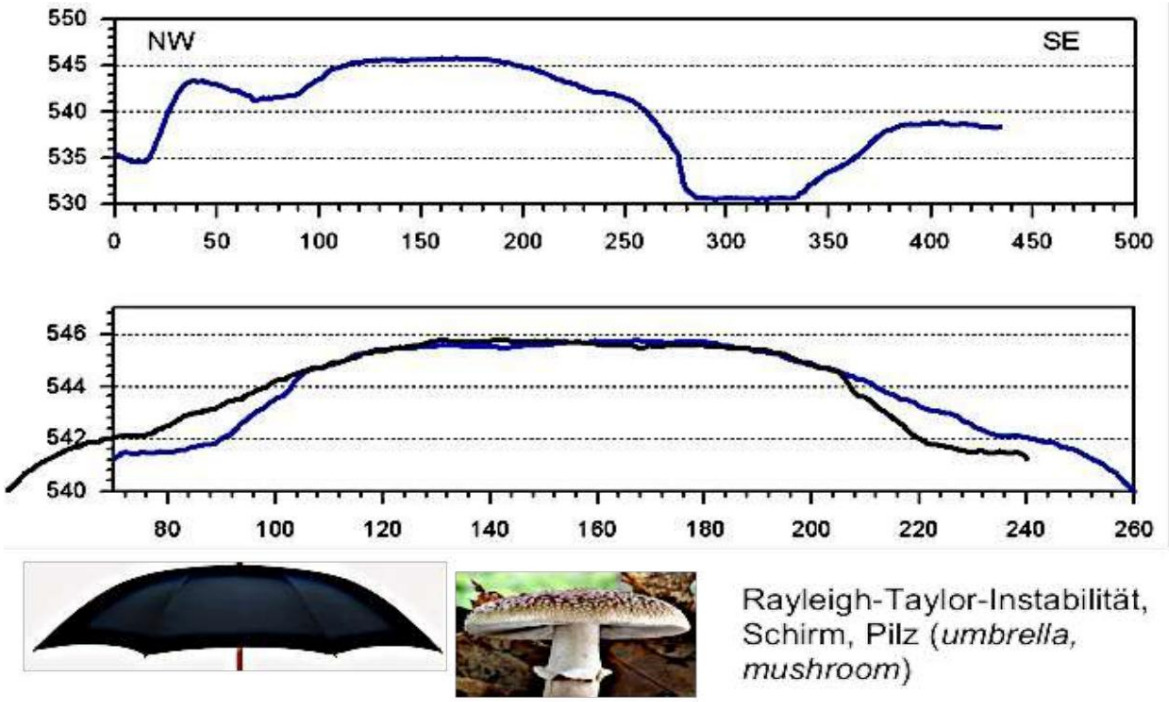

Fig. 84. The blue profile in Figs. 82 and 83 above (mirrored below for the section) is a good example of the umbrella/ mushroom comparisons for RT crater instabilities. The dimensions of the highly exaggerated DTM 1 are of course not transferable to reality, but the characteristic shapes justify the terms used in the literature.

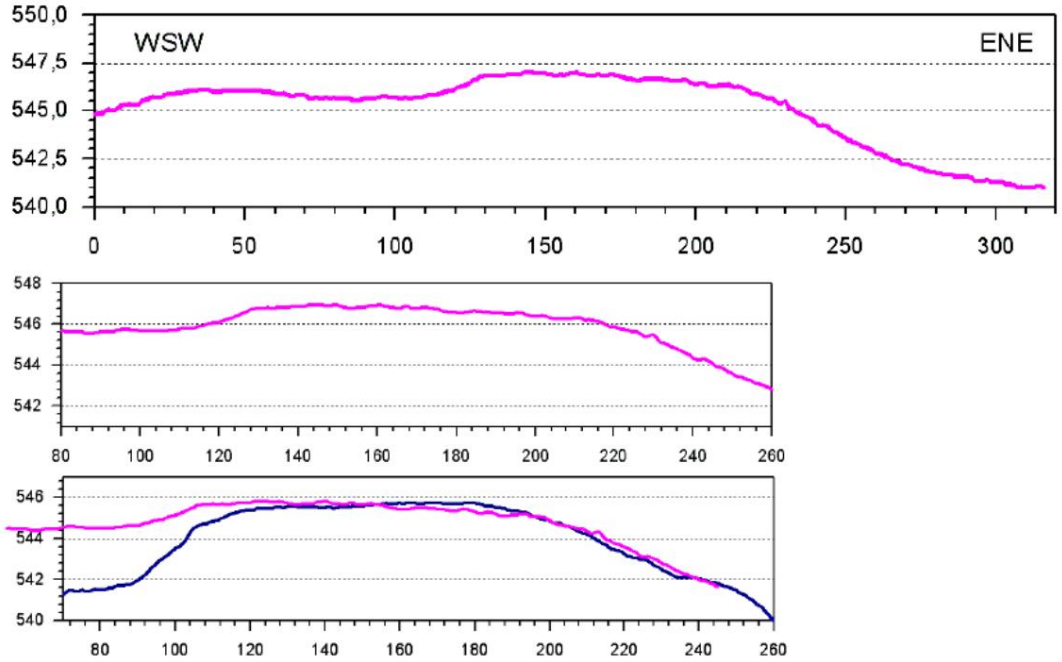

Fig. 85. The pink profile in Fig. 82 below, section and superimposed blue mushroom profile (from Fig. 84). The similarity of both humps over a profile length of 150 m is remarkable.

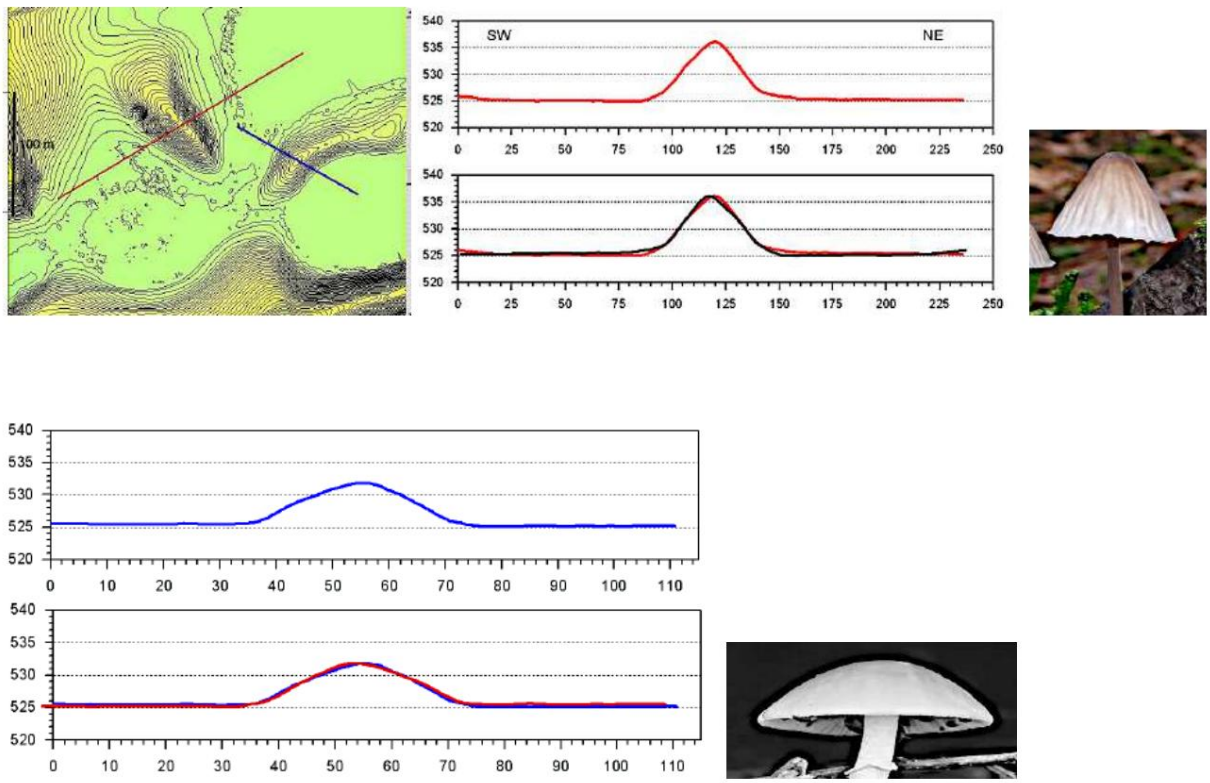

Fig. 86. DGM 1 profiles over rim ridges of two secondary craters show RTI mushroom cross-sections with perfect track symmetry.

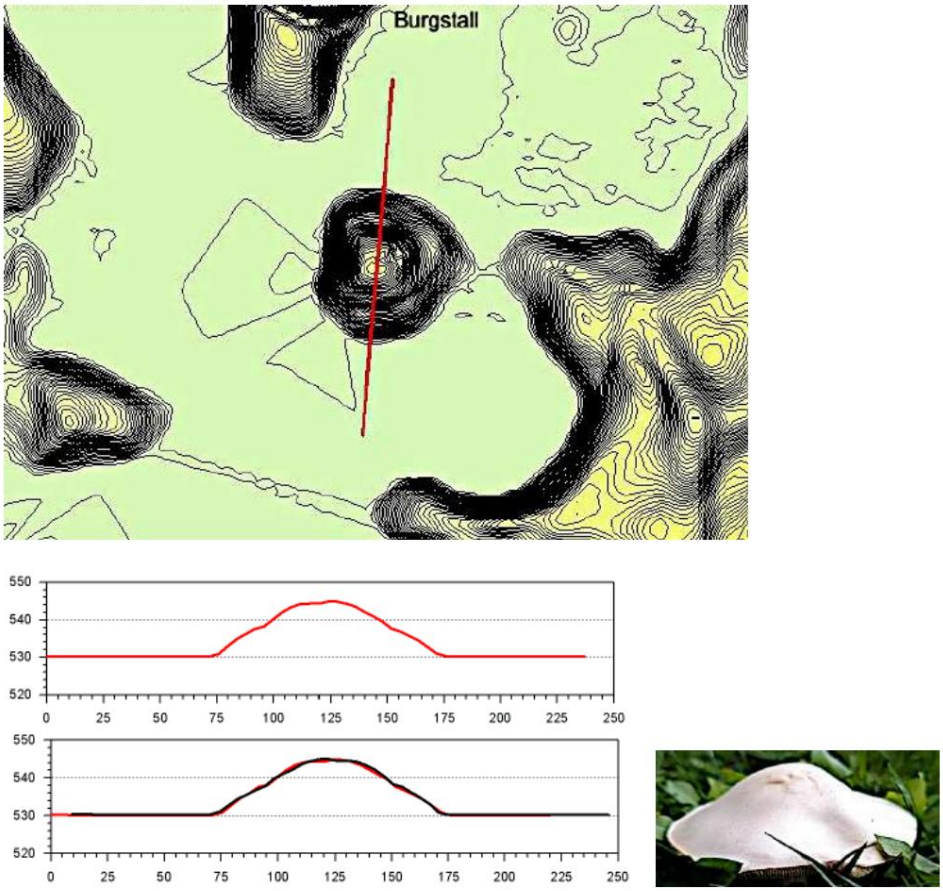

Fig. 87. 100 m wide and 15 m high, slightly terraced mushroom hill according to KHI with perfect symmetry in the decimeter range over 100 m, black mirrored profile.

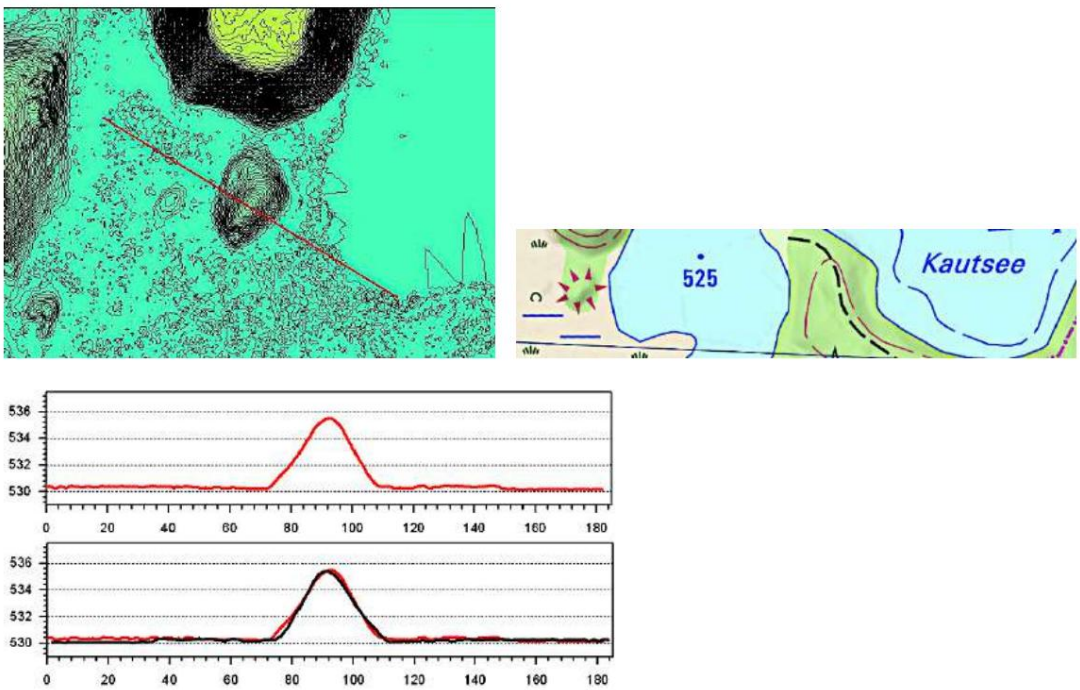

Fig. 88. The hump, specially marked on the topographic map of Bavaria, with perfect mushroom symmetry according to RTI.

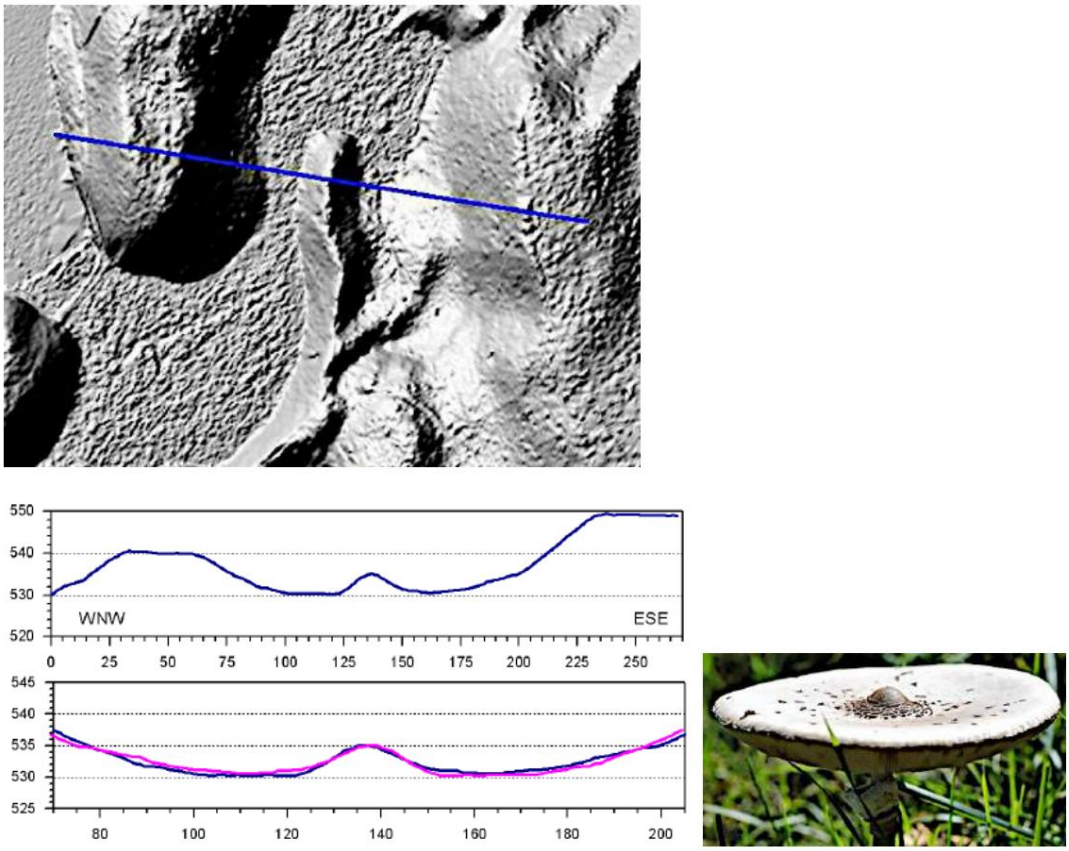

Fig. 89. Eastern edge of the Kesselsee. Rib-shaped RTI finger structure with a distinctive mushroom cross-section and perfect trace symmetry.

Fig. 90. DGM 1 3D terrain: Complex structures at Kesselsee with triangular formations within marginal ridges and with internal structures made of coarser block material. Details in the following figures.

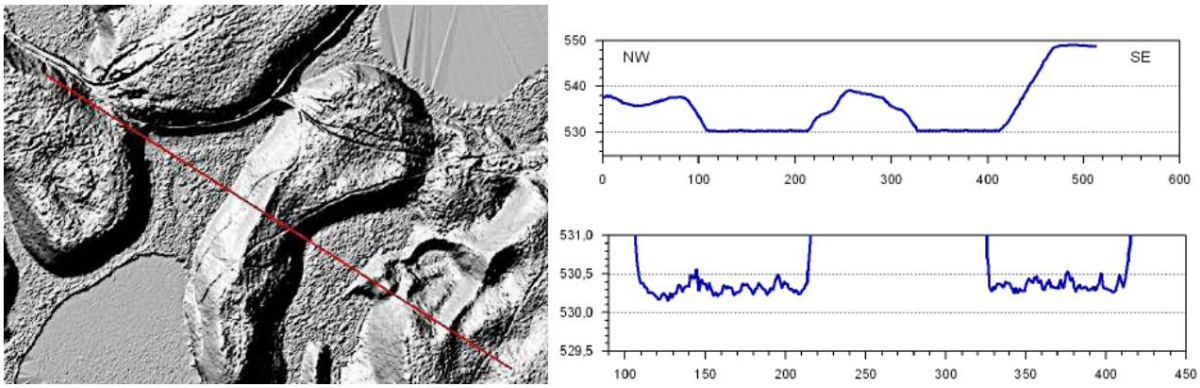

Fig. 91. The triangular structures in the shaded relief and DTM 1 profile. The geometry of the
The inner block material indicates a very complex impact process.

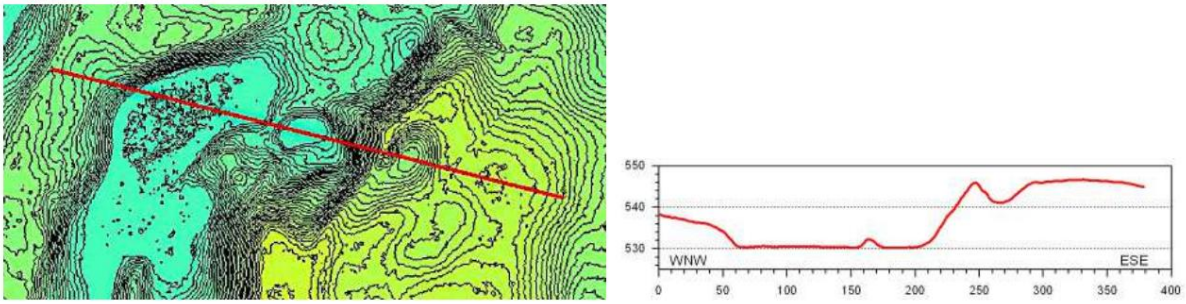

Fig. 92. The southeastern triangle as a DEM 1 isoline map (50 cm) showing the parallel geometry of the uplifted internal coarse material. The smaller accompanying craters support the idea of a very complex impact process.

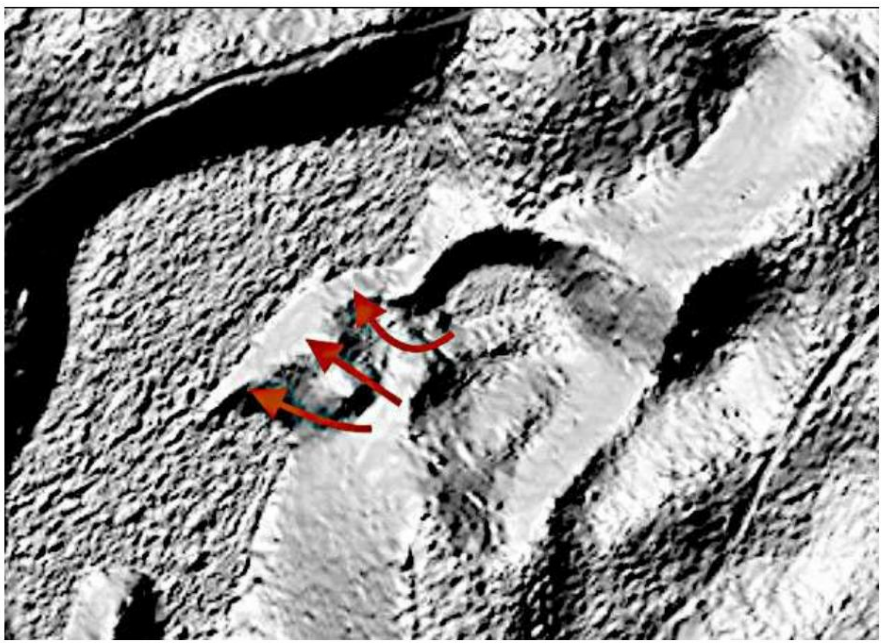

Fig. 93. A temporal sequence in the complex impact process.

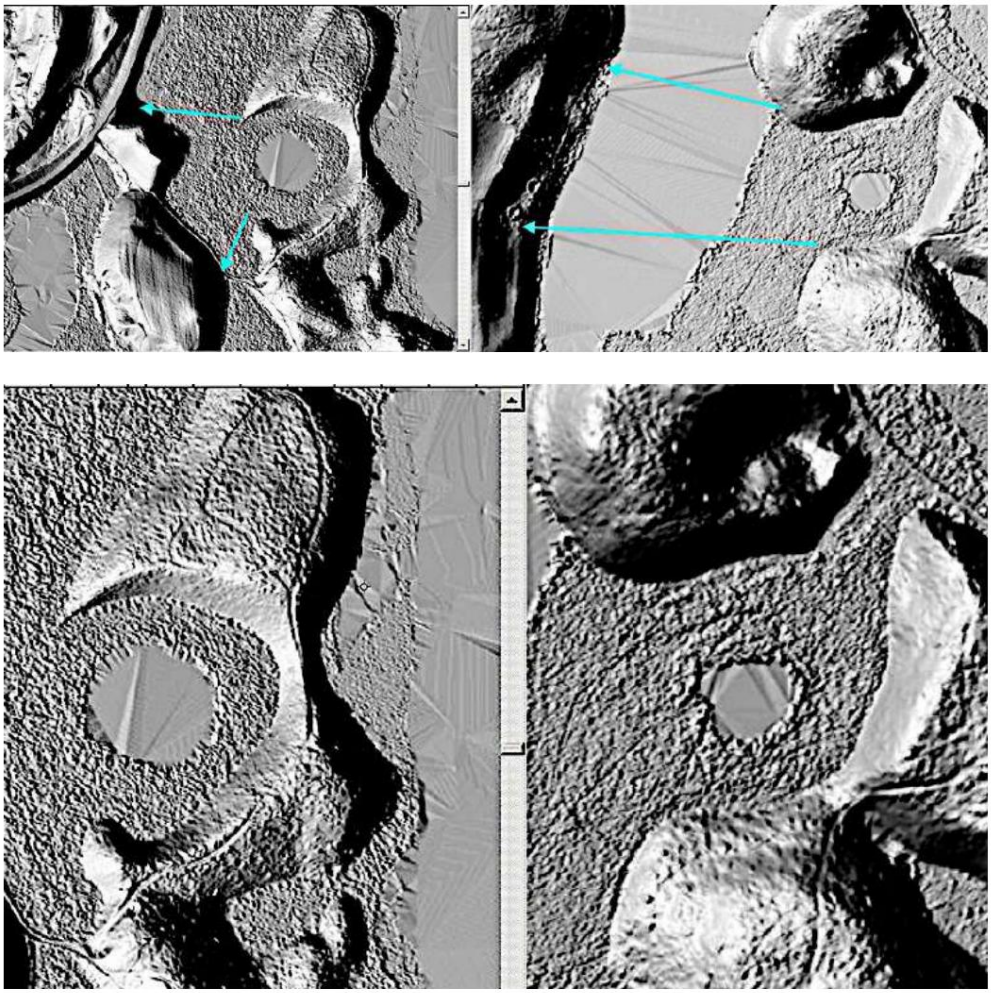

Fig. 94. DGM 1 shaded relief. Schernsee crater and Dürnbiehler See crater striking

similar, although 1 km apart. This applies to both the ring wall structure and the internal material distribution. The identical opening to the southwest caused by the wall displacement could indicate an airburst impact direction from the northeast, which corresponds to the orientation of the main axis of the Chiemgau impact ellipse (Fig. 1).

6. Dating

Considered part of the Chiemgau impact crater strewn field, recent dating suggests the lake district originated between 900 and 600 BC. This finding is supported and refuted by the observation of the widespread historical remnants of ridge and furrow fields in the Rosenheim area of Bavaria (according to Wikipedia). These are a characteristic agricultural cultivation method used in parts of Europe. Evidence of their use dates back to the Middle Ages, but based on findings in direct association with burial mounds, they may have been in use since the Bronze Age. This is particularly noteworthy for the Eggstätt-Hemhofen lake district because the impact and the resulting enormous landscape changes, including those around the lakes and directly at the lakeshores, are documented in the Digital Terrain Map 1 (DGM 1). The following illustrations show some characteristic examples.

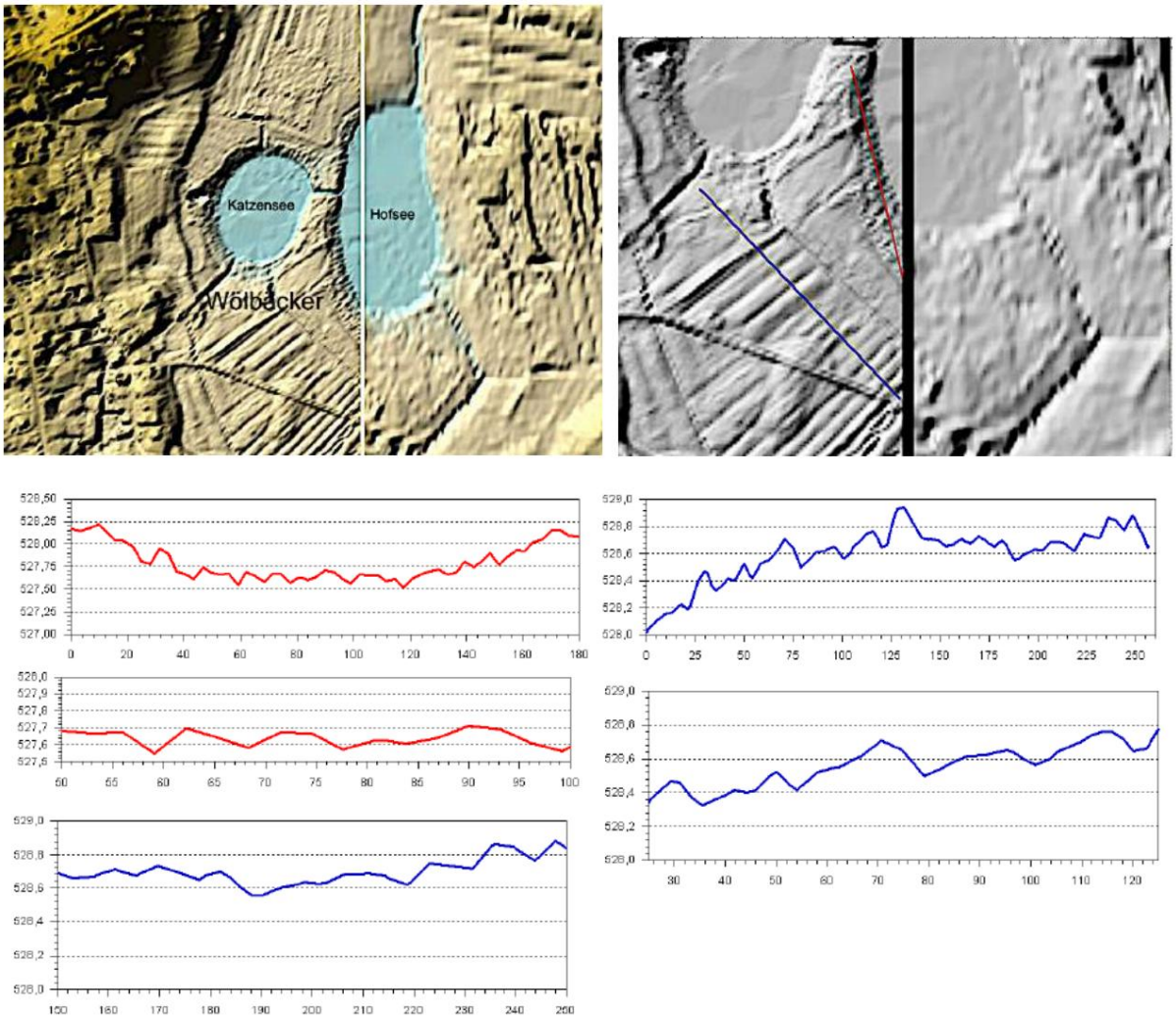

Fig. 95. Widely preserved morphologies of ridge and furrow fields around Hofsee and Katzensee near Eggstätt. The ridge patterns, some sharply cut off from the lakeshore, demonstrate the age sequence of cultivation and subsequent impact. The DGM 1 profiles with enlarged sections show identical patterns on the southwestern field (red) and at the shoreline (blue). The scales indicate the true amplitudes of the furrows.

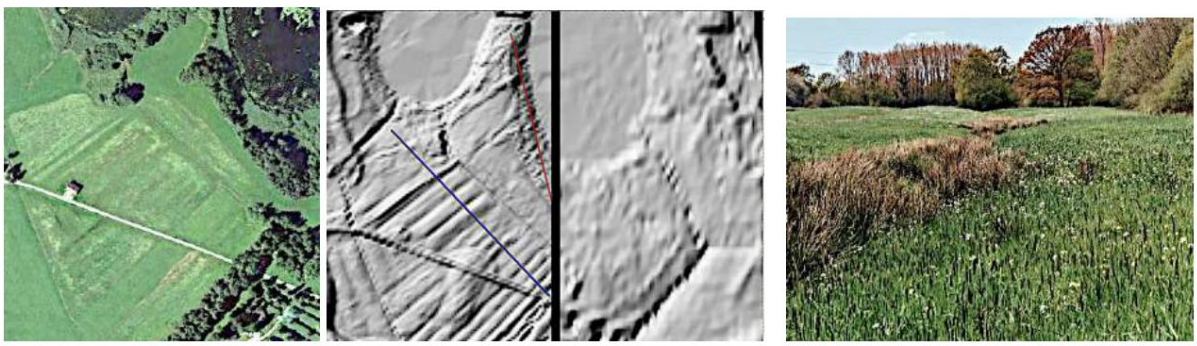

Fig. 96. The pattern of the large ridge and furrow system is still visible in the Google Earth image. In another area (right), the historical ridges are still clearly visible.

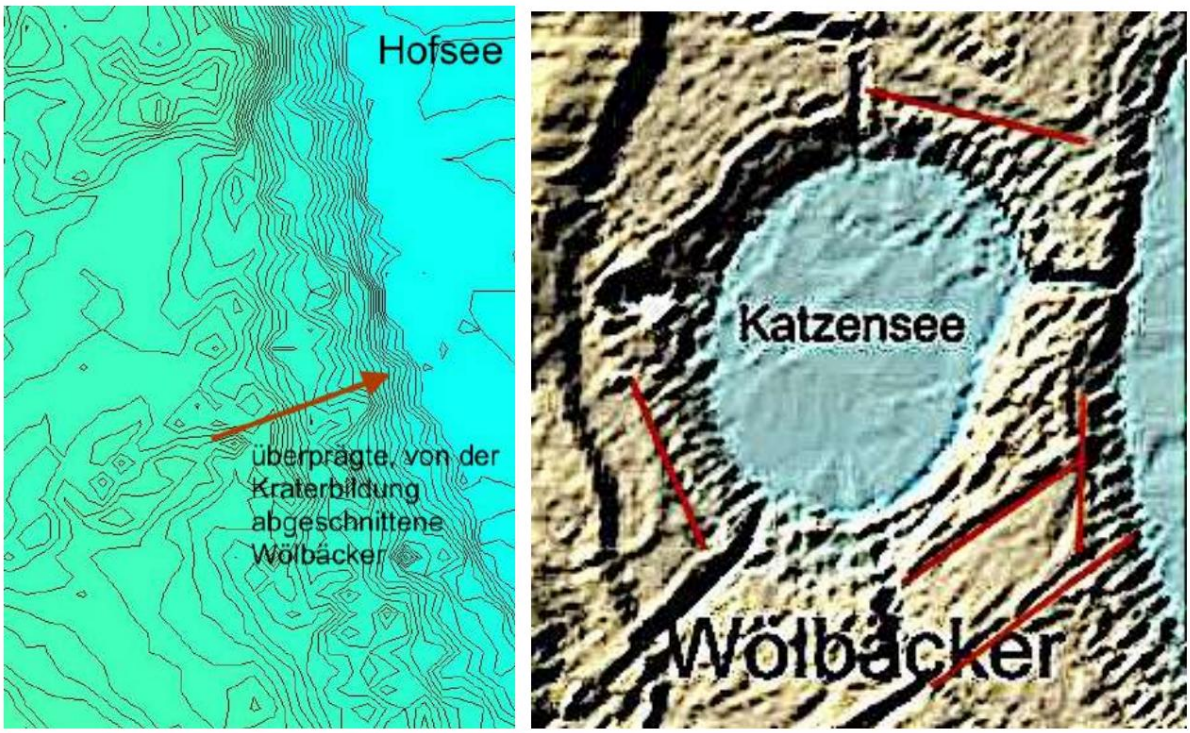

Fig. 97. The sharply cut-off ridge and furrow fields indicate the recent impact formation of the lake.
and rule out the Ice Age. The red lines trace the old boundaries of individual ridge and furrow fields.

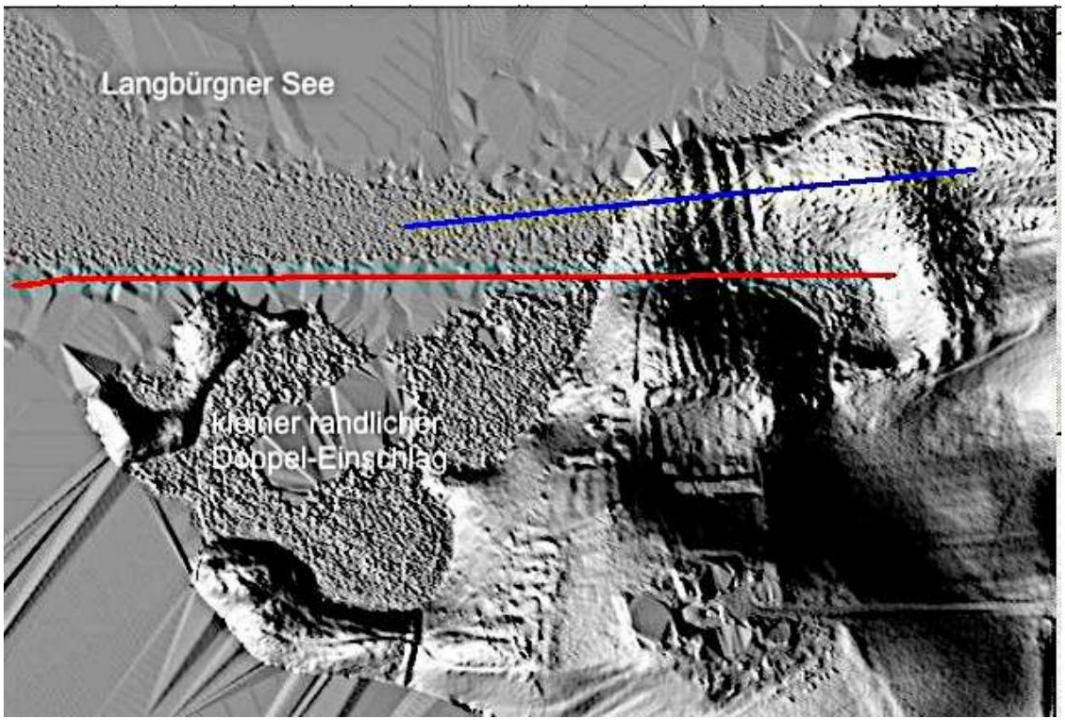

Fig. 98. DGM 1 shaded relief: Impact-modified ridge and furrow fields on the southern edge of Lake Langbürgner. As the subsequent profiles also indicate, faint ridge structures can still be traced beyond the shore. The abrupt changes in period, parallel to the profiles, also point to former field boundaries.

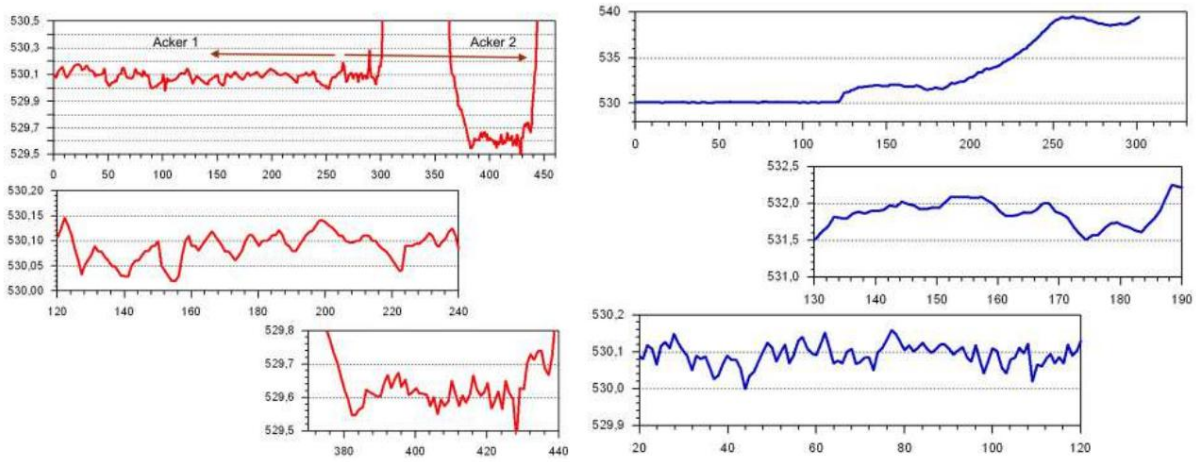

Fig. 99. Profiles of the ridge and furrow system, remnants of which are apparently still visible beyond the bank in the DGM 1. Sudden changes in periods indicate possible old, altered field margins where the technique was changed.

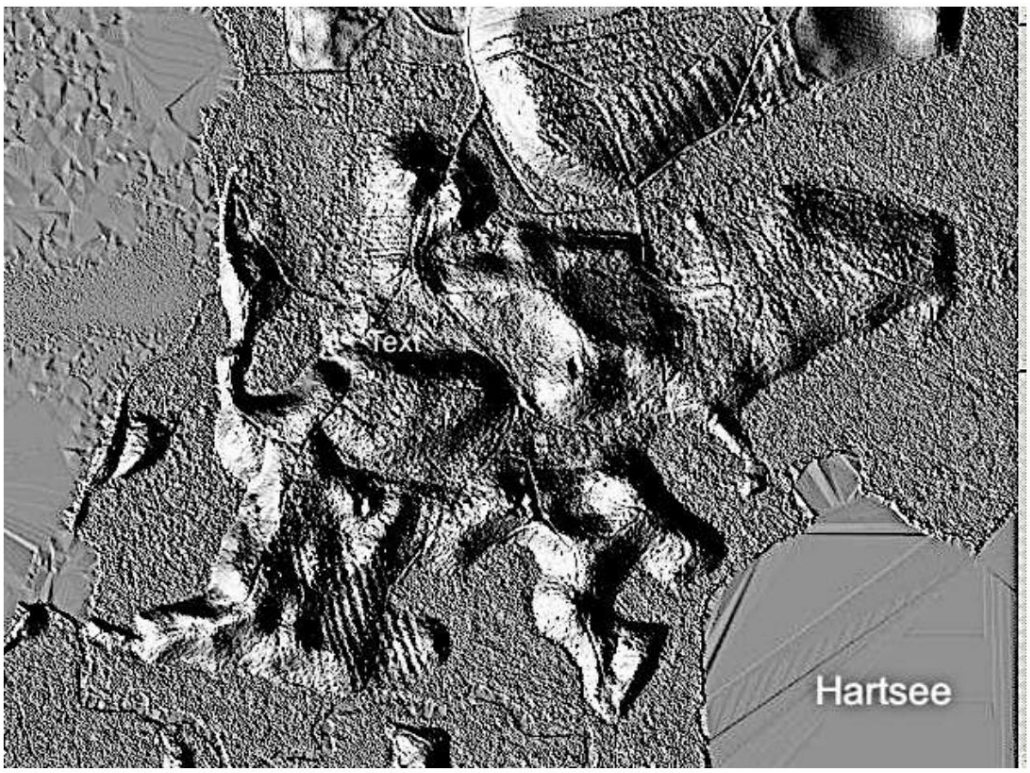

Fig. 100. DTM 1 shaded relief. Note, as always, the strong terrain elevation.
The ridge and furrow fields appear on the western, fragmented rim of the Hartsee crater.
equally fragmented with obviously erased field edges.

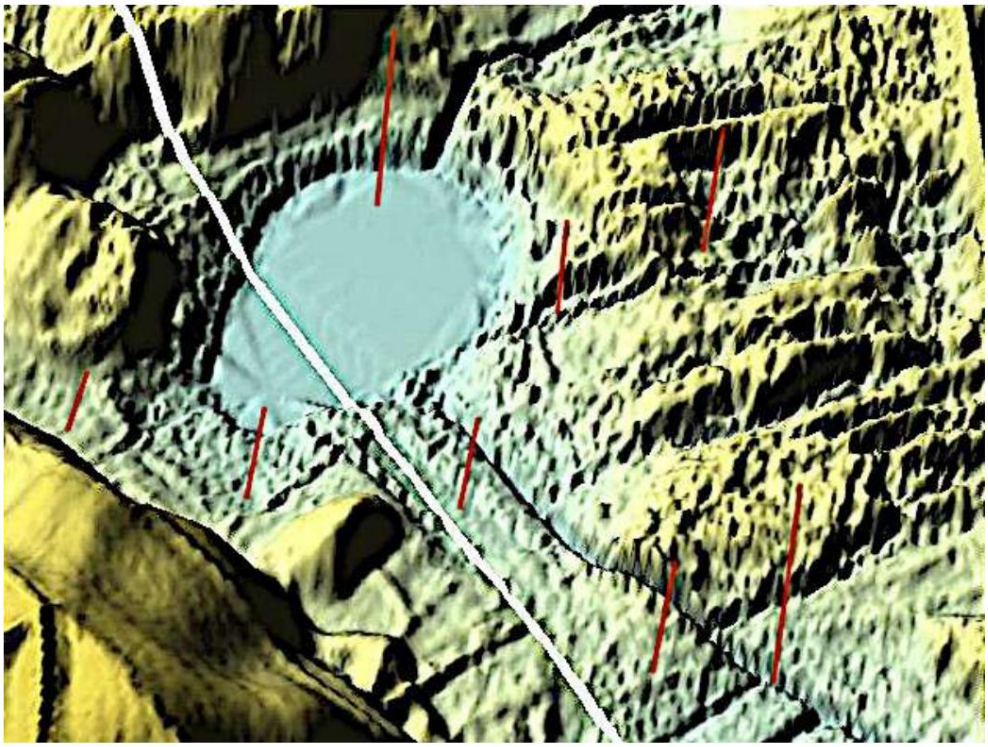

Fig. 101. DGM 1 surface 3D, slight oblique view. Lake Liensee appears here as if punched into the large field of ridge and furrow fields. Kettle hole excluded.

7. Summary Discussion

The Eggstätt lake district did not originate during the Ice Age. It is not a glacial meltwater landscape, considered one of the most important in Bavaria, and the lakes are not kettle holes (dead-ice depressions, kettle holes, or kettle holes). Geological evidence for such an origin has never been provided, which is true for all so-called kettle holes in the Alpine region, many of which are officially designated as special geotopes. The lake district is even listed by the Bavarian State Office for the Environment (LfU) as valuable geotope No. 187R001.

The glacial origin of the lake district in the course of the Prien Glacier is described in detail by Darga [11]: *On the trail of the Inn-Chiemsee Glacier* and has never before been seen in a comprehensible way in another geological context.

With the discovery and subsequent verification of the Holocene Chiemgau impact event, recently dated to around 900-600 BC during the Bronze Age/Iron Age [xy], impact researchers are questioning fundamental findings and extensive literature from Bavarian Ice Age geologists and geomorphologists, and instead declaring impact models to be correct in many cases: impact craters instead of kettle holes, crater rims instead of terminal moraines. To this day, despite all the internationally recognized, clear, and widely significant impact evidence, Ice Age geologists have only expressed rejection, albeit without ever providing any conclusive evidence.

Counterarguments have been presented. It is likely that this line of reasoning will be maintained by Bavarian Ice Age geology regarding the Eggstätter Lakes.

We are keeping pace with the extremely high-resolution Digital Terrain Model DGM 1 (horizontally interpolated down to the decimeter range, vertically interpolated down to the
(centimeter range) is, however, conclusively valid:

Beyond the known and approximately two dozen listed lakes, the lake area is covered with a dense, morphologically enormously complex network of small and large structures, which—like the lakes themselves—are to be understood as the result of a " low-altitude touchdown airburst impact" during the Chiemgau impact event. This refers to the impact of a significant portion of the Chiemgau impactor, presumably a massive comet of at least 1 km in diameter (as estimated and modeled), which exploded at a low altitude above the Earth's surface and, according to a hydrocode model, literally covered large areas with shallow impacts and the resulting very shallow craters.

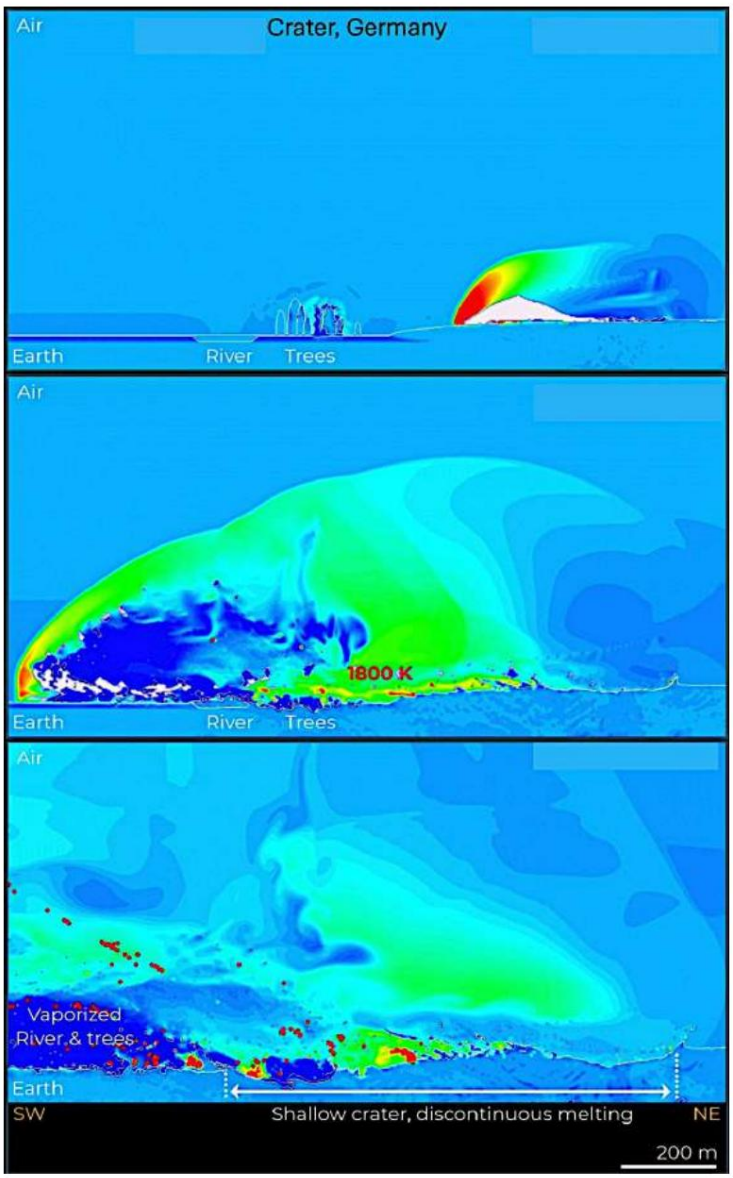

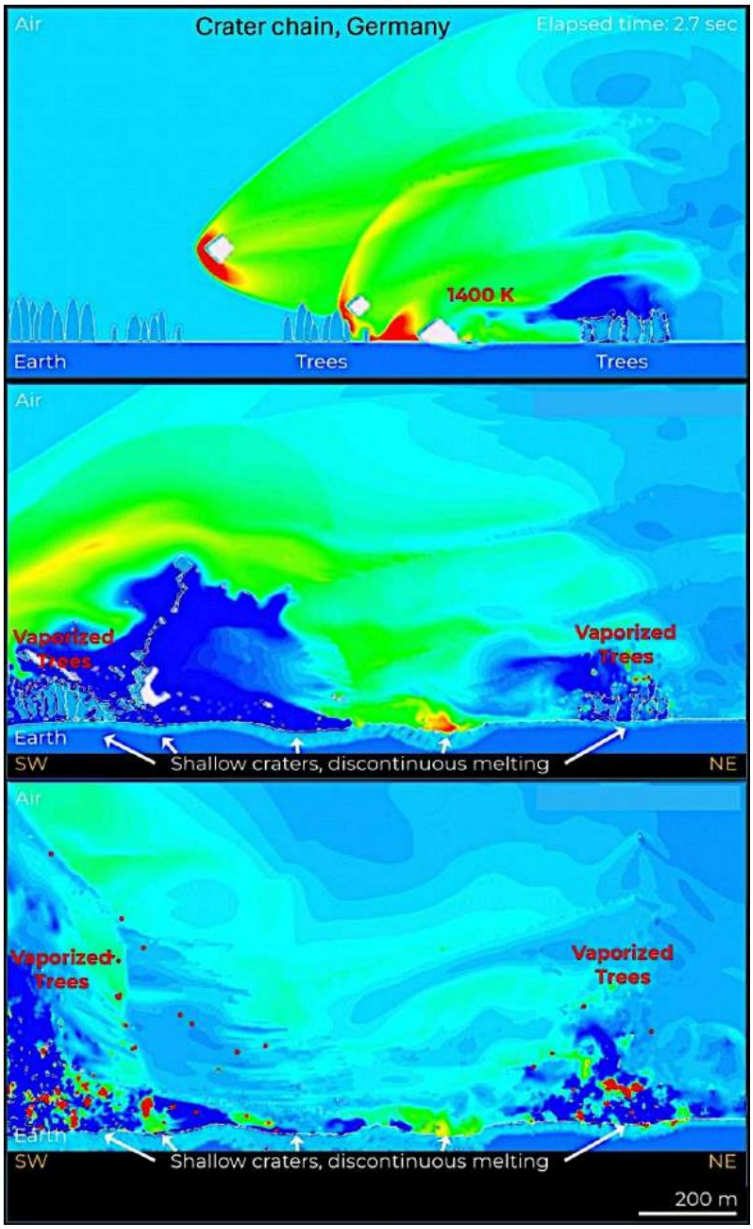

Fig. 102. Two still images from videos of hydrocode modeling of the Chiemgau impact caused by a comet impactor (by Allen West, Comet Group). Top: Modeling of the impact for a single crater (Eglsee crater), bottom: for a chain of craters (at Lake Chiemsee). The Chiemgau impact models explain how, given the lake district and the extent of the impact, larger, very shallow single craters (e.g., Lake Eschenau, Lake Laubensee, Fig. 53) and chains of craters (e.g., at Lake Einbessee, Fig. 82) could have formed.

What definitely rules out the lake district as a relic of the Ice Age:

* The dating of its origin to after the Bronze Age is based on the fact that the dense covering of the lake district with remnants of agricultural ridge and furrow fields was continuously overlaid by the impact, and ridge and furrow fields were not created until the Bronze Age at the earliest.

* Numerous Rayleigh-Taylor and Kelvin-Helmholtz instability structures (mushrooms/umbrellas, fingers, waves, block-dissected crater rims) are widely documented in DGM 1.
from liquid-gas interactions in experiments, in nature, but also from the
Astronomy (Crab Nebula, supernova explosions), and mushroom cloud formations
known forms occur widely in the Chiemgau airburst impact and explicitly in the
Eggstätter Lakes District. Here, it is the layered Würm sediments (possibly also) that form the rock.
Contributions from the cracking period and the lying molasse) of different densities and viscosities
in conjunction with the groundwater, which is subject to the pressure from above through the
Airburst impact according to the RTI and KHI.

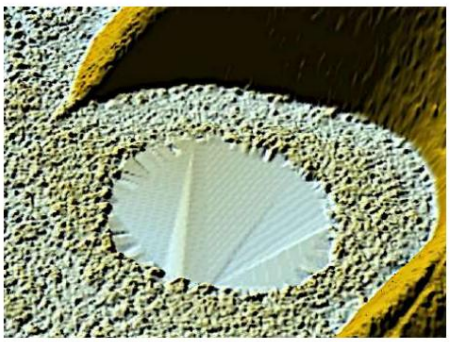
Fig. 33

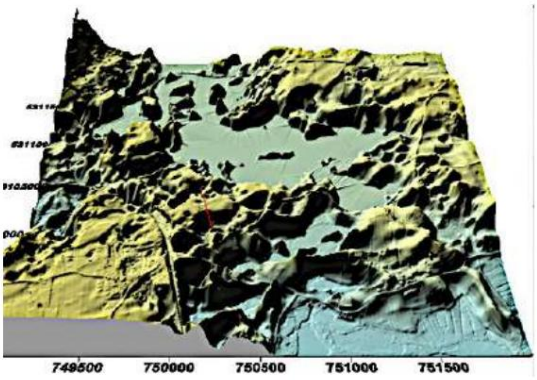

Fig. 71

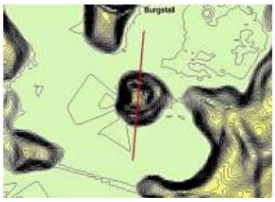

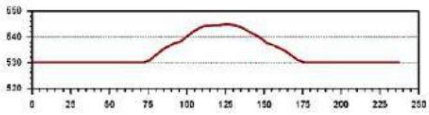

Fig. 87

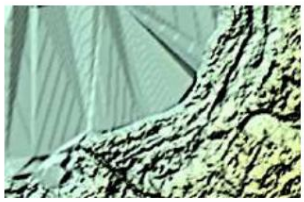
Fig. 56

Fig. 103. Examples of characteristic RTI/KHI impact structures from the lake district.
Block-like, fragmented lake rim, Schernsee crater; a dense finger-like pattern forms the southern edge.
of Lake Langbürgner; mushroom hill south of the castle ruins; waves in the terraced crater rim,
Eschenauer See.

* Widely occurring clusters of craters and humps, often mixed, which do not fit into a
Ice-decay landscape.

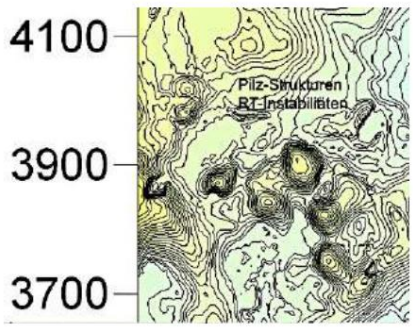

Fig. 13

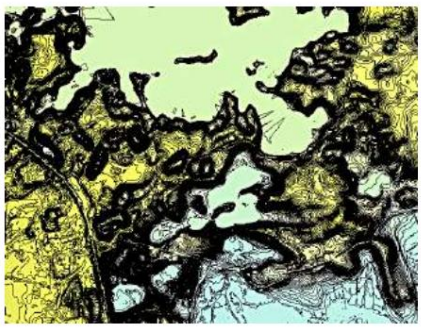
Fig. 33

Fig. 104. 300 m cluster of RTI fungi, southwestern edge of Lake Pelham; cluster of around 60 craters and
hummock structures, measuring about 50 - 100 m, southern edge of Lake Langbürgner.

* Complex craters with inner rings and central bulges.

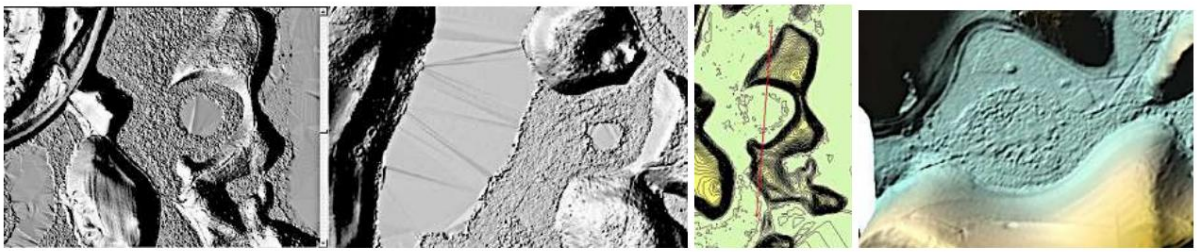

Fig. 105. Complex outer and inner crater structures at the Schernsee crater and the Dürnbiehler See crater in the shaded relief of the DGM 1; highlighting of the inner ring in the Schernsee crater in the DGM 1 isoline map; accompanying crater at the Stettner See crater, 3D block image with concentrically structured uplift.

* The morphological resolution of the DGM 1 down to the decimeter and centimeter range prohibits the formation of an ice age, which is widespread among many, even very large, structures. Lake district due to extreme trace symmetries (mirror symmetries) on intersecting DEMs 1-profiles.

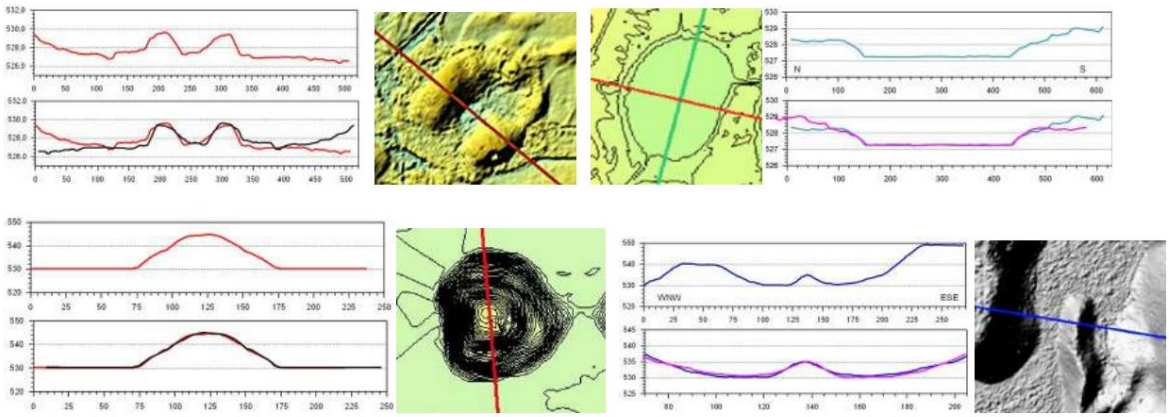

Fig. 106. Small selection of trace symmetries over different impact structures.
Double finger, crater rim Eschenauer See; Katzensee, turquoise profile; Mushroom hump Fig. 87;
Rib (“finger”), Fig. 89.

This compilation of a selection of DGM 1 structures underlines once again
without reservation the new finding that the Eggstätt-Hemhofen lake district within the framework
of the Touchdown Airburst Chiemgau impact and additionally datable to the Bronze Age
The latest Hydrocode modeling, specifically for a Chiemgau comet airburst impact, supports a picture that the LiDAR DGM 1 data analysis and
-Interpretation is drawn.

Bavarian Ice Age geology, and with it the Ice Age geologists who still study the Chiemgau region today,
Impact against all "relevant" submissions and publications made over the last 20 years
Those who reject findings and evidence as non-existent are once again confronted here with the enormous impact confronted them, leading to even more far-reaching rethinking and revisions of important

constellations of the Würm glaciation with Inn, Chiemsee and Prien glaciers should stimulate what we have already formulated earlier for Prien and Chiemsee glaciers [12, 13].

Based on our experience over the past 20 years with the LfU and local geologists, this will not happen; a scientifically substantiated counter-argument will not be forthcoming, and the
The Eggstätt-Hemhofen airburst impact is being ignored and continues to be treated as very significant.
Invite a tourist Ice Age attraction.

Interestingly, this situation bears a striking parallel to the not-so-distant Nördlinger Ries crater and the story of its transformation from a 100-year-old volcano to a recognized impact crater. After the US geologists Shoemaker and Chao provided irrefutable proof of the coesite shock effects in suevite in the early 1960s, the resistance, protest, and rejection from German geologists were enormous, even bitter, and persisted for a long time. Ries: volcano versus impact; Chiemgau: Ice Age versus impact.

New ideas and considerations will also be generated for the Chiemgau impact as a whole, particularly regarding the extent, inventory, and phenomena of the airburst impact, together with the new findings and application possibilities of the DGM 1.
must include.

literature

[1] Rappenglück, B., Hiltl, M., Poßekel, J., Rappenglück, MA, Ernstson, K. (2023) People experienced the prehistoric Chiemgau meteorite impact - geoarchaeological evidence from southeastern Germany: a review. Medit. Archeology Archaeometry, 23, no. 511, 209-234. doi: 10.5281/zenodo.7775799.

[2] Allen West, Marc Young, Luis Costa et al. (2024) Modeling airbursts by comets, asteroids, and nuclear detonations: shock metamorphism, meltglass, and microspherules. Airbursts and cratering impacts. Vol. 2(1). DOI: 10.14293/ACI.2024.0004.

[3] Ernstson, K. and Poßekel, J. (2024) The Chiemgau Meteorite Impact Strewn Field and the Digital Terrain Model: "Earthquake" Liquefaction from Above and from Below. - AGU 2024.
Abstract and poster.

[4] Martin, MR (2014) Ice Age Glaciology Theory, 17, 18, viademica.verlag, Berlin.

[5] Ernstson, K., Mayer, W.; Neumair, A.; Rappenglück, B.; Rappenglück, MA; Sudhaus, D.; Zeller, K. (2010) The Chiemgau crater strewn field: Evidence of a Holocene large impact event in Southeast Bavaria, Germany. Journal of Siberian Federal University Engineering & Technologies, 1(3), 72–103.

[6] Rappenglück, M.; Rappenglück, B.; Ernstson, K. (2017) Cosmic collision in early history. The Chiemgau impact: The exploration of a Bavarian meteorite crater strewn field. Zeitschrift für Anomalistik 2017, 17(3), 235-260, and extensive citations therein.

[7] CIRT (2019) https://www.chiemgau-impakt.de/2019/07/16/tuettensee-meteoritenkrater-ein-bayerisches-geotop/

[8] Ernstson, K. and Poßekel, J. Paradigm shift in impact research: the Holocene Chiemgau meteorite impact crater strewn field and the digital terrain model. 55th LPSC, Abstract and Poster 1658.pdf.

[9] Google AI 2006)

[10] West, A. and Ernstson, K. (2026) Hydrocode modeling of impact craters: Chiemgau low-altitude airburst impact strewn field, Germany. 57th LPSC (2026), 1085.pdf.

[11] Darga, R. (2009) In the footsteps of the Inn-Chiemsee Glacier – Excursions. Darga, R.
Ed.; Pfeil: Munich.

[12] Ernstson, K. and Poßekel, J. (2024) The Chiemgau Meteorite Impact Strewn Field and the Digital Terrain Model: "Earthquake" Liquefaction from Above and from Below. - AGU 2024.
Abstract and poster.

[13] Ernstson, K. and Poßekel, J. (2025) Lake Bärnsee in the Chiemgau Holocene impact strewn field (Germany): ice-age tongue basin lake vs. Holocene low-altitude touchdown airburst impact formation. 87th Annual Meeting of the Meteoritical Society 2025 (LPI Contrib. No.
3088) Abstract and Poster, #5134.pdf.